THE USE OF REMOTE SENSING AND GIS FOR DROUGHT RISK ASSESSMENT: THE CASE OF SOUTHERN PROVINCE, ZAMBIA.

Micheal Katongo Phiri

University Of Zambia, IWRM Centre

C/O School Of Mines

A thesis submitted to the School of Mines, University of Zambia in fulfilment of the requirement for the Degree of Master of Science in Integrated Water Resource Management

2019

DECLARATION

This thesis was written and submitted in accordance with the rules and regulations governing the award of the Master of Science in Integrated Water Resources Management in the School of Mines of the University of Zambia. I further declare that I am the sole author of this thesis and that all content is my original work that has not been presented before for an award at any university or learning institution:

Signature of author: .....

Date: .....

APPROVAL

This thesis of Michael Katongo Phiri is approved as fulfilling the requirements of the Degree of Master of Science in Integrated Water Resources Management of the University of Zambia.

Signature: Chairperson ……..

1st Examiner ……..

2nd Examiner ……..

External Examiner ……..

EXTENDED ABSTRACT

Water plays a major role in human livelihoods and has significant implications to food security. Hydrological extremes are a major threat to society and can have extensive effects. Droughts compound the already increasing pressures on water resources from population growth, economic activities and escalating competition between users. Remote Sensing and Geographic Information Systems (GIS) have emerged as essential tools in the assessment and analysis of natural resources and hazards for drought prone areas such as the Southern Province of Zambia. The Southern Province is drought prone and is typified by unreliable rainfall and arid conditions despite being one of the food baskets of Zambia. Therefore, it is important to assess the risk of drought in the region. However, there are only 11 meteorological stations present in the vast region, of which only six have historical records of more than 10 years. This limits the use of conventional drought risk assessments techniques as they require well populated networks of weather stations. Remote sensing and GIS are not reliant on station based data. Satellite data is easily obtainable in almost real-time and at high resolutions from several platforms. Therefore, it is important to explore the use of Remote Sensing and GIS to assess drought in the Southern Province.

In this study, Normalised Difference Vegetation Index (NDVI) and Land Surface Temperature (LST) for the years 2000 to 2016 were obtained from Moderate Resolution Imaging Spectroradiometer (MODIS). Climate Hazards Group InfraRed Precipitation with Station (CHIRPS) gridded rainfall estimates and in situ rainfall data were also obtained. Standardised Precipitation Index (SPI) and rainfall anomaly percentage were calculated using monthly CHIRPS in SPIRITS software and used to assess meteorological drought. NDVI was transformed to Vegetation Condition Index (VCI) in order to assess agricultural drought. Soil Moisture Index (SMI) was determined using NDVI and LST. Correlations analyses were conducted between NDVI and in situ rainfall, NDVI and CHIRPS, VCI and maize production and yield, and SMI and Soil Moisture. Drought risk comprised of three components, which were hazard, exposure and vulnerability. Meteorological drought hazard was determined using rainfall anomaly percentage and SPI, whilst agricultural drought hazard was determined using VCI and SMI. Drought exposure comprised of two elements, which were human populations and land

cover. Drought vulnerability was a combination of socioeconomic indicators, rainfall variability and slope.

The results show that NDVI responded quickly to increments in rainfall but slower to reductions due to residual soil moisture. Droughts of the Southern Province were categorised as aggressive or regressive in nature. Aggressive droughts were those that increased in magnitude and/or intensity as the season advanced, whereas regressive droughts where those that saw reductions in intensity/magnitude as the season progressed. Aggressive and regressive behaviour were true for both meteorological and agricultural droughts. The 2001/2002 season saw an aggressive drought occur as the average SPI for the Southern Province dropped from -0.26 (normal) in November 2001 to - 2.29 (extremely dry) in January 2002. In the 2002/2003, SPI rose from - 1.55 (severely dry) in November 2002 to 0.57 (normal) in March 2003, which indicated a regressive drought. Similarly, VCI dropped from 53 (no drought) in November 2001 to 36 (mild drought) in January 2002, whereas it rose from 36 in November 2002 to 50 in Mach 2003. Regressive droughts occurred as a result of El Niño and were characterised by higher surface temperatures. SMI was lower in agro-ecological Region I and higher in Region IIa. NDVI was positively correlated to in situ rainfall measurements (0.59) and was reliable as an index to assess drought. VCI was correlated to maize production and yield (0.66 and 0.84, respectively). Similarly, SMI was correlated to soil moisture at 5 centimetre depth with a correlation of 0.71. The most at risk to drought districts in the province were Kalomo, Sinazongwe and Zimba. The least at risk were Mazabuka and Chikankata, which were both in Region IIa. Kalomo and Zimba had a combined population of 258,570 people of which about 75% were estimated to be living under the poverty line of 96.37 Zambian Kwacha rebased in 2015. The two districts were also estimated to have planted 96,427.53 hectares of maize in 2015, which at the time was the most in the Southern Province. However, 37.62% was estimated to have been harvested.

Remote sensing and GIS were successfully used to assess meteorological and agricultural drought in the Southern Province of Zambia. It was possible to assess areas in which meteorological data was absent as the remote sensing data used covered the whole province. Furthermore, remote sensing data had a few gaps and correlated well with precipitation values. It is recommended that the Disaster Management and Mitigation Unit (DMMU) integrate remote sensing drought indices and GIS work flows to drought early warning systems. It is also

recommended that further studies be carried out in the drought hot spot districts of Kalomo, Sinazongwe and Zimba by the Zambia Meteorological Department and the DMMU in collaboration with the University of Zambia Integrated Water Resources Management Centre (UNZA IWRM).

DEDICATION

To my wife Zondiwe, for her patience and understanding.

To my parents, for their consistent encouragement.

To Dr Augustine Mulolwa, for his mentorship.

ACKNOWLEDGEMENTS

I wish to acknowledge the following for their contribution, in one way or another, to the realisation of this dissertation:

I wish to extend my heartfelt thanks to all the staff of the Integrated Water Resource Management (IWRM) Centre, who assisted in one way or another during the course of this study. In particular, I am thankful to those that provided the necessary guidance and supervision.

I wish to thank the National Remote Sensing Centre (NRSC) for awarding me the opportunity to further my studies and in awarding me the time to complete the study. I would love thank the Acting Director, Mr. Samuel Maango for his constant support and Mr. Lusekelo Kasunga for his brilliant contributions and critiques.

I wish to thank all those who assisted me in gathering and processing data. I wish, most importantly, to express my appreciation for the contributions that came from my Principal Supervisor, Dr Kawawa Banda and my Co-supervisor Professor Imasiku Nyambe. Thank you very much for the commitment in providing me the needed guidance. Succinctly put, you made this document intelligible.

TABLE OF CONTENTS

DECLARATION i

APPROVAL ii

EXTENDED ABSTRACT iii

DEDICATION vi

ACKNOWLEDGEMENTS vii

LIST OF FIGURES xii

LIST OF TABLES xvi

LIST OF ACRONYMS xvii

CHAPTER ONE: INTRODUCTION 1

1.1 Background 1

1.2 Statement of the Problem 2

1.3 Main Objectives 2

1.3.1 Specific Objectives 2

1.3.2 Research Questions 3

1.3.3 Significance of the study 3

CHAPTER TWO: DESCRIPTION OF STUDY AREA 4

2.1 Location and Administration 4

2.2 Topography and Drainage 5

2.3 Weather and Climate 5

2.4 Land Cover 7

2.5 Demography, Economy and Livelihood 8

CHAPTER THREE: LITERATURE REVIEW 11

3.1 Definitions of Drought 11

3.2 Types of Drought 12

3.3 Drought Hazard, Vulnerability and Risk....12
3.4 Principles of IWRM and Drought....14
3.5 Conventional Drought Indices....15
3.5.1 Deciles....16
3.5.2 Standardised Precipitation Index (SPI)....17
3.5.3 Palmer Drought Severity Index (PDSI) and Palmer Hydrological Drought Index (PHDI)....18
3.5.4 Standardised Water Level Index (SWI)....19
3.6 Remote Sensing Drought Indices....19
3.6.1 Normalised Difference Vegetation Index (NDVI)....20
3.6.2 Vegetation Condition Index (VCI)....21
3.6.3 Soil Moisture Index (SMI)....22
3.7 Relationship between NDVI and Precipitation as an Indicator of Drought....24
3.8 Drought Risk Assessments in Southern Africa....26
3.8.1 Monitoring for Environment and Security in Africa (MESA)....27
3.8.2 Famine Early Warning Systems Network....29
3.9 El Niño Events and Drought in Southern Africa....30
3.10 History of Drought in Zambia (2000 to 2016)....33
3.11 Remote Sensing and GIS in Drought Risk Assessment....33
CHAPTER FOUR: METHODOLOGY....35
4.1 General Remarks....35
4.2 Data Selection Criteria for Remote Sensing Data....35
4.3 Description of Selected MODIS and Gridded Rainfall Data Used in this Study....36
4.4 Pre-processing of Selected MODIS Data Used in this Study....37
4.5 Rainfall Anomaly Percentage and Rainfall Variation....39

4.6 Calculation of Standardised Precipitation Index (SPI) 40
4.7 Calculation of Vegetation Condition Index (VCI) 42
4.8 Calculation of Soil Moisture Index (SMI) 44
4.9 Correlation Analysis for Validation of NDVI Based Indices 45
4.10 Drought Risk Mapping 48
4.11 Limitations to Study 53
CHAPTER FIVE: RESULTS AND DISCUSSION 55
5.1 General Remarks 55
5.2 The Changes in NDVI Due to Rainfall Variation 55
5.3 Rainfall Anomaly and Variability 61
5.4 Standardised Precipitation Index (SPI) and Drought in the Southern Province 67
5.5 Drought Assessment Using Vegetation Condition Index (VCI) 74
5.6 Surface Temperature and Soil Moisture Conditions during Drought 77
5.7 Validation of NDVI Based Drought Indices 83
5.8 Drought Risk Mapping of the Southern Province, Zambia 92
5.8.1 Drought Hazard of the Southern Province of Zambia 92
5.8.2 Drought Exposure of the Southern Province, Zambia 95
5.8.3 Drought Vulnerability of the Southern Province, Zambia 97
5.8.4 Drought Risk of the Southern Province of Zambia 99
5.9 Discussion of Results 106
5.9.1 Calculation of Remotely Sensed to Determine Meteorological and Agricultural Drought Indices Drought Hazard for the Southern Province of Zambia 106
5.9.2 Relationship between Normalised Vegetation Index (NDVI) and in situ Rainfall, NDVI and Remotely Sensed Rainfall Estimates, Maize

Production and Yield versus Vegetation Condition Index (VCI), and Soil Moisture and Soil Moisture Index (SMI) 108

5.9.3 Identification of Drought Hotspots in the Southern Province of Zambia using Drought Hazard, Exposure and Vulnerability 109

CHAPTER SIX: CONCLUSION AND RECOMMENDATIONS 111

6.1 Conclusions 111

6.2 Recommendations 115

REFERENCES 117

APPENDICES 124

Appendix 1: Coordinates of meteorological stations in the Southern Province, Zambia 124

Appendix 2: Livelihood zones of Zambia (FEWS NET, 2014) 125

Appendix 3: Coordinates of sample points used for correlation analysis for the Southern Province of Zambia 126

Appendix 4: Maize production and yield of the Southern Province, Zambia (CSO, 2016b) 127

Appendix 5: Ward Population, Number of Poor and Poverty Headcount of Southern Province Zambia (De la Fuente, et al. 2015) and (CSO 2012) 128

Appendix 6: Correlations in different land cover classes of the Zambia Scheme II Land Cover Map 132

Appendix 7: District area planted and harvested for Maize in the Southern Province, Zambia (CSO, 2015) 133

LIST OF FIGURES

Figure 1: Location of the Southern Province of Zambia, the study area 4

Figure 2: Agro-ecological zones of the Southern Province of Zambia, modified from FEWS NET (2014) 6

Figure 3: Locations of Meteorological Stations in Southern Province of Zambia 7

Figure 4: Zambia Forestry Department 2014 Scheme I Landcover of Southern Province 8

Figure 5: Area planted of maize, sorghum, millet and soya beans in Southern Province from 1987 to 2014 (CSO, 2015). 9

Figure 6: Livelihood zones of the Southern Province after FEWS NET (2014) 10

Figure 7: Relationship between different types of droughts (NDMC, 2006) 12

Figure 8: Typical reflectance spectrum of a healthy and a stressed plant 21

Figure 9: Typical scatterplot in NDVI-LST space 23

Figure 10: Example of a Boolean-type drought risk map 28

Figure 11: Example of a Graded-type drought risk map 29

Figure 12: Historical El Niño Intensities and Rainfall Patterns in December-March, 1981-2010 31

Figure 13: Southern Africa October to January rainfall, ranked within 1981-2016 32

Figure 14: GIS pre-processing model for MODIS imagery used in this study 38

Figure 15: The gamma probability density function plots 41

Figure 16: VCI Calculation Model used in this study 43

Figure 17: Changes in monthly NDVI and monthly CHIRPS rainfall estimates from January 2000 to October 2016 over the Southern Province of Zambia 56

Figure 18: Average monthly NDVI from January 2000 to October 2016 for the Southern Province of Zambia 58

Figure 19: Average monthly rainfall versus actual monthly rainfall from January 2000 to October 2016 for the Southern Province of Zambia 59

Figure 20: Pattern of rainfall and NDVI during drought seasons over the Southern Province of Zambia 60

Figure 21: Rainfall anomaly percentage for the months of December, January and February during drought periods in the Southern Province of Zambia 63

Figure 22: Areal and temporal rainfall variabilities of the Southern Province, Zambia..... 66

Figure 23: Standardised Precipitation Index (SPI) at the manual meteorological stations in Southern Province 68

Figure 24: Temporal SPI of the Southern Province of Zambia 69

Figure 25: SPI at Kafue and Choma Meteorological stations for the 2001/2002, 2002/2003 ans 2004/2005 rainfall seasons 72

Figure 26: Spatial frequency of each drought severity occurrence for the Southern Province of Zambia 73

Figure 27: Changes in VCI across the seasons of 2001/2002 and 2015/2016 over the Southern Province of Zambia 75

Figure 28: The trends of VCI, maize yield and maize production in the Southern Province of Zambia 76

Figure 29: NDVI-LST space depicting (a) LST maximum (b) LST minimum (c) NDVI for bare soil, and (d) maximum NDVI of the Southern Province, Zambia..... 78

Figure 30: Fractional vegetation cover versus scaled land surface temperature in Southern Province of Zambia 78

Figure 31: Land Surface Temperature (LST) during November for the drought seasons of 2002/2003 and 2015/2016 for the Southern Province of Zambia 79

Figure 32: Fractional vegetation cover – scaled land surface temperature space (a) February 2002 drought month with triangular shaped (b) November 2015 drought month with trapezoid shape (c) February 2004 normal year with triangular shape (d) November 2003 normal, in the Southern Province of Zambia 80

Figure 33: SMI during the months of January and February, 2005 in the Southern Province of Zambia 82

Figure 34: Q-Q plots for monthly NDVI, rainfall and CHIRPS rainfall estimates for the Southern Province of Zambia 84

Figure 35: Rainfall-NDVI correlation of the Southern Province of Zambia 85

Figure 36: Monthly NDVI – RFE correlation of the Southern Province of Zambia 86

Figure 37: NDVI-Rainfall Correlation in different land cover classes, Southern Province, Zambia 88

Figure 38: Q-Q plots of VCI, maize production and yield, Southern Province of Zambia 89

Figure 39: Maize production – VCI and Maize Yield – VCI correlations, Southern Province of Zambia 90

Figure 40: Q-Q plots for soil moisture at different depths and SMI, Southern Province of Zambia 91

Figure 41: Soil Moisture-SMI Correlation for the Southern Province of Zambia..... 92

Figure 42: Meteorological drought hazard of the Southern Province of Zambia presented by district 93

Figure 43: Agricultural drought hazard of the Southern Province of Zambia presented by district 95

Figure 44: Drought exposure of the Southern Province, Zambia 96

Figure 45: Drought exposure of each district of the Southern Province of Zambia 97

Figure 46: Drought Vulnerability of the Southern Province of Zambia 98

Figure 47: Average drought vulnerability of each district of the Southern Province, Zambia..... 99

Figure 48: Meteorological drought risk of the Southern Province of Zambia..... 101

Figure 49: Agricultural drought risk of the Southern Province, Zambia 102

Figure 50: Integrated drought risk of the Southern Province of Zambia derived by the combining meteorological and agricultural drought 103

Figure 51: Average integrated drought risk of each district in the Southern Province of Zambia104

Figure 52: Area Planted for Maize in the Southern Province of Zambia 105

Figure 53: Area Planted and area harvested of maize in the Sothern Province of Zambia from 2010 to 2015 106

LIST OF TABLES

Table 1: Principles of IWRM and their applicability to drought risk management..... 14

Table 2: Summary of the commonly used drought indices 16

Table 3: Decile Classification..... 17

Table 4: SPI values (WMO, 2012) 18

Table 5: SWI classes (Mishra & Nagarajan, 2013) 19

Table 6: VCI drought severity classes (Amalo, et al., 2017)..... 22

Table 7: MESA SADC-THEMA Drought Service Products..... 27

Table 8: Satellite data selection criteria used in this study based on spatial, spectral and temporal resolutions, historical record and cost 36

Table 9: Rainfall anomaly percentage classes used in this study 39

Table 10: Example of formatting of data used in this study..... 40

Table 11: Ranks of land cover based on the strenth of correlation between NDVI and rainfall .. 50

Table 12: Ranks and weights of inputs in vulnerabilty determination used in this study 52

Table 13: Probability of drought recurrence defined by this study 70

Table 14: Correlation at each station used in this study 85

LIST OF ACRONYMS

AVHRR	Advanced Very High Resolution Radiometer
CCD	Cold Cloud Duration
CHIRPS	Climate Hazards Group Infrared Precipitation with Stations
CMAP	Centre Merged Analysis of Precipitation
CRU	Climatic Research Unit
CSO	Central Statistics office
DMMU	Disaster Management and Mitigation Unit
DN	Digital numbers
EA	Enumeration Area
ENSO	El Niño/Southern Oscillation
EOS	Earth Observing System
EROS	Earth Resources Observation and Science
EVI	Enhanced Vegetation Index
Fr	Fractional Vegetation Cover
GIS	Geographical Information Systems
GPCP	Global Precipitation Climatology Project
HC	Poverty Headcount
HPRCC	High Plains Regional Climate Centre
IEV	Integrated exposure values
ISFC	Index of Segmentation of Fourier Components
ITF	Inter-Tropical Front
IWRM	Integrated Water Resource Management
LST	Land surface temperature
MESA	Monitoring for Environment and Security in Africa
MODIS	Moderate Resolution Imaging Spectrometer
NDVI	Normalized Difference Vegetation Index
NOAA	National Oceanic and Atmospheric Administration
NRSC	National Remote Sensing Centre
PASG	Percentage Average Seasonal Greenness

PDSI	Palmer Drought Severity Index
PHDI	Palmer Hydrological Drought Index
RCMRD	Regional Centre for Mapping Resource for Development
RIHN	Research Institute for Humanity and Nature
RWSI	Regional Water Stress Index
SMDI	Soil Moisture Deficit Index
SMI	Soil Moisture Index
SPI	Standardized Precipitation Index
SRTM	Shuttle Radar Topography Model
SWI	Standardized Water-Level Index
SWSI	Surface Water Supply Index
T*	Scaled Surface Temperature
TARCAT	TAMSAT African Rainfall Climatology And Time
TCI	Temperature Condition Index
TVDI	Temperature-Vegetation Dryness Index
USGS	United States Geological Survey
VCI	Vegetation Condition Index
WMO	World Meteorological Organisation
WRSI	Water Requirement Satisfaction Index
ZMD	Zambia Meteorological Department

CHAPTER ONE: INTRODUCTION

1.1 Background

Water is major part of life and has significant implications to food security. Hydrological extremes such as droughts and floods are a major threat to social security and can have extensive effects (Kundzewicz & Matczak, 2015). The increasing pressures on water resources from population growth, economic activities and escalating competition between users are compounded by droughts, posing more challenges to socioeconomic and environmental security. Droughts pose a threat to security due to the way they impact society, the economy and the environment. These impacts vary from region to region because societies, economic activities and environments are different around the world. Common impacts of droughts on the society include (but are not limited to) losses of human life, reduced income and increased health problems related to water (National Drought Mitigation Centre, 2019). Economic impacts include loss of money due to crop failure, increased food prices, increased water tariffs and reduced electricity production from hydroelectric power stations (National Drought Mitigation Centre, 2019). Examples of the impacts of drought on the environment comprise of poor soil quality, loss of wetlands, destruction of wildlife habitats and increased pressure on endangered species (National Drought Mitigation Centre, 2019). Ultimately, drought impacts are dynamic and far reaching because water plays a cardinal role in environmental processes, society and the economy. In contemporary times, droughts have been more intense and have lasted longer than usual. This has been partly due to global warming and climate change. Many regions of the world have been experiencing higher air temperatures, drier air and more severe or frequent droughts (The Climate Reality Project, 2016).

Zambia is largely dependent on rain fed agriculture with the largest part of the grain crops produced by small scale farmers. However, insufficient public investment in small scale agriculture has left the country in difficult positions during times of drought (Lekprichakul, 2008). Several droughts have occurred in Zambia for the past 40 years. These droughts have differed in magnitude and some were as a result of El Nino events. The Southern Province has been amongst the hardest hit regions (Relief Web, 2003), despite being one of the largest producers of maize and other crops in the country (Central Statistics Office (CSO), 2015). The province has received considerably lower rainfall compared to the provinces in the north and has been prone to drought (Relief Web, 2003). It is, therefore, important to assess

drought risk in the area. In order to make an assessment of drought using conventional methods, meteorological data is required. However, the Southern Province, and the country at large, have very few meteorological stations, most of which are along the line of rail. Therefore, remote sensing and Geographical Information Systems (GIS) can supplement or provide an alternative. Normalized Difference Vegetation Index (NDVI), remote sensing derived rainfall estimates and drought indices are used to assess drought by analysing the changes in vegetation due to rainfall variations. Several remote sensing drought indices have been developed for monitoring and evaluating drought. The advantages of these indices are that they are not dependent on station-based meteorological data and they offer near real-time measurements over the globe at relatively high resolutions (Chopra, 2006). In a region such as the Southern Province of Zambia, where meteorological stations are scarce and sparsely distributed, such indices offer a feasible alternative to assess drought risk. Therefore, the study was conceived to assess drought risk in the Southern Province of Zambia using remote sensing and GIS.

1.2 Statement of the Problem

There is evidence that Southern Province of Zambia has inadequate infrastructure (weather stations) to perform drought assessments despite experiencing an increased frequency of dry spells in recent times, thus, it is important to explore remote sensing and GIS as an alternative or supplement to weather stations for the evaluation of droughts.

1.3 Main Objectives

The main objective of the study was to assess meteorological and agricultural droughts using remote sensing and GIS and to identify the drought prone areas in the Southern Province of Zambia.

1.3.1 Specific Objectives

The following were the specific objectives:

(i) To determine remotely sensed drought indices in order to characterize meteorological and agricultural drought hazards for the Southern Province of Zambia;

(ii) To investigate the relationship between NDVI based indices and appropriate physical parameters in order to validate the use of remotely sensed drought indices in the assessment of drought for the Southern Province; and

(iii) To identify and outline the drought hotspots in the Southern Province using drought hazard, exposure and vulnerability.

1.3.2 Research Questions

The following are the research questions of the study:

(i) What is the nature of drought hazard in the Southern Province?

(ii) Are there any significant relationships between NDVI based indices and appropriate physical parameters? and

(iii) Which areas are most prone to drought in the Southern Province?

1.3.3 Significance of the study

Drought risk assessment plays a cardinal role in mitigating impacts of water shortages during drought periods. A remote sensing and GIS approach of assessing drought risk over the Southern Province will provide an evaluation of the vulnerability of the Southern Province to drought on a continuous scale and fill in the gaps that exist due to the lack of a well populated meteorological station network. The study will assess the spatial and temporal drought occurrences and identify the drought prone areas within the province by integrating remote sensing drought indices with socioeconomic and biophysical data. The data and information generated will be important in forecasting future droughts and provide water resource managers with data to better plan during periods of water stress.

CHAPTER TWO: DESCRIPTION OF STUDY AREA

This section provides a description of the Southern Province of Zambia. The socioeconomic activities present in the province are described as well as the biophysical nature of the region such as climate, land cover and topography.

2.1 Location and Administration

The Southern Province is located in the southern region of Zambia. It is located between the latitudes 15˚S and 18˚S, and on the longitudes 25˚E and 29˚E (Figure 1) and is bordered by Central, Lusaka and Western provinces. It shares an international border with Botswana, Namibia and Zimbabwe.

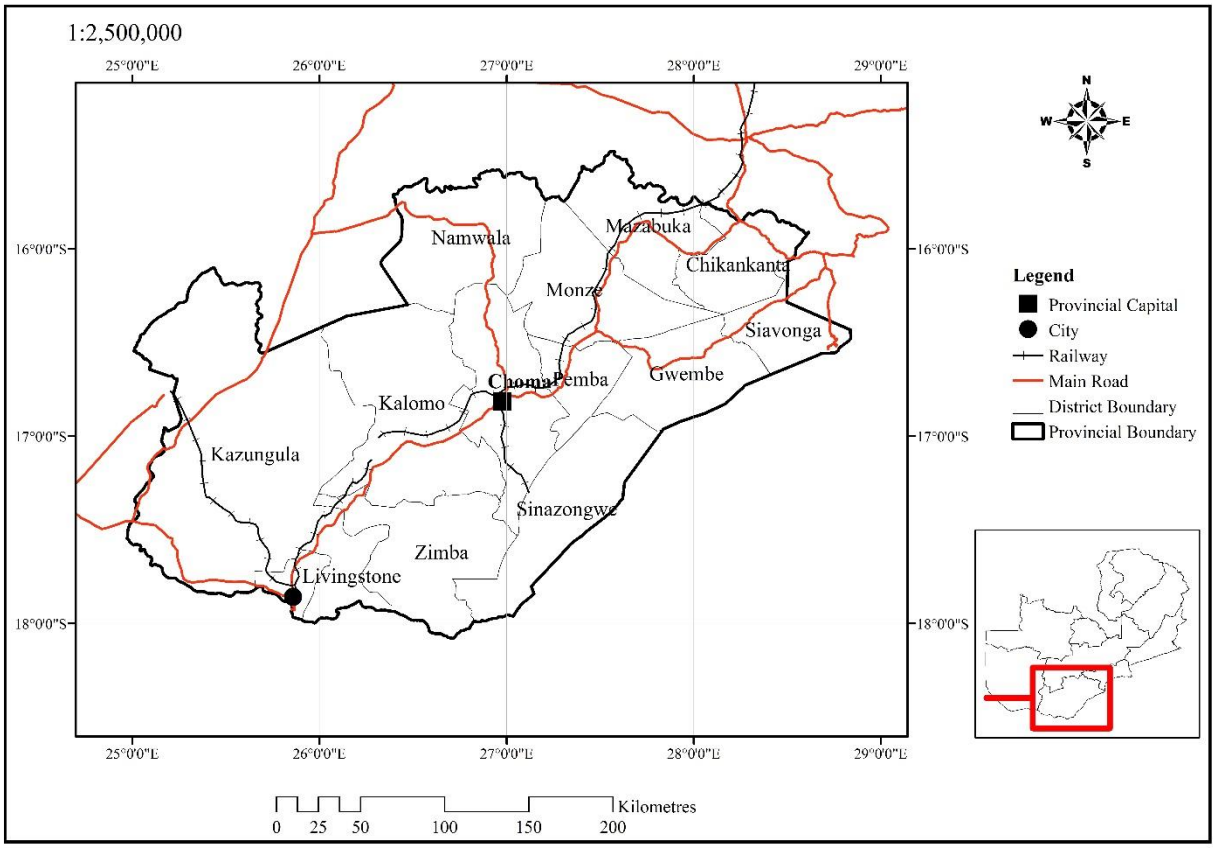

Figure 1: Location of the Southern Province of Zambia, the study area

There are 13 districts in the Southern Province with Choma as the provincial capital. Livingstone is the only city in the province and is the tourist capital of Zambia (Figure 1 above).

2.2 Topography and Drainage

The Southern Province is located in the low lying area of the country with a relief of 1,000 metres above sea level with many valleys. The Gwembe Valley is the lowest area in the province at an elevation of 500 metres above sea level. The main river in the area is the Zambezi, flowing along the southern borders from west to east were it is joined by the Kafue River.

2.3 Weather and Climate

The Southern Province is found in two of the four agro-ecological zones in Zambia. These are Region I and Region IIa (Figure 2). Region I stretches along the western and southern parts of the province, along the Zambezi and the Luangwa Escarpment. The region sits on valleys and plains that are less than 1000 metres above seas level. The region has limited production potential due to poor sandy soils (Famine Early Warning Systems Network (FEWS NET), 2014). Annual rainfall is less than 800 millimetres and the growing season is short. Furthermore, temperatures are relatively higher than other places in the country. The region is most suitable for small scale farming of drought resistant crops such as millet, sorghum, sesame seed and cotton (FEWS NET, 2014).

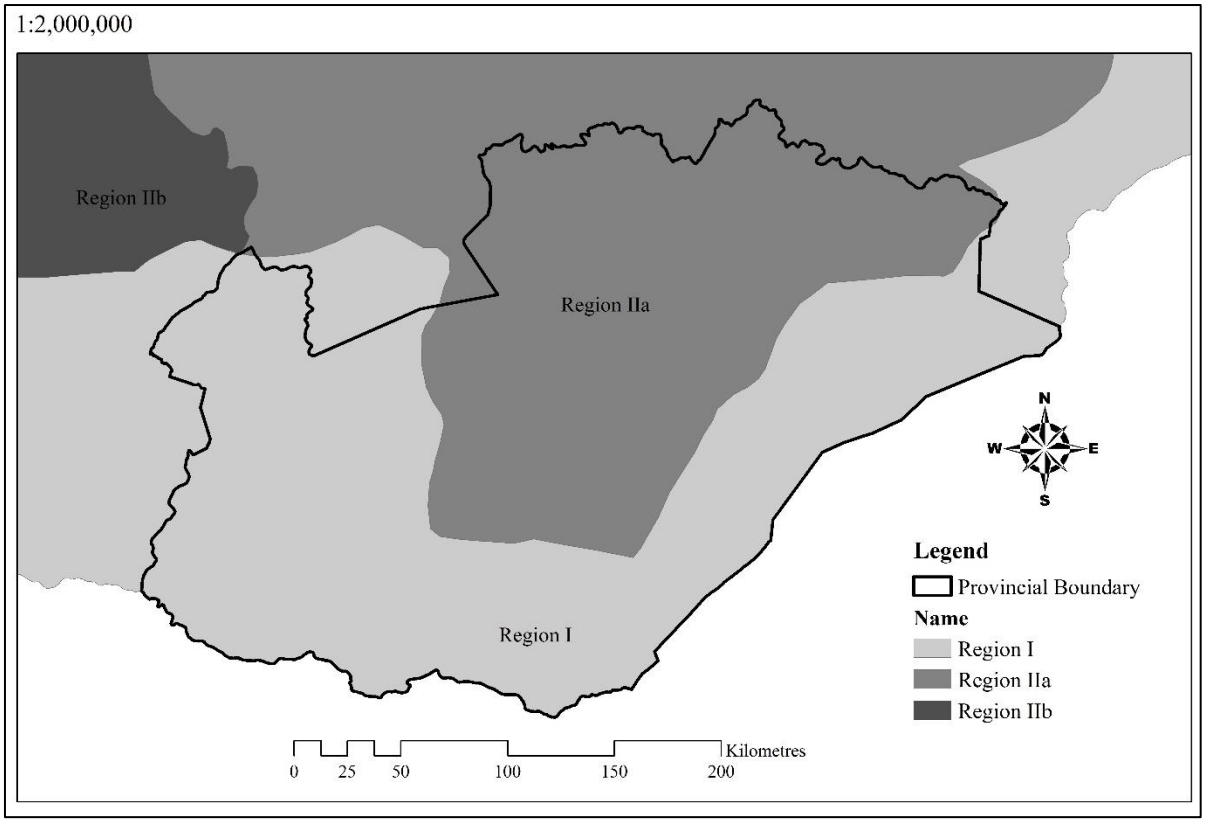

Figure 2: Agro-ecological zones of the Southern Province of Zambia, modified from FEWS NET (2014)

Agro-ecological Region II is at the centre of the province. The region sits on a plateau and altitudes vary from 1000 to 1400 metres above sea level. Annual rainfall is 800 to 1000 millimetres and the growing season ranges from 120 to 160 days, which supports growth of medium to long-term crop varieties (FEWS NET, 2014). The region is divided into two, Region IIa and Region IIb. The Southern Province is only covered by Region IIa. Along with the central and eastern plateaus, the southern plateaus are considered to have the best agricultural potential in Zambia because the land is suitable for the growth of a diversified base of primarily rain-fed crops and livestock production (FEWS NET, 2014). The land is laid with fertile soils that support maize, wheat, soya beans and tobacco.

There are eleven meteorological stations in the Southern Province (Figure 3). Of the eleven, six are automatic and five are manual (Appendix 1). The automatic meteorological stations became operational in 2013 and have insufficient historical data. Therefore, the study relied on data from the manual stations. All eleven of the stations are operated and run by the Zambia Meteorological Department (ZMD).

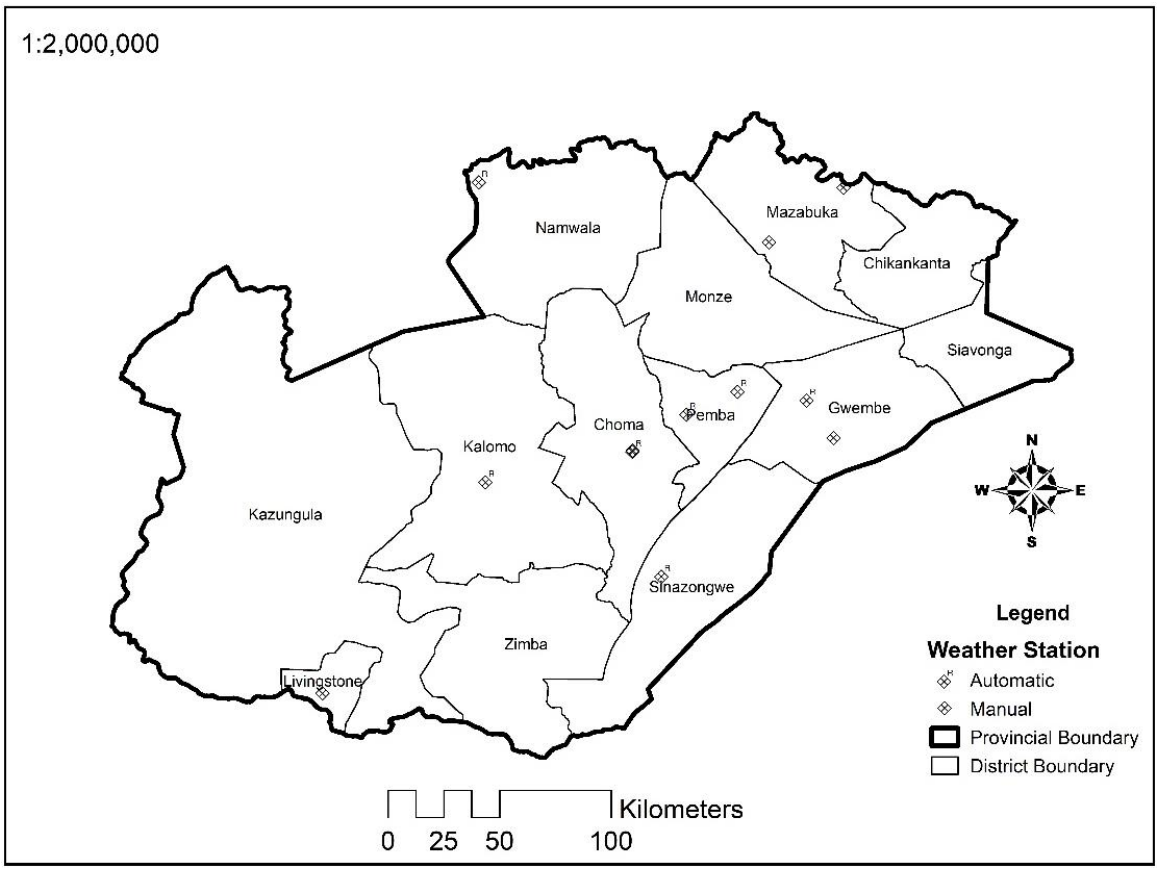

Figure 3: Locations of Meteorological Stations in Southern Province of Zambia

2.4 Land Cover

The Regional Centre for Mapping Resource for Development (RCMRD) developed land cover maps of the entire Zambia for the years 2000, 2010 and 2014. The maps were developed for the Zambia Forestry Department under the United Nations Programme on Reducing Emissions from Deforestation and Forest Degradation (UN-REDD). The land cover maps had two schemes that is Scheme I and Scheme II. Scheme I had six classes whilst Scheme II had ten. For this study, the 2014 Scheme I map was used for land cover (Figure 4).

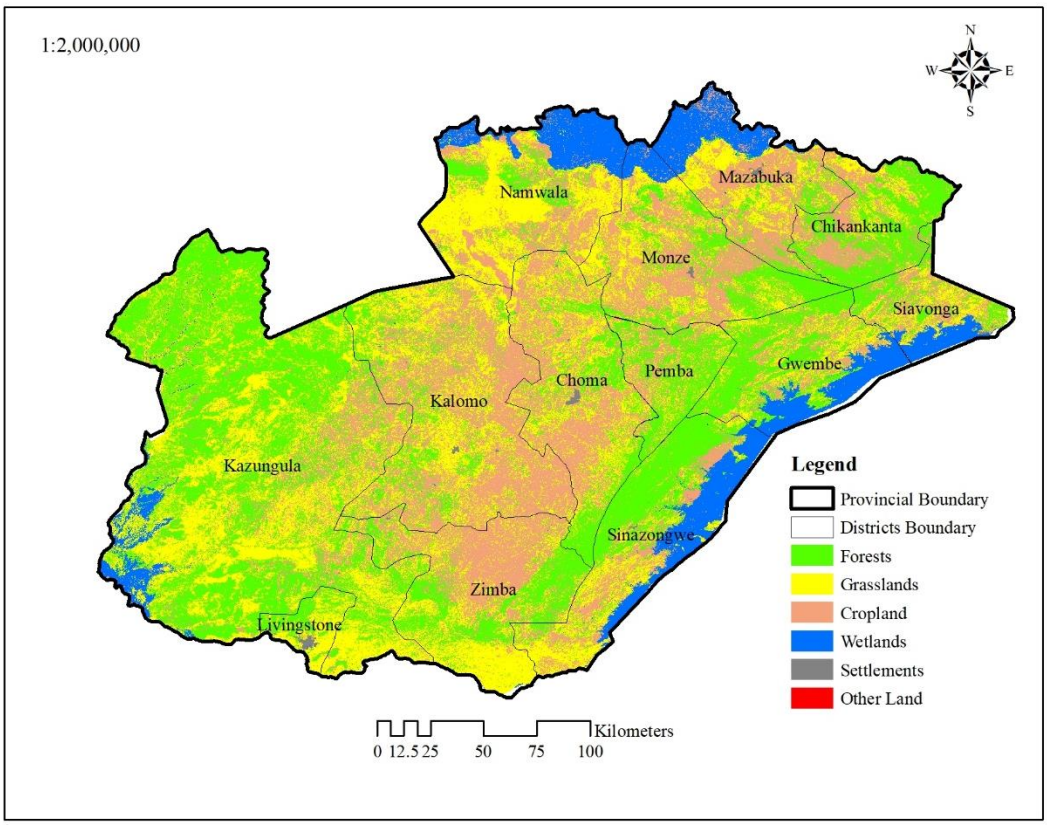

Figure 4: Zambia Forestry Department 2014 Scheme I Landcover of Southern Province

The major land cover classes of the Southern Province are Forests, Grasslands, Cropland, Settlements and Otherlands.

2.5 Demography, Economy and Livelihood

As of 2010, there were 1,589,926 people in the Southern Province (CSO, 2012). About 49% of the population were males whilst 51% were female. The annual growth rate was 2.8% per annum. The population density of the province was 18.6 people per square kilometre in 2010, an increase from 14.2 people per square kilometre in 2000. The main languages spoken were English and Tonga.

Agriculture is the biggest industry in the region. The majority of people are small-scale farmers and the most grown crop is maize (Figure 5). Moreover, there are a number of commercial farms in the province such as the Nakambala Sugar Estates in Mazabuka. Secondary and ancillary industries of agriculture are also present.

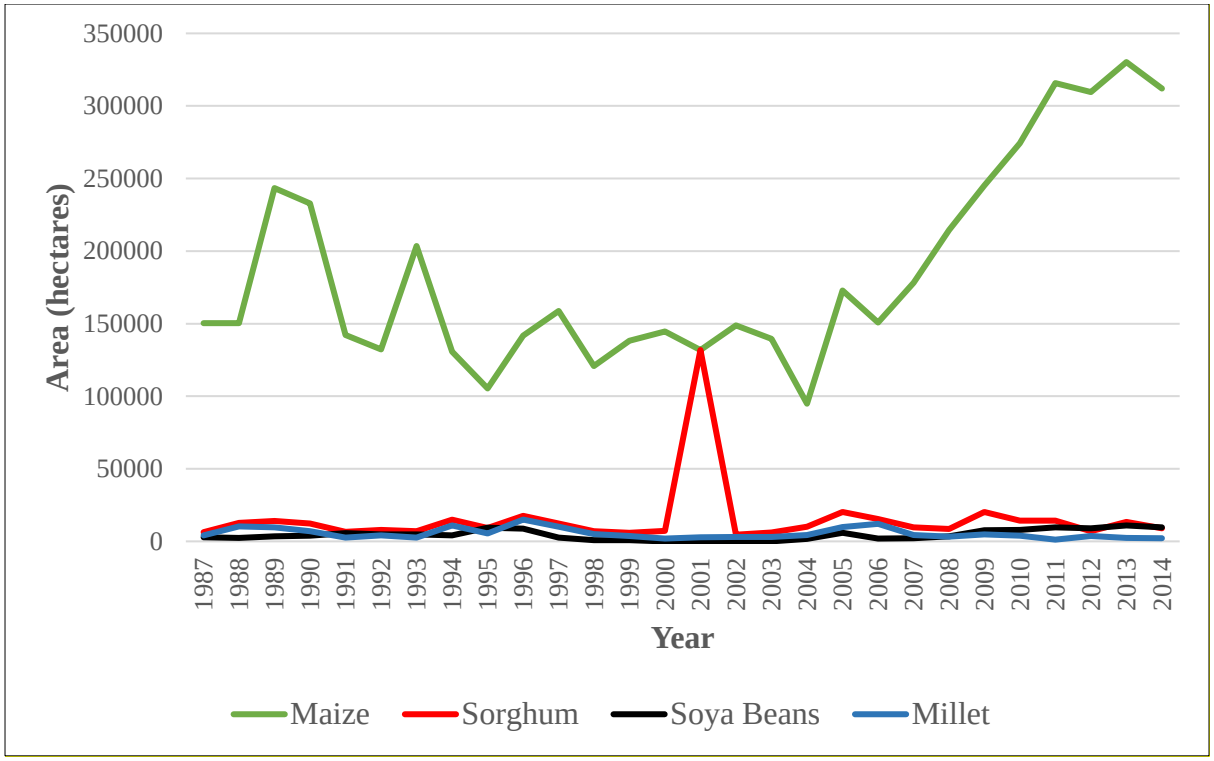

Figure 5: Area planted of maize, sorghum, millet and soya beans in Southern Province from 1987 to 2014 (CSO, 2015).

Other economic activities include fishing on Lake Kariba, power generation at the Kariba North Bank Power Station in Siavonga and Kafue Gorge Lower in Chikankata and tourism in Livingstone.

FEWS NET (2014) zoned Zambia into 21 livelihood zones and created the Livelihood Zoning Plus Product (Appendix 2). The product showed that there are five livelihood zones in the Southern Province (Figure 6). These are the ZM02 (Southern cereal, livestock and timber), ZM07 (Kafue plain maize, cattle and fishing), ZM08 (commercial rail line maize, livestock and cotton), ZM09 (Southern plateau cattle, maize and tobacco) and ZM10 (Zambezi valley agro-fisheries). ZM02 is located in the northern part of Kazungula and falls under agro-ecological Region I. The population density is 10 inhabitants per square kilometre and the main economic activities include crop and livestock production, formal employment related to timber and tourism, timber, handicrafts related to tourism, fishing and the sale of wild fruits (FEWS NET, 2014). ZM07 is located in the extreme north of the province, in the northern parts of Namwala and Mazabuka. In the province, the zone is found in agro-ecological Region II. The zone is sparsely populated with only 3 people per square kilometre

and the main forms of livelihood revolve around cattle rearing, crop production and fishing (FEWS NET, 2014).

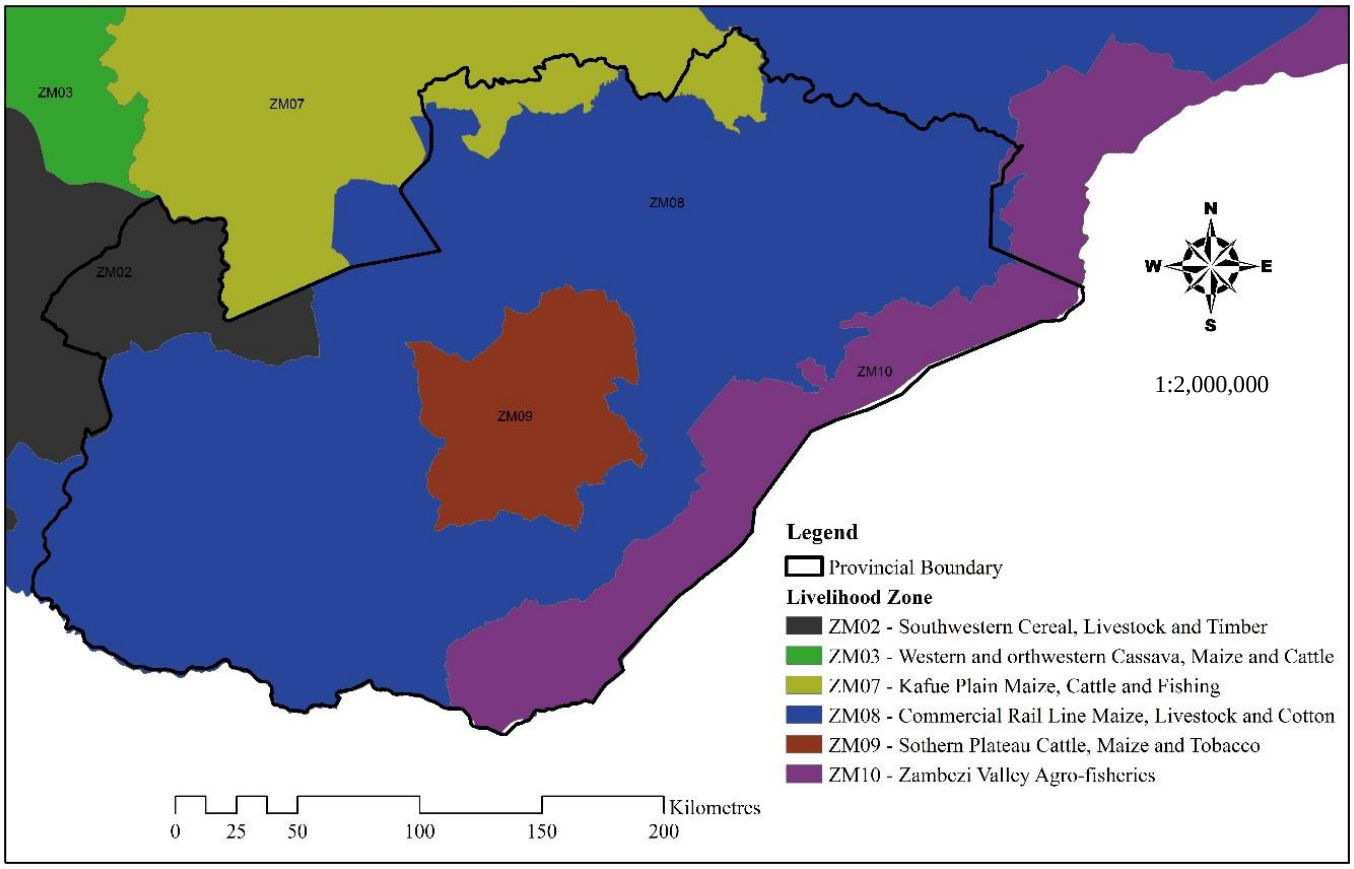

Figure 6: Livelihood zones of the Southern Province after FEWS NET (2014)

Livelihood zone ZM08 covers the majority of the province extending from Kazungula and Livingstone, through Monze and Pemba to Mazabuka and Chikankata. The zone is located in two agro-ecological regions (I and IIa) and the main economic activities are rainfed and irrigated agriculture using manual labour or animal traction, with a population density of 19 people per square kilometre (FEWS NET, 2014). Located between Kalomo and Choma, ZM09 is moderately populated with 13 people per square kilometre. The zone is found in agro-ecological Region IIa and the main forms of livelihood are commercial agriculture using draft power or by tractor and the production of tobacco (FEWS NET, 2014). Lastly, ZM10 is located along the shores of Lake Kariba covering Gwembe, Siavonga, Sinazongwe and Zimba districts. The zone is found in agro-ecological Region I and has a high population density of 26 inhabitants per square kilometre (FEWS NET, 2014). The main economic activities in the zone is fishing, despite the presence of livestock and arable farming.

CHAPTER THREE: LITERATURE REVIEW

A significant part of the arable land in Zambia is found in the semi-arid regions. With only three percent under irrigation, the country critically depends on rain fed subsistence agriculture (Lekprichakul, 2008). Coupled with insufficient investment, the country finds herself in a difficult situation during times of drought.

Agriculture accounts for 67% of the labour force in the country and contributes 18-20% of GDP (CSO, 2011). It is also a principle source of income for the majority of women in rural areas. Therefore, drought is bound to have detrimental effects on the welfare of the country such as a drop in maize yield and livestock production.

3.1 Definitions of Drought

Drought does not have a worldwide definition. Definitions are region specific due to different climatic characteristics as well as different ecological and socio-economic factors between regions. Nonetheless, some common definitions of drought are:

(i) A drought can be defined as a deficiency in rainfall over a prolonged period, usually a season or more, that results in a water shortage causing adverse impacts on vegetation, animals and/or people (National Weather Service, 2012)

(ii) "Drought is an interval of time, generally of the order of months or years in duration during which the actual moisture supply at a given place rather consistently falls short of the climatically expected or climatically appropriate moisture supply." (Palmer, 1965)

(iii) "Drought can be conceived as a temporary lack of water, which is, necessarily but not exclusively, caused by abnormal climate and which is damaging to an activity, a group, or the environment" (Cap-Net, 2015).

(iv) In 1965, the Director of Commonwealth Bureau of Meteorology suggested a general definition of drought as "Severe Water Shortage".

The common theme is that there is a shortage of water for a given period of time. Drought differs to other hazards in that it is creeping and develops slowly.

3.2 Types of Drought

There are four main types of droughts, namely, the meteorological, agricultural (vegetation), hydrological and socioeconomic drought (Figure 7). Meteorological droughts occur where rainfall is reduced by a defined degree from the normal in a given area. Meteorological droughts are natural occurrences that occur as a result of climatic events. The other forms of drought are as a result of interaction between meteorological droughts and human activity (Meshu & Berhan, 2013). Agricultural droughts link various characteristics of meteorological (or hydrological) droughts to agricultural impacts, and are focused on precipitation shortages, differences between actual and potential evapotranspiration and soil water deficits. Hydrological drought associated with deficiencies of surface water and/or groundwater due to shortfall of precipitation. Socio-economic droughts are associated with supply and demand of some economic good with elements of meteorological, hydrological, and agricultural droughts.

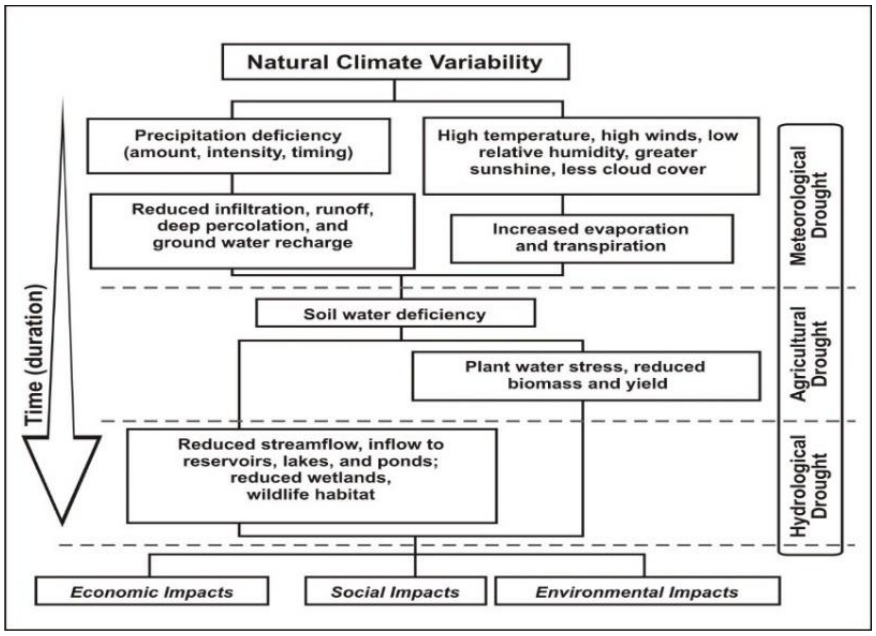

Figure 7: Relationship between different types of droughts (NDMC, 2006)

3.3 Drought Hazard, Vulnerability and Risk

Cap-Net (2015) described drought risk as dependent on hazard and vulnerability. On their own, drought hazards do not form disasters. Disasters are mainly described in terms of the

harmful impacts hazards have had on society, that is, the adverse impacts on lives; property and infrastructure; the environment; and the cost of mitigation (Cap-Net, 2015). A relationship exists between the ability of a society to withstand the impacts of drought hazards with their own resources and drought risk. Therefore, drought risk is the sum of two elements, vulnerability and hazard (Cap-Net, 2015). Similarly, Shahid (2008) defined risk as the likelihood of damaging effects, or expected losses as a result of the interactions between drought hazards and vulnerability.

The Joint Research Centre (2018) identified the three components of global drought risk analysis as a combination of the hazard, the exposure and the vulnerability. The hazard was characterised as the magnitude of hydro-meteorological deficit and the required data were meteorological, hydrological and/or biophysical indicators. The exposure was the extent to which elements and assets were subject to a drought hazard and the required data were human population, infrastructure, economic activities and/or ecosystems. Lastly, vulnerability was characterised as the sensitivity of exposed elements to the negative effects of droughts and the required data were composite indicators that include social, economic, environmental and/or infrastructural components. Overall, drought risk was characterised as possible damages and losses from drought to defined assets (Joint Research Centre, 2018). The Center for International Earth Science Information Network (CIESIN) (2015) described the Spatial Index Approach used to determine vulnerabilty hotspots of disasters. The approach involved the development of vulnerability scores of 0 to 100, where 0 was least vulnerable and 100 the most. In this context, vulnerability consisted of exposure, sensitivity and adaptive capacity. Each of the three components was also scored 0 to 100 so as to make them comparable.

Drought hazard was determined and assessed using the remote sensing drought indices. These indices were in types, meteorological drought indices (Standardised Precipitation Index (SPI) and rainfall anomaly percentage) and agricultural drought indices (Vegetation Condition Index (VCI) and Soil Moisture Index SMI)). Drought exposure was determined using two elements, human population (CSO, 2012) and land cover (FD & FAO, 2016). Vulnerability was the summation of socioeconomic indicators (De la Fuente, et al., 2015) and physical data. Socioeconomic indicators were at ward level and included poverty Head Count (HC) ratio and the number of poor. Physical data included rainfall variability (spatial and temporal) and terrain (slope).

Poverty HC ratio, or poverty incidence is the proportion of the population whose income is under a defined poverty line (Development Initiatives, 2016). De la Fuente, et al. (2015) evaluated poverty based on the two poverty lines set by the Central Statisticts Office (CSO) during the 2010 livelihood survey. The extreme poverty line was set at ZMK96, 366 (ZMW96.37) which was the cost of the food basket at the time. The moderate poverty line was set at ZMK146,009 (ZMW146.01) and was obtained by dividing the food poverty line by its corresponding food budget ratio (De la Fuente, et al., 2015). At ward level, HC was the percentage of people living under the poverty lines within the ward. The number of the poor was the total number of people living under the poverty line in each ward. Both inputs can be used to assess vulnerability because HC was a relative take to the number of poor compared to the entire population of the ward.

3.4 Principles of IWRM and Drought

IWRM is process which promotes the coordinated development and management of water, land and related resources, in order to maximize the resultant economic and social welfare in an equitable manner without compromising the sustainability of vital ecosystems (Cap-Net, 2015). An integrated approach to water management offers opportunities to drought risk management by reducing exposure and vulnerability to droughts. IWRM has become the dominant approach to water management. Based on its four principles, it offers water managers an opportunity to reduce exposure and vulnerability to droughts by managing the entire water cycle, rather than using old uncoordinated sectoral approaches that alter water systems to benefit humankind. The four principles of IWRM are applicable to drought risk management (Table 1). The principles can be applied to reduce exposure and vulnerability to drought as a holistic approach is taken to water resources management. The resource is evaluated based on the ability to sustainably contribute to economic goals, social equity and environmental sustainability.

Table 1: Principles of IWRM and their applicability to drought risk management (Cap-Net, 2015)

IWRM principle	**Applicability to drought risk management**
Water is a finite and vulnerable resource	Using participatory evaluation of water allocations regimes under different water availability conditions and putting in place conditional water use licenses that depend on the available water can dampen the conflict around water uses during times of stress.

Participatory approach	This calls for the involvement of key stakeholders in the planning cycle, implying engagements of organisations tasked with drought planning and management. Institutions such as disaster teams or agencies and others key to drought risk management should be involved in risk preparedness and mitigation
Role of women	Since the impacts of drought differ for the different genders, the inclusion of women in capacity building and water management would lead to more relevant planning and actions. There are many parts of the world where women have direct responsibility for household water security and food security.
Social and economic value	This principle accepts that water has an economic value and should be priced and allocated as such. In times of drought, appropriate pricing that reflects that the resource is in short supply can drive behaviour change that reduces wastages by domestic users, agriculture and industry. It also incentivises the development and adoption of water use efficient technology in the home, in agricultural fields and in industry. However, the same principle states that water is a social good and implies that access to basic amount of water should be promoted for good health and dignity. This is an important principle to be applied to emergency situations as it places the burden on the government to protect its citizens.

3.5 Conventional Drought Indices

Many drought indices have been developed across the globe for drought assessment and monitoring. These range from local and regional scales to global scale. Drought indices combine a large amount of data, such as precipitation, evapotranspiration, snowfall, streamflow and other water supply indicators, into a single number to monitor drought severity and determine how the climate has deviated from the normal over a given period (Narasimhan & Srinivasan, 2005). In this section, a brief review of the most commonly used drought indices is given.

There are many drought indices such as the Palmer Drought Severity Index (PDSI) and Palmer Hydrological Drought Index (PHDI) (Palmer, 1965), Standardized Precipitation Index (SPI) (Mckee, et al., 1993) and the Surface Water Supply Index (SWSI) (Doesken, et al., 1991), which are used extensively in water resources management, drought assessment,

monitoring and forecasting. However, each index has its own weaknesses and strengths (Table 2).

Table 2: Summary of the commonly used drought indices (Mu, et al., 2013)

Indices	Description	Strength	Weakness	Citation
Deciles	A simple calculation by grouping precipitation into deciles distributed from 1 to 10. The lowest value indicates conditions drier than normal and the higher value indicates conditions wetter than normal.	Accurate statistical measurement of drought response to precipitation, and providing uniformity in drought classifications.	Accurate calculations require a long climatology record of precipitation.	Gibbs and Maher (1967)
SPI	A simple calculation based on the concept that precipitation deficits over varying periods or time scales influence ground water, reservoir storage, soil moisture, snowpack, and streamflow.	Computed for flexible multiple time scales, provides early warning of drought and help assessing drought severity.	Precipitation is the only input data. SPI values based on long-term precipitation may change. The long time scale up to 24 months is not reliable.	McKee et al. (1993)
PDSI	Calculated using precipitation, temperature, and soil moisture data. Soil moisture algorithm has been calibrated for relatively homogeneous regions.	The first comprehensive drought index used widely to detect agricultural drought.	PDSI may lag emerging droughts. Not effective for mountainous areas with frequent climatic extremes, or in winter and spring.	Palmer (1965)
PHDI	Derived from PDSI to quantify long-term impact from hydrological drought.	Same as PDSI, but more effective to determine when a drought ends.	PHDI may change more slowly than PDSI.	Palmer (1965)
SWSI	Developed from the Palmer index by combining hydrological and climatic features.	SWSI takes into account reservoir storage, streamflow, snowpack, and precipitation. Effective under snowpack conditions.	SWSI is difficult to compare between different basins. SWSI cannot detect extreme events effectively. Not a suitable indicator for agricultural drought.	Doesken et al (1991)

3.5.1 Deciles

Deciles (Gibbs & Maher, 1967) are used to assess meteorological drought and are a technique developed that divides the distribution of occurrences over a long-term record of rainfall into tenths of the distribution (Sivakumar, et al., 2010). These distributions are ranked as deciles with the first comprising of rainfall amounts in which the lowest 10% of values are not

exceeded, and the fifth is the median (WMO and GWP, 2016). Deciles can be calculated at daily, weekly, monthly, seasonal and annual intervals. The methodology is fairly simple and flexible as only a single variable is considered (WMO and GWP, 2016). Deciles are categorised to five classes, as shown in Table 3:

Table 3: Decile Classification (Gibbs & Maher, 1967)

Deciles	Description	Class
1 and 2	Much below normal	Lowest 20%
3 and 4	Below normal	Next lowest 20%
5 and 6	Near normal	Middle 20%
7 and 8	Above normal	Next highest 20%
9 and 10	Much above normal	Highest 20%

3.5.2 Standardised Precipitation Index (SPI)

Standardised Precipitation Index (SPI) is a meteorological drought index. It was developed by McKee et al. in 1993 for the purpose of assigning a single value to the precipitation that can be compared across regions with different climates. SPI is defined as the difference of precipitation from the average for a defined time period divided by the standard deviation, where the average and standard deviation are determined from past records (Mckee, et al., 1993). It is expressed as:

$$SPI = \frac{(P_i - P_m)}{\sigma} \quad (1)$$

Where $P_i$is the seasonal precipitation, P_m is the long-term mean and σ is the standard deviation of the long-term record.

For any location, the calculation of SPI is based on long term precipitation records. McKee et al. (1993) first calculated the index for 3, 6, 12, 24 and 48 months, representing precipitation as single values where negatives represented drought and positives sufficient moisture (Table 4). SPI determines magnitude and duration of droughts, as well as the probability of emergence droughts (Hunt, et al., 2008). SPI quickly responds to rainfall anomalies making it ideal for drought detection.

Table 4: SPI values (WMO, 2012)

SPI Value	Interpretation
2.0+	Extremely wet
1.5 to 1.99	Very wet
1.0 to 1.49	Moderately wet
-0.99 to 0.99	Near normal
-1.49 to -1.0	Moderately dry
-1.99 to -1.5	Severely dry
-2 and less	Extremely dry

The disadvantage of SPI is that precipitation is not normally distributed over cumulative periods of 12 months or less. However, this can be overcome by transforming the distribution using a Gaussian function. (Mckee *et al.* 1993). Another disadvantage is that SPI only has precipitation as input data. Despite SPI being a conventional drought index, it can be derived using remote sensing through the use of remote sensing rainfall estimates.

3.5.3 Palmer Drought Severity Index (PDSI) and Palmer Hydrological Drought Index (PHDI)

Palmer Drought Severity Index (PDSI) was introduced by Palmer (1965). He based the index on supply and demand considering daily precipitation, temperature and the available holding capacity of the soil. PDSI is a meteorological drought index, which follows the water balance equation and the main goal is to provide standardised measurements of moisture for comparison between locations and between months. A two layer soil moisture model is used to compute the index. It is assumed that runoff starts only when both layers are saturated. The range of PDSI is between -6 (extremely dry) and +6 (extremely wet).

Palmer (1965) designed PDSI specifically for semi-arid and sub humid regions and suggested extrapolation beyond these conditions may lead to impractical results. Therefore, PDSI is not applicable globally as some regions are so close to deserts that there is no point in analysing drought severity using the PDSI. Other regions have high levels of precipitation such that abnormal dryness rarely occurs. The index also requires strict adherence to the procedures Palmer (1965) described. Any deviation from the methods described would result in values incompatible with the equation. Similar to other traditional drought indices, the spatial resolution of PDSI is dependent on the density and distribution of meteorological stations

(Ganesh, 2013). Lastly, PDSI does not consider the influence of soil type, land use and management practices in calculating runoff (Ganesh, 2013).

Palmer Hydrological Drought Index (PHDI) is a hydrological drought index that utilises a modification of PDSI to evaluate long-term moisture anomalies that affect streamflow, groundwater and water storage (Mishra & Singh, 2012). The index has the capability to anticipate when a drought will end based on the rainfall required by using a ratio of moisture received to moisture needed to terminate a drought (Mishra & Singh, 2012). Similar to PDSI, PHDI ranges from -6 to +6 where negative values represent dry spells and positive values wet spells.

3.5.4 Standardised Water Level Index (SWI)

Standardised Water Level Index (SWI) is a hydrological drought index. It was developed to scale the groundwater recharge deficit. SWI is defined as:

$$SWI = \frac{(W_{ij} - W_{im})}{\sigma} \qquad (2)$$

Where W_{ij} is the seasonal water level for the i^{th} well and j^{th} observation, W_{im} its seasonal mean and σ is its standard deviation. SWI is divided into four classes (Table 5). Positive anomalies correspond to drought and negative anomalies correspond to normal condition because groundwater level is measured down from the surface (Mishra & Nagarajan, 2013).

Table 5: SWI classes (Mishra & Nagarajan, 2013)

Drought Classes	Criterion
Extreme drought	SWI>2.0
Severe drought	SWI>1.5
Moderate drought	SWI>1.0
Mild drought	SWI>0

3.6 Remote Sensing Drought Indices

Conventional drought indices assimilate data from precipitation, stored soil moisture and/or water supply but do not express much local spatial detail and are only valid for a single location when calculated at one meteorological station (Chopra, 2006). Remote sensing indices assimilate surface features and have more spatial detail. Several remote sensing

drought indices rely on changes in vegetation due to rainfall variations and water stress. Common remote sensing drought indices include NDVI, VCI, Temperature Condition Index (TCI), Soil Moisture Index (SMI) and Temperature Vegetation Dryness Index (TVDI).

3.6.1 Normalised Difference Vegetation Index (NDVI)

Normalised Difference Vegetation Index (NDVI) is a numerical indicator that uses the near infrared and red bands to assess whether the feature being observed has live green biomass or not (Thenkabail, et al., 2004). The index is used for various applications ranging from crop yield estimation to forest assessments. The underlying principle of NDVI is that healthy green plants will absorb a large amount of energy in the red band and reflect away a large portion of energy in the near infrared band (Figure 8). Inversely, unhealthy green plants reflect away a large amount of energy in the red band and absorb more infrared energy. This behaviour of green plants across the electromagnetic spectrum is used to extract information on the health of green plants by focusing on the red and near infrared bands. The bigger the difference observed between the near infrared band and the red band, the more green plants there are. Therefore, NDVI is defined by equation 3:

$$NDVI = \frac{NIR-RED}{NIR+RED} \quad (3)$$

Where *NIR* is the reflectance in the near infrared band and *RED* is the reflectance in the red band. NDVI is a dimensionless index and varies from -1 to 1, where a value of -1 represents the poorest or absence of greenness (chlorophyll) and 1 represent the richest and greenest.

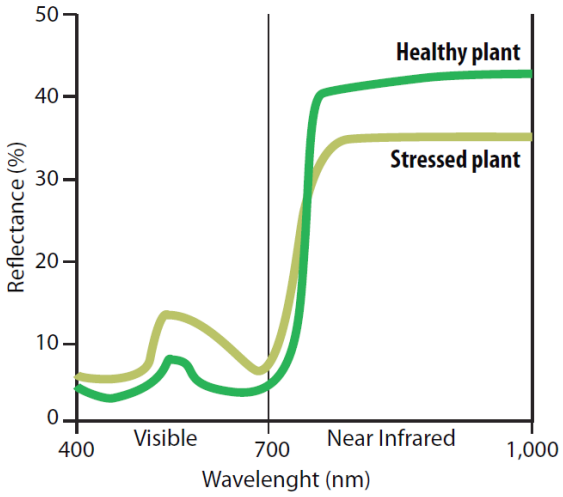

Figure 8: Typical reflectance spectrum of a healthy and a stressed plant(Govaerts & Verhulst, 2010)

NDVI is the most commonly used vegetation index in remote sensing. However, it only uses two bands and is not sensitive to the soil background reflectance at low vegetation cover. It has a delayed response to drought because of a lagged vegetation response to developing rainfall deficits due to residual moisture stored in the soil (Thenkabail, et al., 2004).

NDVI has been successfully used to identify stressed and damaged crops and pasture in homogeneous terrains (Chopra, 2006). Studies by Unganai and Kogan (1998) showed a correlation between NDVI derived from NOAA-AVHRR satellites, rainfall, vegetation cover and corn yield ratios in Southern Africa.

3.6.2 Vegetation Condition Index (VCI)

Vegetation Condition Index (VCI) is an indicator of the status of vegetation cover as a function of NDVI minimum and maximum of an area over several years. It is defined using equation 4 (Kogan, 1997):

$$VCI = 100 * \frac{(NDVI_i - NDVI_{min})}{(NDVI_{max} - NDVI_{min})} \quad (4)$$

Where $NDVI_i$ is the NDVI of the year of interest, and $NDVI_{min}$ and $NDVI_{max}$ are the minimum and maximum NDVI respectively, for each pixel over the period of interest from a multi-layered temporal NDVI data cube.

VCI is divided into four classes ranging from 0 to 100 (Table 6). All values below the 40 threshold represent droughts of different severity. All values above 40 indicate the absence of drought.

Table 6: VCI drought severity classes (Amalo, et al., 2017)

Severity class	**Values**
Extreme Drought	< 10
Severe Drought	< 20
Moderate Drought	< 30
Mild Drought	< 40
No Drought	> 40

VCI was used successfully to assess drought and showed a strong correlation with agricultural production in the United States of America, South America and Africa (Kogan, 1997). VCI was also used to assess the feasibility of area-yield drought insurance in Zimbabwe (Makaudze & Miranda, 2008). Unganai and Kogan (1998) used VCI for crop yield estimation, and to detect, track and map drought in Southern Africa.

A limitation of VCI is that it does not account for the condition of the soil. It also indicates a drought each time crops are stressed even though the cause of the stress is not a shortage of water.

3.6.3 Soil Moisture Index (SMI)

Soil moisture varies in space and time, which makes it difficult to obtain measurements over wide areas. However, remote sensing has the capability to infer the availability of moisture in soil. The derivation of soil moisture from satellite data has been of special interest for many researchers since 1978 (Kasim & Usman, 2016). Therefore, the SMI was developed by the High Plains Regional Climate Centre (HPRCC) as a user-friendly index that can detect a quick onset of agricultural drought by demonstrating the observed dryness of soil relative to the ability of a plant to extract water as scaled over the range from field capacity to wilting point (Hunt, et al., 2008). SMI is directly linked to rainfall as it is defined through soil water (Hunt, et al., 2008).

The basis of SMI is the empirical parameterization of the relationship that exists between land surface temperature (LST) and NDVI (Potic, et al., 2017). It is defined by the equation 5 (Potic, et al., 2017):

$$SMI = \frac{(LST_{max} - LST)}{(LST_{max} - LST_{min})} \quad (5)$$

Where LST_{max} and LST_{min} are the maximum and minimum land surface temperatures for a specific NDVI and LST is land surface temperature of a pixel for a given NDVI.

SMI is determined using the triangle method, which emerged in the 1990's (Kasim & Usman, 2016). The method relies on the relationship between LST and NDVI when the two are plotted against each other (Figure 9). The underlain principal is that surface radiant temperature is sensitive to and dependant on soil surface wetness, and hence, spatial and temporal variations of soil moisture are reflected in LST (Kasim & Usman, 2016).

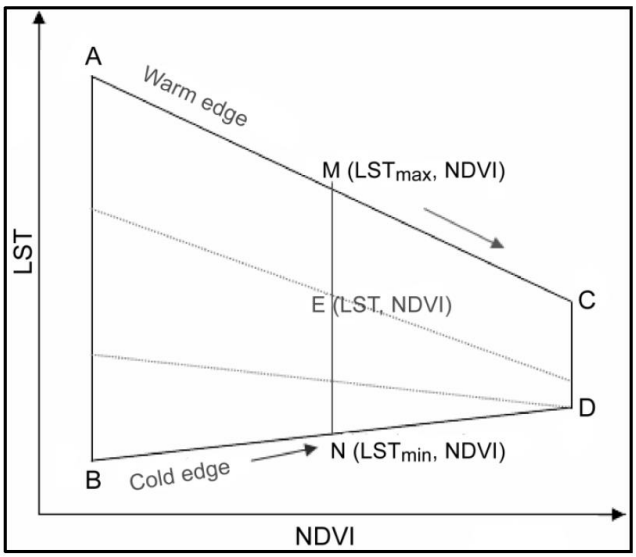

Figure 9: Typical scatterplot in NDVI-LST space (Parida et al. 2008 in Potic, et al., 2017)

Other scholars have preferred to scale NDVI and surface radiant temperature. NDVI has been transformed to Fractional Vegetation Cover (Fr) which is scaled from 0 to 1, whilst surface radiant temperature is rescaled to a range of 0 to 1 (T*). The advantage of this is that both axes are scaled 0 to 1 regardless of the net radiation or ambient air temperature (Carlson, 2007). Therefore, 0 becomes the well-watered vegetation (T_{min}) and 1 the dry and bare soils (T_{max}). Scaling also reduces the sensitivity of Fr and T* to atmospheric correction, helps isolate cloud and water pixels which lie outside the triangle, allows comparison of pixel data from different days and seasons within the same framework (Carlson, 2007).

The key importance of using the triangle method is that it does not require ancillary atmospheric and surface data (Kasim & Usman, 2016). On the other hand, the main limitation of the triangle method is that the identification of the triangle in the scatter plot requires a flat

surface and a large number of pixels over an area with wide range of soil moisture and vegetation cover (Carlson, 2007). This makes the method more effective in higher resolution imagery such as Landsat. However, across a large space, such as the Southern Province, there are a sufficient number of pixels to define the triangle. Another limitation of the triangle method is hat subjectivity is required to determine the vegetation limits of bare soil and full vegetation cover. Lastly, it is necessary to mention that remotely sensed measurements based on the thermal signal only has the capability of sensing soil moisture only over the top centimetre or two of a bare soil surface (Carlson, 2007). However, the values achieved are appropriate as they give a relative indication of soil moisture in an area.

The advantage of SMI over conventional means of monitoring soil moisture is that it has spatial and temporal continuity, which benefits many applications. In situ measurements cannot provide continuous data because of financial and physical constraints (Leeuwen, 2015). Compared to microwave methods of assessing soil moisture, optical sensors offer higher resolution imagery than passive microwave sensors and higher temporal resolutions than strong sensitive active microwave sensors (Leeuwen, 2015).

3.7 Relationship between NDVI and Precipitation as an Indicator of Drought

Remote sensing has been used extensively to detect, monitor, track and assess droughts. In several studies, NDVI based drought indices have been utilised in drought risk assessment. Cardinal to this has been the relationship between NDVI and precipitation. It was important to establish a correlation between rainfall and vegetation in order to validate the use of remote sensing as a tool for assessing drought. Several studies have established a correlation between NDVI and rainfall in different parts of the globe. The relationship between vegetation and precipitation varies spatially across the globe (Chopra, 2006) due to different species of plants having different requirements of water and different tolerance levels to water stress. Furthermore, rainfall levels differ from one region to another. Hence, one of the aims of this study was to establish a correlation between the condition of local vegetation and rainfall of the Southern Province in Zambia. This was cardinal in assessing the drought risk of the area as vegetation condition and amount are a function of environmental variables (Chopra, 2006).

A study was done on vegetation change and its relation to rainfall in the Kol River Basin in the southwest semi-arid region of Iran (Damizadeh, et al., 2001). The study utilized cloud

free NOAA images over the period 1995 to 1997. NDVI was transformed into 10 day images using maximum 10 day composite technique. A varying degree of correlations were found. The correlation between vegetation and precipitation was investigated in different land units and the results of the study displayed a varying of correlations. The correlation was strongest in alluvial and flood plain mapping units. NDVI showed the highest dependence on rainfall in previous months using the multi-variable relationship.

The relationship between NDVI and extracted rainfall from the Global Precipitation Climatology Project (GPCP) was investigated in Central Africa between latitudes 15˚S and 20˚N, and longitudes 0˚E and 31˚E (Rousvel, et al., 2013). Monthly NDVI and GPCP datasets for the period 1982 to 2000 were utilized. Index of Segmentation of Fourier Components (ISFC) was applied to NDVI to segment the study area into four climatic bioclimatic ecoregions (BCERs). Inter-annual, intra-annual and seasonal variability were scrutinized for each BCER, so as to compare the differential response of vegetation growth to rainfall. The correlation found was relatively high, especially in the brush-grass savannah. A strong similarity between temporal patterns of NDVI and rainfall was found, displaying that NDVI can be considered a sensitive indicator of the inter-annual variability of rainfall.

Vegetation response to inter-annual precipitation in Tropical Africa was examined over 20 years (1981-2000) using NDVI from AVHRR data (Camberlin, et al., 2007). Linear regressions and correlations were calculated between annual rainfall and NDVI at 0.5˚ latitude/longitude resolution based on two gridded precipitation datasets, the Climate Prediction Centre Merged Analysis of Precipitation (CMAP) and Climatic Research Unit (CRU). One third of the study area displayed significant correlations between annual NDVI variations and rainfall. The largest correlation was found distinctively in semi-arid open grassland and croplands.

The temporal responses of NDVI to rainfall and temperature in the Great Plains in Kansas, USA for the period 1989 to 1997 were investigated (Wang, et al., 2003). Biweekly and monthly precipitation data were derived from 410 weather stations and 17 weather stations were used to derive biweekly temperature data. NDVI values were calculated using NOAA-AVHRR datasets. Interpolation was used to derive biweekly and monthly climate maps. A strong and significant correlation was found between growing season NDVI and rainfall. Temperature and NDVI were positively correlated in the early and late growing season, whilst they were negatively correlated in the mid growing season. It was concluded that

rainfall was the primary influence on NDVI, and consequently productivity. Precipitation and NDVI had a strong and predictable relationship, when observed at an appropriate spatial scale.

A comparative analysis of the sensitivity of NDVI and Enhanced Vegetation Index (EVI) to rainfall variability was conducted for different land covers and uses in the southwest of Burkina Faso (Zoungrana, et al., 2015). Land cover/use maps for the years 1999, 2006 and 2011 were produced and change detection was applied to identify the persistent areas. Correlation analysis was performed to measure the relationship between the vegetation indices and rainfall. Similarities between the NDVI and EVI were found with both indices showing strong and significant positive correlations for all the land covers/uses. It was concluded that NDVI was more sensitive to rainfall, even though the difference between the two indices was insignificant. In this study, only NDVI shall be used to test whether there are any correlations with rainfall. Furthermore, land cover from the Zambia Scheme II Land Cover Map of 2014 shall be used to assess correlations between NDVI and rainfall in different classes. A similar study to that of Zoungrana et al. (2015) was carried out by Davenport & Nicholson (1993) who investigated the relationship between NDVI and rainfall for diverse vegetation types in East Africa. Ten vegetation formations were analysed. There was a strong similarity between the spatial and temporal patterns of NDVI when annual rainfall was below 1000 millimetres and monthly rainfall around 200 millimetres. In the same range, NDVI was a strong indicator of inter-annual rainfall variability. In this study, correlation analysis shall be done only at monthly time steps due to the gaps that are found in in situ annual rainfall data from the Zambia Meteorological Department (ZMD).

3.8 Drought Risk Assessments in Southern Africa

This section highlights the drought assessments carried out in Southern Africa. The Southern African Development Community (SADC) and United States Agency for International Development (USAID) have both had regional food security programmes where drought assessment and monitoring were undertaken. Under SADC, Monitoring for Environment and Security in Africa (MESA) programme had a drought component where 17 drought services were offered to SADC countries. USAID created the Famine Early Warning Systems Network (FEWS NET) to provide information and analysis on food security. FEWS NET provides data to support drought monitoring efforts globally. This information has been used in the SADC region for various food security analyses. This study was partly intended to fill

in the gaps that exist in both the MESA and FEWS NET programmes by assessing both meteorological and agricultural drought. This study took advantage of local information as opposed to regional data in order to localise the products.

3.8.1 Monitoring for Environment and Security in Africa (MESA)

Monitoring for Environment and Security in Africa (MESA) under the Southern African Development Community Thematic Action (SADC-THEMA) offer a drought service aimed at aiding the relevant national institutes in the SADC region, to monitor drought for informed decision making during drought periods (MESA SADC-THEMA, 2017). The service relies on remote sensing data to model drought conditions and provide regular drought maps and drought risk forecasts (MESA SADC-THEMA, 2017). Several drought services are provided (Table 7) and are categorised as vegetation performance maps and rainfall maps and graphs.

Table 7: MESA SADC-THEMA Drought Service Products (MESA SADC-THEMA, 2017)

Vegetation Performance Maps		**Frequency**
1	DP01: NDVI difference	10 days
2	DP02: Long-term average NDVI	10 days
3	DP03: Long-term average cumulative NDVI	10 days
4	DP04: Long-term standard deviation of NDVI	10 days
5	DP05: Long-term maximum of NDVI	10 days
6	DP06: Long-term minimum of NDVI	10 days
7	DP07: VCI	10 days
8	DP08: SDVI	10 days
9	DP09: PASG	10 days
Rainfall maps and graphs		
10	DP10: Total cumulative rainfall	10 days
11	DP11: Long-term average rainfall	10 days
12	DP12: Percentage of long-term average rainfall	10 days
13	DP13: Drought risk map (Boolean type)	1 month
14	DP14: Drought risk map (Graded type)	1 month
15	DP15: R Graphs – Percentage of LTA rainfall	10 days
16	DP16: Graphs – Cumulative NDVI	10 days
17	DP17: Rainfall Decile	1 month

MESA SADC THEMA have developed two types of drought risk maps for the Southern African Region. These are the Boolean-type and the Graded-type drought risk maps. The Boolean-type drought risk map (Figure 10) shows areas where drought risk exists according to cut-off values of current Percentage Average Seasonal Greenness (PASG) or cumulative rainfall as a percentage of the average input (MESA SADC-THEMA, 2014). The map is binary and consists of only two classes, possible drought (1) and other (2). The product is

used to identify areas affected by drought. In this study, different levels of severity were used, ranging from extremely dry droughts to extremely wet conditions.

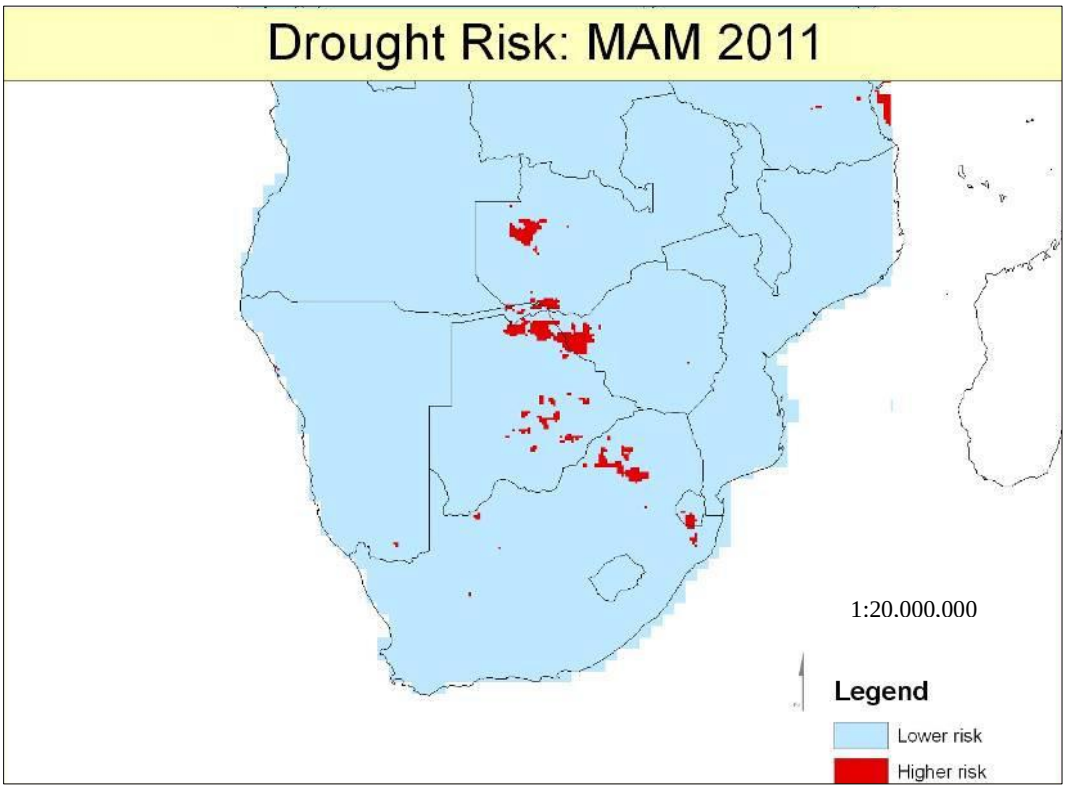

Figure 10: Example of a Boolean-type drought risk map (MESA SADC-THEMA, 2014)

The Boolean-type drought risk map is a regional product and lacks detail over smaller areas such as the Southern Province of Zambia. As shown in Figure 10 above, the whole Southern Province of Zambia was classed as a lower risk area based on data from the whole of Southern Africa. No details were provided of the different levels of risk within the province. Furthermore, the Boolean-type drought risk map does not display combined risk of both meteorological and agricultural drought. Each risk map only provides details of risk for one type of drought at a time.

The Graded-type drought risk map (Figure 11) displays varying occurrences of drought currently and into the near future (3 months), and it is based on the prevailing conditions of PASG or percentage of cumulative rainfall (MESA SADC-THEMA, 2014). Similar to the Boolean-type drought risk map, it is used to identify areas affected by drought. However, it is also shows the intensities of drought in different shades. The degree of risk is divided into deciles, with the first decile representing the highest risk and the tenth decile representing the lowest risk.

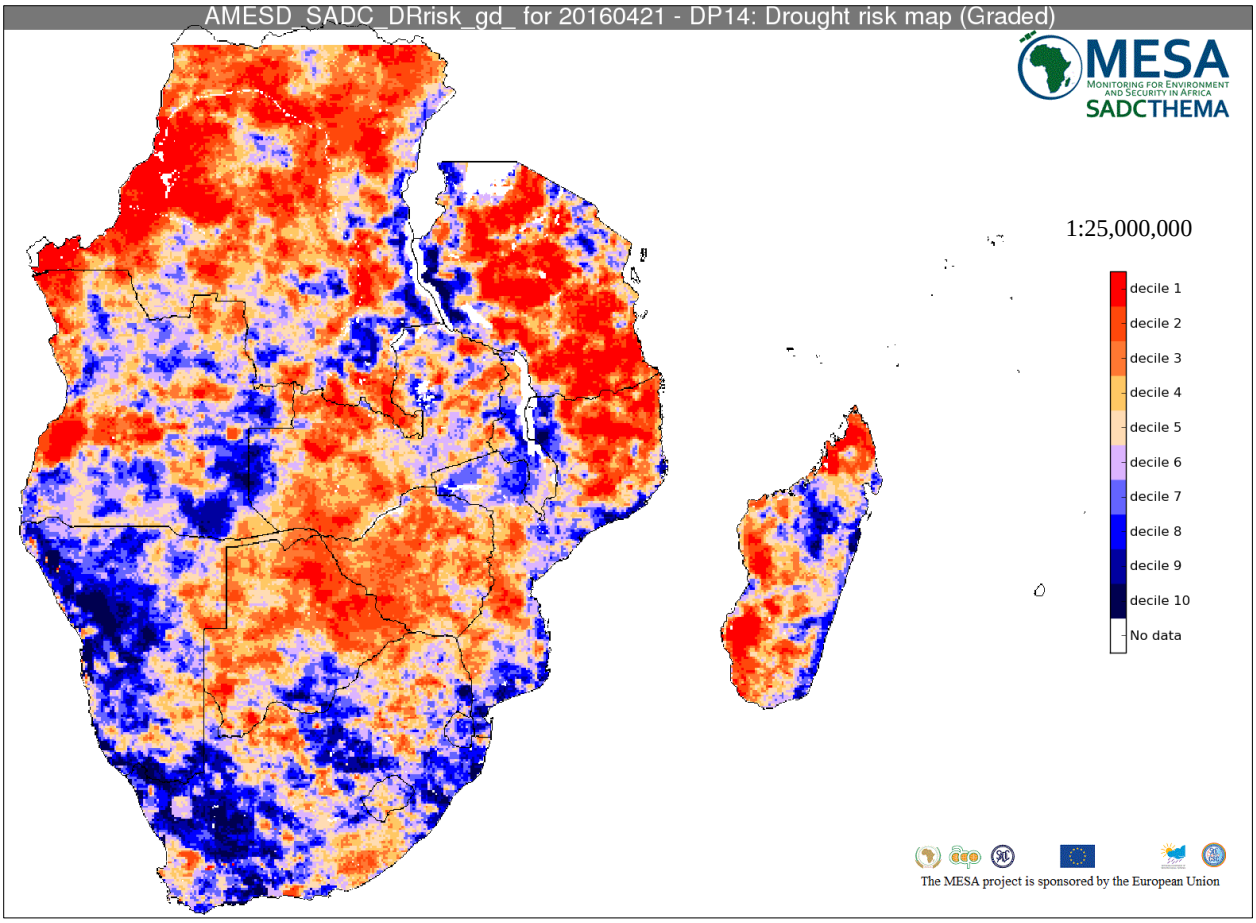

Figure 11: Example of a Graded-type drought risk map (MESA SADC-THEMA, 2017)

Despite the degree of differentiation in the levels of drought displayed by the Graded-type drought risk map, it is a regional map based on regional information and the spatial resolution is 10 kilometres. Applied to the Southern Province of Zambia, the levels of drought risk become generalised as they are defined by regional parameters. Moreover, the map does not display combined risk of both meteorological and agricultural drought. As is the case for the Boolean-type drought risk map, the Graded-type only provides details of risk for one type of drought at a time.

3.8.2 Famine Early Warning Systems Network

The United States Geological Survey (USGS) Famine Early Warning System Network (FEWS NET) Data Portal provides geo-spatial data, satellite image products and derived data products to support drought monitoring efforts throughout the world (FEWS NET, 2017). It is part of the Early Warning Focus Area at the USGS Earth Resources Observation and Science (EROS) Centre (FEWS NET, 2017).

Products such as continental eMODIS NDVI, SPI, actual evapotranspiration, evapotranspiration anomaly (ET), NOAA rainfall estimates (RFE), Inter-Tropical Front (ITF) position and moisture index are available for the whole of Africa at the data portal. However, there are no risk maps available at the portal.

3.9 El Niño Events and Drought in Southern Africa

El Niño is a Spanish phrase that directly translates to "boy child" and is a phenomenon that was first noticed in the nineteenth century by fishermen in Peru and Ecuador to refer to the abnormally warm waters that reduced their catch just before Christmas (WMO, 2014). The atmospheric counterpart of El Niño is called the Southern Oscillation, thus, the combination of the two is termed as El Niño/Southern Oscillation (ENSO). ENSO has three phases, namely: El Niño which is the warm phase; La Niña (girl child) which is the cold mikaphase; and the neutral phase (WMO, 2014). El Niño events (the warm phase) usually begin mid-year with extensive heating of surface water in the central and eastern equatorial Pacific Ocean and changes in the tropical atmospheric circulation (that is, winds, pressure and rainfall) (WMO, 2014). The phenomenon peaks during the months of November to January and subsides during the first half of the next year. The event occurs every two to seven years and can last for period of about eighteen months (WMO, 2014). Moderate and strong events lead to an increase in average global surface temperatures (WMO, 2014).

The impacts of El Niño in Southern Africa include a late start of the rainfall season, rainfall deficits, and poor distribution that mostly lead to significant dry spells (WFP, 2016). In turn, there is a delay in planting, a reduction in planted areas and a reduction in yield, which ultimately translates to reduced food supply (WFP, 2016). Coupled with intense multi-year droughts, the events have compounded an already deteriorating food and nutrition security situation in Zambia (WFP, 2016). El Niño events have occurred over a number of years across Southern Africa (Figure 12). Over the years, for example, Zambia has experienced several El Niño events of different magnitudes. Coupled with intense multi-year droughts, the events have compounded an already deteriorating food and nutrition security situation in Zambia (WFP, 2016). However, each El Niño event is unique and a strong signal does not always correspond with the magnitudes of impacts nor does it result in erratic and reduced rainfall (WFP, 2016). For instance, the El Niño event of the 1997/1998 rainfall season was the strongest recorded yet it resulted in near normal rainfall conditions, whilst the moderate 2002/2003 event resulted into a humanitarian crisis of extraordinary proportions because it

was preceded by a poor agricultural season (due to the 2001/2002 drought). Therefore, it is important to note that El Niño events do not always translate to droughts and droughts are not always as a result of El Niño events.

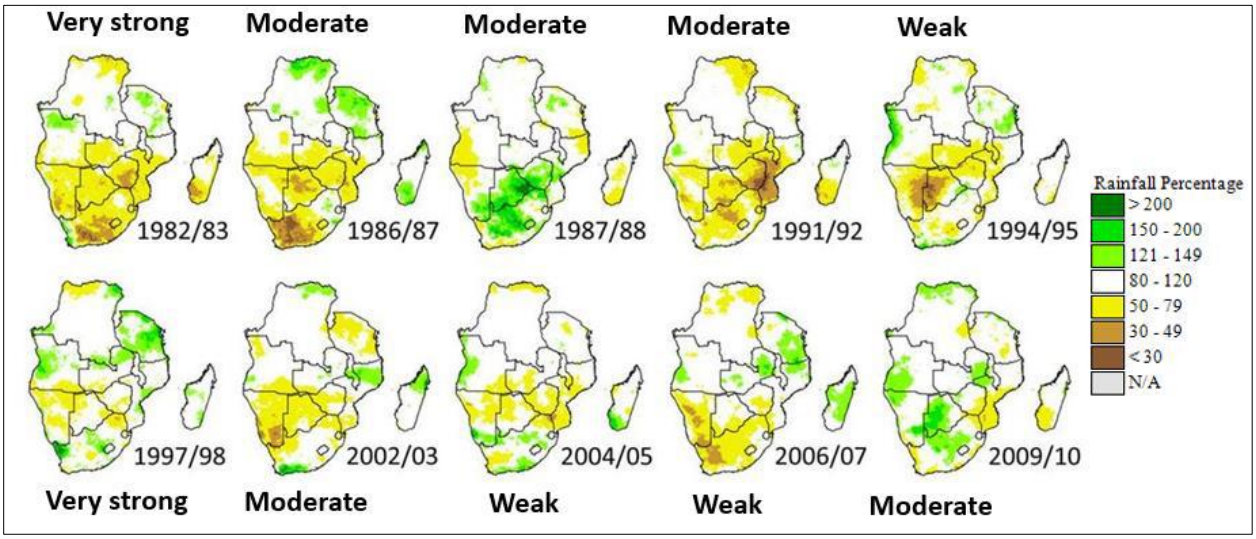

Figure 12: Historical El Niño Intensities and Rainfall Patterns in December-March, 1981-2010 (WFP, 2016)

Most recently, an El Niño event occurred in Southern Africa and affected most of the region. In Zambia, the southern and western regions were the most affected (Figure 13).

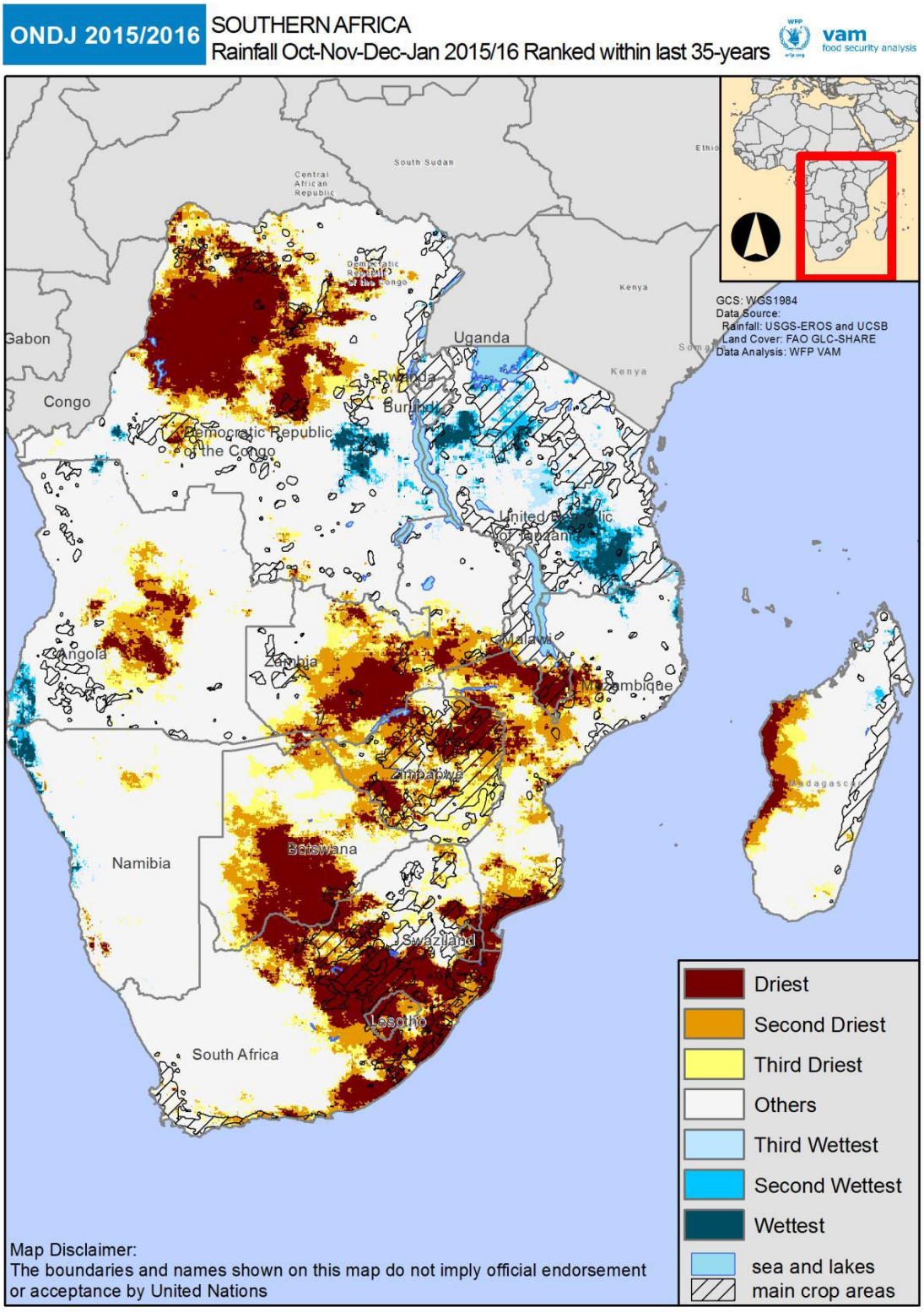

Figure 13: Southern Africa October to January rainfall, ranked within 1981-2016 (WFP, 2016)

3.10 History of Drought in Zambia (2000 to 2016)

In the 2001/2002 season, Zambia experienced a drought that resulted in a maize deficit of 0.6 million tons (which was 50% of the annual domestic consumption requirements) which translated to approximately 2.9 million people experiencing food shortages (World Bank, 2007). The hardest hit areas of the 2001/2002 drought were the Southern and Western Provinces of Zambia. In May 2002, the Government of the Republic of Zambia declared a national disaster due to the food crisis and appealed to the international community for assistance (World Bank, 2007). The following season (2002/2003) marked the second consecutive season of drought over the country, with Southern Province being the hardest hit (Relief Web, 2003). The drought was exacerbated by the El Niño conditions that prevailed over the region at the same time (WFP, 2016). Millions of farmers in the province faced severe food shortages and were forced to sell or consume grain seed indispensable for the next farming season (Relief Web, 2003). Zambia experienced late planting rains, below average quantities, poor and erratic rainfall distribution in the 2004/2005 rainfall season (Lekprichakul, 2008). Despite the shortfall of rain, the province still remained one of the main suppliers of maize and other cereal crops in the country. However, maize and other cereal crop production dropped that season as the province experienced greater crop failure than in non-drought seasons. In this case, the most affected regions are those in the southern and western regions, which experience fewer rains than their northern counterparts (Lekprichakul, 2008). In the 2015/2016 rainy season, Zambia experienced an El Niño induced drought that impeded rain-fed agriculture (UNOCHA, 2017). Lusaka, Southern and Western provinces, which are part of the main cropping areas in the country, experienced prolonged dry periods which resulted in wilting and stunted growth of crops (FAO, 2016). Previously a net exporter, Zambia implemented an export ban on grain and began importing maize (RisCura, 2017). Low water levels in the country's largest dam, the Kariba, forced a reduction in hydro-electric power generation, which led to wide spread power outages (RisCura, 2017).

3.11 Remote Sensing and GIS in Drought Risk Assessment

Drought assessment using remote sensing is built on properties of vegetation to reflect, absorb and emit solar energy. In years with no drought, healthy green vegetation reflects little energy in the visible part of the magnetic spectrum, owing to high chlorophyll absorption, and much in the near-infrared because of scattering of the light by leaf internal tissues and

water content (Kogan, 2001). In drought years, canopy area is reduced due to plant-stress from a reduction in chlorophyll and water content. An increase in reflected visible light is observed while the reflected near-infrared dwindles (Kogan, 1997). This principle is used in Normalized Vegetation Index.

Real time information about a disaster is cardinal for mitigation, monitoring and prediction. Since droughts have extensive effects that cause huge socio-economic and ecological disturbances over large areas, it is difficult to effectively collect continuous data using conventional methods. In Zambia, and the Southern Province in particular, this difficulty is pronounced as meteorological stations are few and far in between. However, remote sensing and GIS tools and techniques offer magnificent possibilities. Data can be collected rapidly and repeatedly over global, regional and local scales. The digital form of data enables analysis and manipulation by powerful computer systems whilst easing data sharing and communication.

Remote sensing data has temporal properties that enable assessment before, during and after a drought. The data can be used as a baseline which future changes can be compared to while the GIS techniques provide a suitable environment for integrating and analysing many types of data sources required for drought assessment (Chopra, 2006). Moreover, remote sensing and GIS are highly useful in detecting, quantifying and delineating drought, which has proved to be very difficult over several generations. Satellite data can provide details about vegetation condition and surface temperature at scales, ranging from the entire globe to a crop field, using few instruments and at relatively low cost (Unganai & Kogan, 1998). The development of Earth Observation technology for the detection, monitoring, assessment and forecast of drought hazard has been dealt with successfully around the world. The same concepts and technology can be adjusted and applied to the Southern Province of Zambia. Being a relatively drought prone area, which contributes significantly to the food security of the country, it is important to assess drought risk within the province to improve planning and preparedness. Many studies have utilised National Oceanic and Atmospheric Administration (NOAA) Advanced Very High Resolution Radiometer (AVHRR), Moderate Resolution Imaging Spectrometer (MODIS) and Landsat as these platforms are continuously monitoring the Earth's surface. The imagery is widely available as it is free and easy to access.

CHAPTER FOUR: METHODOLOGY

4.1 General Remarks

This chapter outlines the method used to achieve the objectives of this study. The initial step was the selection of the satellite data to be used in the study. Upon selection, the satellite data was downloaded (2000 to 2016) and then pre-processed in a GIS model. Pre-processing involved reprojection and rescaling of data to physical units. Pre-processed satellite data was used to calculate Vegetation Condition Index (VCI) and Soil Moisture Index (SMI). Correlation analysis was undertaken between NDVI based indices and the appropriate physical parameters. Correlation methods depended on the distribution of data. The three methods used were the Spearman, Kendall and Pearson.

Rainfall anomaly percentage and rainfall variation were determined using gridded rainfall data from January 1981 to March 2016. Standardised Precipitation Index (SPI) was calculated using both in situ rainfall measurements and gridded rainfall data. Data was redistributed to the gamma distribution before SPI was calculated. Drought risk mapping involved rescaling of data using the Spatial Index Approach described by CIESIN (2015). Drought risk was a combination of hazard, exposure and vulneraility, which was in line with Cap-Net (2015) and Joint Research Centre (2018) methods.

4.2 Data Selection Criteria for Remote Sensing Data

It was important to understand the specific requirements of an application in order to select the appropriate data (Tempfli, et al., 2009). Therefore, the spatial temporal properties of the phenomenon at hand had to be considered. In the case of drought, the temporal resolution of data was very important. Drought risk assessment required a dataset with a consistent historical record. Furthermore, to study the changes of vegetation within the wet season required a sensor on a satellite platform which frequently revisited the study area (high temporal resolution). The number of usable images within the time frame was also important. Despite a relatively high temporal resolution, cloud cover can make an image unusable. This was the case with Landsat which had a return time of 16 days. However, several of the images within the wet season were covered by clouds. The scale and the extent of the area of interest were important. Large areas, such as the whole Southern African region, do not require high spatial resolutions and are well represented at relatively smaller scales. The spectral and radiometric resolutions were important in the data selection exercise. The ability

of a sensor to detect changes in the visible bands and the near-infrared bands was important. This was because the study aimed at assessing drought risk using vegetation. The ability of a sensor to detect the magnitude of change in energy was also cardinal.

The study employed four parameters for sensor selection (Table 8). These were spatial resolution, temporal resolution, spectral resolution and cost. The data selected had to have a spatial resolution of 1 kilometre or less. The temporal resolution had to be less than 14 days with a historical record of greater than 10 years. The sensor had to have the capability to sense in the visible and near infrared bands and it had to be open access.

Table 8: Satellite data selection criteria used in this study based on spatial, spectral and temporal resolutions, historical record and cost

Sensor	**< or = 1km Spatial Resolution**	**<14 days return time**	**>10 year Historical record**	**NIR**	**Visible**	**Cost**
Landsat	✔	✘	✔	✔	✔	Free
MODIS	✔	✔	✔	✔	✔	Free
NOAA/AVHRR	✘	✔	✔	✔	✔	Free
SPOT	✔	✘	✔	✔	✔	Commercial
ASTER	✔	✔	✘	✔	✔	Free
Sentinel-2	✔	✔	✘	✔	✔	Free
Sentinel-3	✔	✔	✘	✔	✔	Free

Based on the data selection criteria for the different remote sensing data, MODIS was selected as it met all the required criteria. Therefore, monthly LST and monthly NDVI were obtained for the purpose of completing the study.

4.3 Description of Selected MODIS and Gridded Rainfall Data Used in this Study

Moderate Resolution Imaging Spectroradiometer (MODIS) is a low resolution instrument found aboard NASA's Earth Observing System (EOS), Terra (EOS AM) and Aqua (EOS PM) satellites. The return time is one to two days which offers a better temporal resolution and continuity than Landsat (Tempfli, et al., 2009). MODIS has a wide swath width of 2300 kilometres and a spatial resolution ranging from 250 metres in the visible bands to 1 kilometre in the thermal band. There are 36 narrow spectral bands in MODIS that are used to generate a number of standard data products such as NDVI, Enhanced Vegetation Index (EVI), Leaf Area Index (LAI), Land Surface Temperature (LST), fire and emissivity. MODIS

data used in this study were MOD13A3 and MOD11A2. MOD13A3 data were monthly NDVI generated from 16 day NDVI averages at 1 kilometre spatial resolution. MOD11A2 were 8 day daytime LST at 1 kilometre spatial resolution.

Climate Hazards Group Infrared Precipitation with Stations (CHIRPS) is based on infrared Cold Cloud Duration (CCD) observations (Funk, et al., 2015). It is an algorithm that is built around a 0.05° climatology that integrates satellite information to represent sparsely gauged locations, incorporating daily, pentadal and monthly 0.05° CCD-based precipitation estimates (1981-present). It fuses station data to produce a preliminary data product with a latency of about 2 days and a final product with an average latency of about 3 weeks (Funk, et al., 2015). CHIRPS was developed to support Famine Early Warning Systems Network (FEWS NET) and is a build-on on other successful thermal infrared precipitation products. It was explicitly designed to fill the gap in the types of gridded precipitation datasets (Funk, et al., 2015), which are important for areas where meteorological stations are scarce and sparse. CHIRPS has a spatial resolution of 0.05° (approximately 5km by 5km) and a daily temporal resolution. CHIRPS data that was used in this study were monthly Rainfall Estimates (RFE). The data was used in correlation analysis, calculation of rainfall anomaly percentage and SPI and determination of rainfall variations.

4.4 Pre-processing of Selected MODIS Data Used in this Study

MODIS imagery was downloaded and partly pre-processed using the MODIStsp (Busetto & Ranghetti, 2018) package in RStudio. MODIStsp is an R package that automates the creation of temporal data and allows the performance of several pre-processing steps on MODIS Land Products (Busetto & Ranghetti, 2018). Using MODIStsp, MODIS monthly NDVI and MODIS 8 day LST were downloaded from the year 2000 to the end of the 2016/2017 rainy season. The data was reprojected from the native MODIS gridded sinusoidal to the EPSG 4326 (geographic coordinates on the WGS 1984 datum) with GeoTiff as the output format.

Further, pre-processing was done in in order to rescale both MODIS products, and this was done using a Raster Calculator tool. The scale of NDVI is -1 to 1, however, NDVI products from MODIS have digital numbers (DNs) ranging from -10,000 to 10,000. Therefore, each NDVI image was multiplied by a factor of 0.0001 (Didan, et al., 2015) to scale the NDVI scenes to a range of -1 to 1. Similarly, LST data from MODIS is originally in DNs ranging

from 7,500 to 65,535 and not in physical units. To convert the scenes to the physical unit of degrees Celsius, equation 6 (Wan, 2013) was used:

$$°C = DN * 0.02 - 273.15 \quad (6)$$

Where $°C$ is degrees Celsius and DN is the raw image in digital numbers.

Once each dataset was rescaled, the images were clipped and resized to the extent of the Southern Province of Zambia. Due to the large number of images that required rescaling and clipping, a model (Figure 14) was created in order to iterate and automate the rescaling and clipping process and save time. Two geodatabases were created, one for NDVI images and the other for LST images. The two geodatabases were the inputs of the model, whilst the outputs were the rescaled and clipped images.

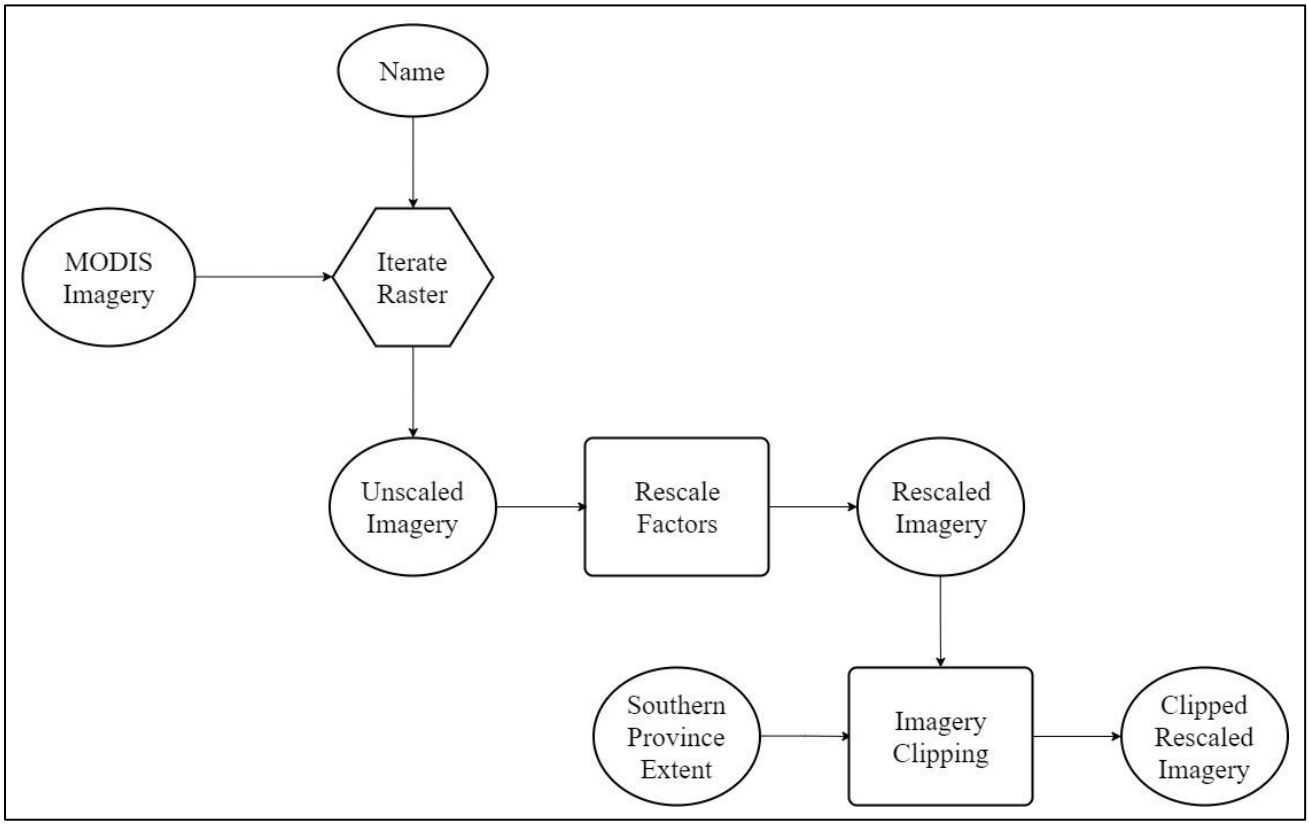

Figure 14: GIS pre-processing model for MODIS imagery used in this study

The last step in the pre-processing of MODIS data was to transform the 8-day LST to monthly LST. This was done using a Cell Statistics tool by calculating the mean of each month. Similarly to MODIS data, CHIRPS data required clipping to the extent of the Southern Province. However, that was the only pre-processing step taken as the data was received in Band Interleaved format and did not require any conversions.

4.5 Rainfall Anomaly Percentage and Rainfall Variation

Monthly rainfall anomaly percentage was used to assess meteorological drought occurrences. It was computed from the year 2000 to 2016 rainy seasons using CHIRPS monthly rainfall estimates, to assess meteorological drought over the Southern Province of Zambia. Rainfall anomaly percentage was calculated using equation 7 (Chopra, 2006):

$$RFA = \left(\frac{ppt_i - \overline{ppt}}{\overline{ppt}}\right) * 100 \quad (7)$$

Where RFA is rainfall anomaly percentage, ppt_i is the precipitation of a given month and $\overline{ppt}$ is the average monthly precipitation.

Rainfall anomaly percentage was calculated for the months of December, January and February throughout the study period. This is because these are the three wettest months of the season (Funk, et al., 2015). Calculation was done using a Raster Calculator. Rainfall anomaly percentage was classified into classes of plus or minus 10%, 25% and 50% (Table 9).

Table 9: Rainfall anomaly percentage classes used in this study

Rainfall Anomaly Percentage	**Severity Class**
< -50	Extremely Dry
-50 to -25	Severely Dry
-25 to -10	Moderately Dry
-10 to 10	Normal
10 to 25	Moderately Wet
25 to 50	Very Wet
> 50	Extremely Wet

Average seasonal rainfall was calculated in order to assess spatial (areal) variability, which is how rainfall amounts vary at different locations across the region. Furthermore, coefficient of variation was calculated using equation 8 (Abdi, 2010) to assess temporal variability:

$$Coefficient\ of\ Variation = \frac{\sigma}{\overline{ppt}} \quad (8)$$

Where σ is the standard deviation of seasonal rainfall and $\overline{ppt}$ is the average seasonal rainfall.

Coefficient of variation was used to assess the temporal variability of precipitation within Southern Province.

4.6 Calculation of Standardised Precipitation Index (SPI)

Standardised Precipitation Index (SPI) was also used to assess meteorological drought occurrences. It was calculated using the spi package in R. A rainfall record of 25 years or more was required in order to have confidence in the results. The five manual stations of the Southern Province had sufficient records as rainfall was recorded from 1980 to 2015. Monthly precipitation values of the wet season (November to March) for each station were taken and arranged in a format that the spi package could read (Table 10). The predefined timescale used was a 1 month moving window.

Table 10: Example of formatting of data used in this study

Month	1980	1981	1982	1983	1984	1985
January	NA	156.5	109.4	191.5	26.9	202.4
February	NA	299	67.9	138.7	94.1	107.9
March	NA	130.1	31.8	34.5	55.3	82.6
April	0	9.1	16.4	74.1	18.8	7.1
October	18.5	7.6	148.1	7.3	24.9	20.2
November	227.7	104.3	25.7	41.5	87.8	29
December	111.8	34.1	111.4	242.2	83.3	205

Cumulative rainfall less than a year tend not to be normally distributed. In order to calculate SPI, monthly rainfall data was normalized using the gamma probability density function of the gamma distribution, which was defined as equation 9 (Guenang & Kamga, 2014):

$$g(x) = \frac{1}{\beta^{\alpha}\Gamma(\alpha)} x^{\alpha-1} e^{-x/\beta} \quad \text{For } x > 0 \qquad (9)$$

Where $\alpha > 0$ is a shape parameter, $\beta > 0$ is a scale parameter, x is the amount of precipitation and $\Gamma(\alpha)$ is the gamma function. The gamma distribution (Figure 15) is not defined for $x = 0$.

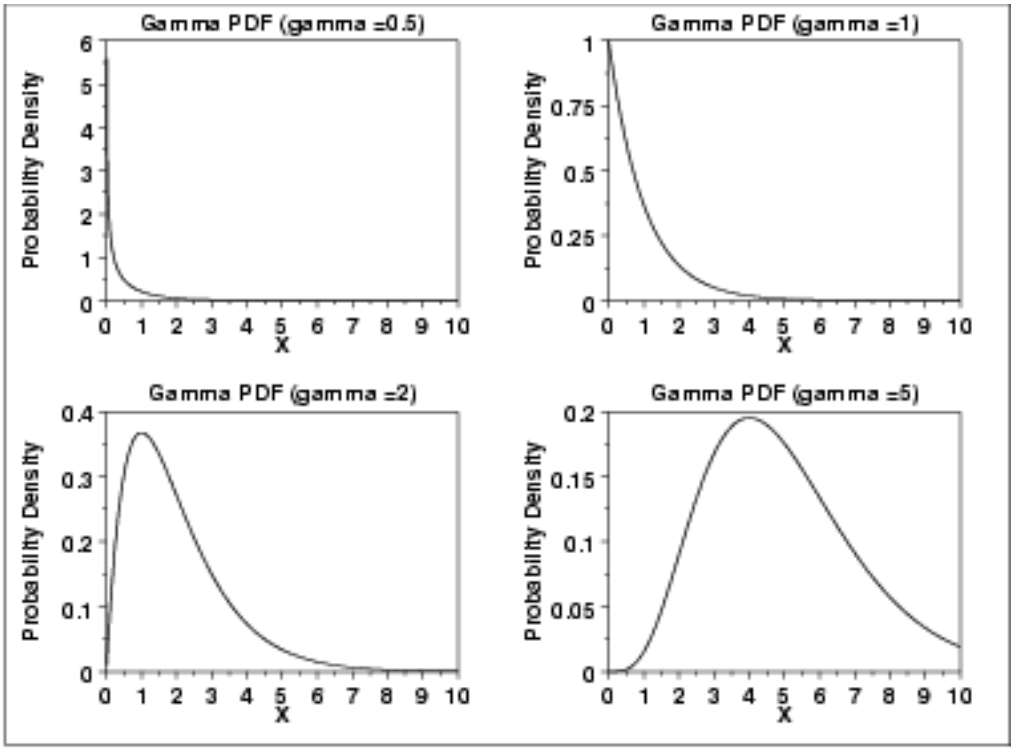

Figure 15: The gamma probability density function plots (NIST, 2016)

The fitted function was used to calculate the cumulative distribution of the data points. Finally, the data points were transformed into standardised normal variates using equation 1.

For CHIRPS rainfall, SPI was calculated using the SPIRIT software. In this case, SPI was calculated from January, 1981 to March 2016. The SPI derived from the CHIRPS was averaged for the whole Southern Province and used to determine the probability of each drought severity occurring. This was done using the frequency of each drought severity class. Spatially, the frequency was determined for each pixel using the Equal To Frequency tool of the Spatial Analyst Toolset in a GIS environment. Before the tool could be applied, constant rasters were created with the required values for each severity class. The tool was then

applied using the constant rasters as reference values to count the number of occurrences for each severity class in each pixel. Three maps were created, which were the moderately dry frequency, severely dry frequency and extremely dry frequency.

4.7 Calculation of Vegetation Condition Index (VCI)

Vegetation Condition Index (VCI) was used to evaluate agricultural drought occurrences in the Southern Province. It was generated for each month of the rainy season (November, December, January, February and March) from the year 2000 to 2016 was generated. An NDVI file geodatabase was created for each month. Using the Cell Statistics tool, $NDVI_{min}$ and $NDVI_{max}$ were determined for each of the five months throughout the study period. $NDVI_{min}$ was an NDVI image representing the minimum value of each pixel in each month across the study period. Conversely, $NDVI_{max}$ was an NDVI image containing the maximum value of each pixel of each month in the time series. The $NDVI_{min}$ and $NDVI_{max}$ were used to calculate VCI using equation 4, using the Raster Calculator tool. Due to the large number of NDVI scenes, a model (Figure 16) was created using a Model Builder that automated the calculation of VCI.

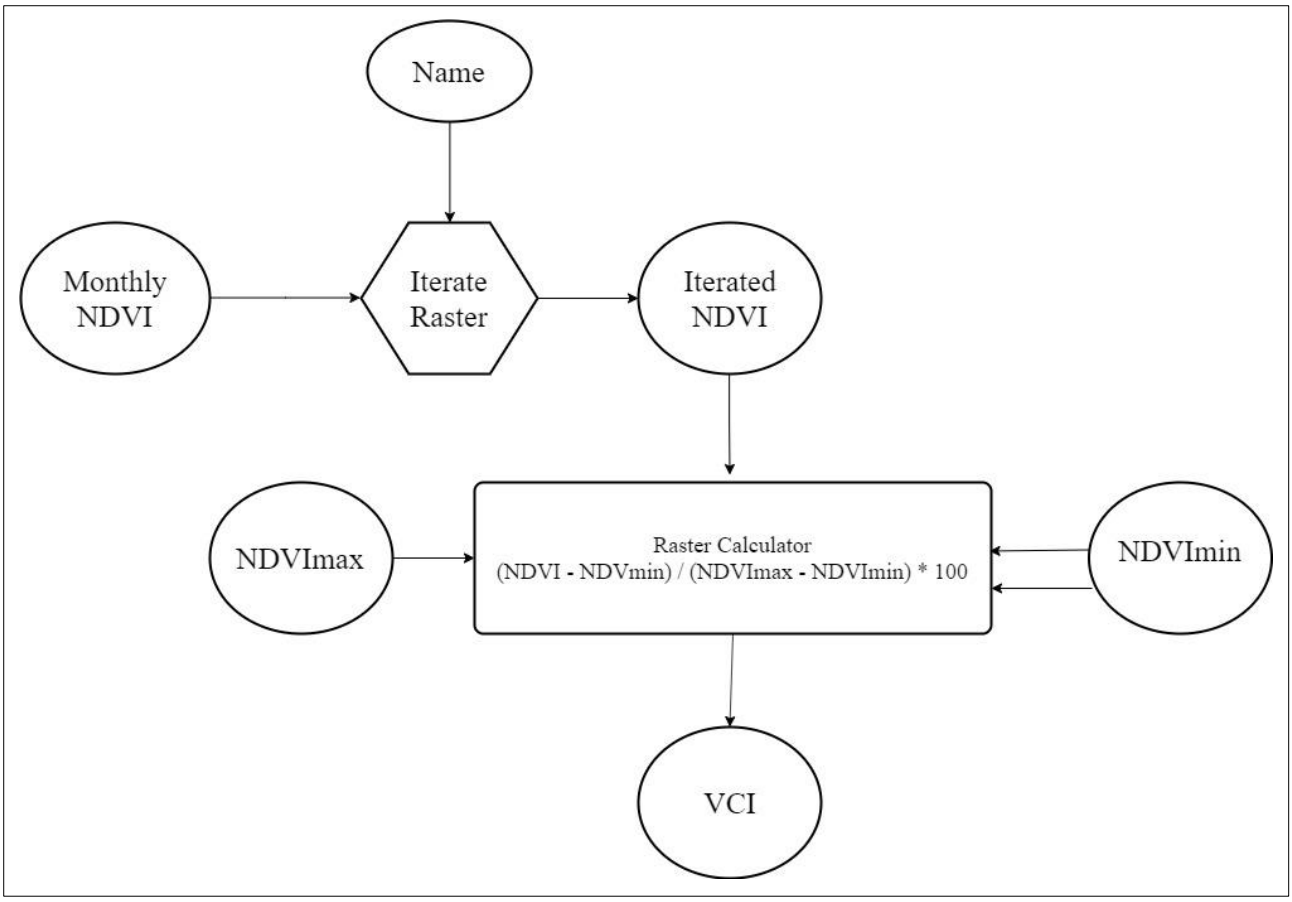

Figure 16: VCI Calculation Model used in this study

4.8 Calculation of Soil Moisture Index (SMI)

Similar to VCI, SMI was used to assess agricultural drought occurrences. It was determined using the triangle method for the drought months detected using SPI. The triangle method involved the plotting of corresponding Fr and T* to determine the wet and dry edges. Equation 10 was used to calculate Fr (Carlson, 2007):

$$Fr = \{\frac{(NDVI - NDVI_0)}{(NDVI_{max} - NDVI_0)}\}^2 \quad (10)$$

Where $NDVI_0$ is the NDVI value of bare soil, and $NDVI_{max}$ is the maximum value of NDVI on each scene (the NDVI value of the greenest pixel). The average NDVI value for soil was 0.1, from data collected in the field. The maximum value of NDVI for all the months calculated was 1.0.

Similarly, LST was rescaled to T* which is scaled from 0 to 1. Equation 11, as defined by Carlson (2007), was used:

$$T^* = \{\frac{(Tir - T_{\min})}{(T_{max} - T_{min}}\} \quad (11)$$

Where Tir is MODIS surface radiant temperature, and T_{max} and T_{min} are the maximum and minimum temperatures in an image.

After the NDVI and LST were scaled to Fr and T*, a scatter plot for each month was created. On each scatter plot, two linear fits (ablines) were done to determine the warm and cold edges. This was in order to determine the necessary empirical parameters for deriving LST_{max} and LST_{min}; which are requirements in the calculation of SMI.

The empirical parameters were the slope and intercept of each linear model. Once the empirical parameters were determined, equations 12 and 13 were used to calculate LST_{max} and LST_{min} (Potic, et al., 2017):

$$LST_{max} = a_1 * NDVI + b_1 \quad (12)$$

$$LST_{min} = a_2 * NDVI + b_2 \quad (13)$$

Where a_1, a_2, b_1 and b_2 are the physical parameters obtained from the linear model (a represents slope, and b represents the intercept) defining both the warm and the cold edge (dry and wet edge).

After the calculation of the LST_{max} and LST_{min}; SMI was calculated using Equation 5.

4.9 Correlation Analysis for Validation of NDVI Based Indices

Due to the temporal nature of the study, correlation analysis was carried out in order to validate the use of NDVI based indices in the assessment of drought in the Southern Province of Zambia. All correlation works were performed in RStudio, which is based on R and is an integrated software suite for data manipulation, calculation and graphical display (Venables, et al., 2018). Monthly NDVI was tested against monthly in situ rainfall measurements and CHIRPS monthly rainfall estimates. VCI was tested against yearly maize production and maize yield. Monthly SMI was tested against monthly in situ soil moisture measurements from Zambia Meteorological Department (ZMD). The correlation test type employed depended on the distribution of data of each variable. Data that was normally distributed was tested using the Pearson's product moment coefficient (r), whilst data that was not normally distributed was tested using Kendall's tau (τ) and Spearman's rank (r_s) correlation coefficients.

Before each correlation test was carried out, the Shapiro-Wilk normality test was used to check the distribution of each dataset. The data was normally distributed if the resulting p-value was greater than the confidence interval level (p-value > 0.05). Furthermore, quintile-quantile plots (q-q plots) were used as a graphical test for normality. Linear distribution of data on the q-q plots represented normal distribution, whilst non-linear distribution meant the sample data was not normally distributed.

To assess the normality and correlation between monthly NDVI and monthly rainfall, the coordinates of the five meteorological stations were used to create a point class feature. Once the point feature was created, the Extract Multiple Values to Point tool of the Spatial Analyst toolset was used to extract the values of monthly NDVI across the study period at each station. Upon extraction, each monthly NDVI value was paired with the corresponding monthly rainfall value to create an NDVI and rainfall matrix. The matrix was exported as a csv file and later tested for normality and correlation analysis.

To assess the normality and the correlation between monthly NDVI and monthly CHIRPS rainfall estimates, 18 random points were generated (Appendix 3). The points fell in all the land cover classes of the Zambia Land Cover Map Scheme I of 2014, from the Zambia Forestry Department. At each point, monthly NDVI values and rainfall estimates were

extracted. Each NDVI value was paired to a corresponding monthly rainfall estimate. The values were formatted as a table and tested for normality and for correlations.

Since all three datasets were not normally distributed, the Kendall tau correlation and Spearman's rank correlation coefficients were used to test if any significant correlation existed between the monthly NDVI and monthly rainfall, and CHIRPS estimates. The Spearman's rank correlation coefficient is a distribution free (non-parametric) test that was proposed by Charles Spearman as a measure of the strength of an association between two variables (Hauke & Kossowski, 2011). The coefficient is a measure of a monotone association, on an ordinal scale, that is used when the distribution of data is not normal and makes Pearson's correlation coefficient undesirable or misleading (Hauke & Kossowski, 2011). The Spearman's rank correlation coefficient was computed using equation 14 (Hauke & Kossowski, 2011):

$$r_s = 1 - \frac{6\sum_{i=1}^{n} d_i^2}{n^3 - n} \qquad (14)$$

Where n is the number of elements in each dataset and d is the rank of each element (Hauke & Kossowski, 2011).

Similar to the Spearman's rank correlation coefficient, the Kendall tau was created in order to compare and capture the association between two ordinal variables (Chok, 2008). The coefficient quantifies the inconsistency between the number of concordant and discordant pairs (Chok, 2008). Concordant pairs are when both members of an observation are larger than their respective members of the other observations, while discordant pairs are when two numbers in one observation differ in opposite directions (Statistics Solutions, 2018). The Kendall tau correlation coefficient was expressed using equation 15 (Statistics Solutions, 2018):

$$\tau = \frac{2(n_C - n_D)}{\sqrt{N(N-1) - T_X}\sqrt{N(N-1) - T_Y}} \qquad (15)$$

Where N is the total number of pairs, n_C is the number of concordant pairs and n_D is the number of discordant pairs.

Kendall's tau values are usually smaller than Spearman's r_s values. The advantages of using Kendall's tau over the Spearman's rank correlation coefficient are that the distribution has superior statistical characteristics and the interpretation in terms of the probabilities of

observing the concordant and discordant pairs is very direct (Statistics Solutions, 2018). However, the Spearman's rank correlation coefficient is much more sensitive to errors and discrepancies in data. The analyses of Kendall's tau and Spearman's rank correlation coefficient are very comparable, and thus, unvaryingly lead to the same interpretations (Statistics Solutions, 2018). Therefore, both methods were used for non-parametric correlation tests

Vegetation Condition Index (VCI) was compared against maize production and yield (Appendix 4) because it is overwhelmingly the main crop grown in the Southern Province, as earlier shown in Figure 5. Furthermore, VCI was used to assess agricultural drought and it was appropriate to correlate it to the most planted crop in the region. The information used to run the correlations were maize production and yield. The maize production –VCI correlation analysis was done using yearly maize production and average seasonal VCI. Maize production was for small-scale and medium-scale farmers who depended on rainfall as a source of water for their crops and harvested at the end of the rain season. Similarly, maize yield was for small-scale and medium-scale farmers and was also compared to average seasonal VCI. Commercial farmer maize production and yields were excluded as the information was not available and because commercial farmers had resilience to drought conditions based on their ability to irrigate. Crop production and crop yield information was only available at provincial level (CSO, 2016b). All datasets were subjected to normality tests before correlations were carried out. In the case of VCI against crop production and yield, all the datasets were normal, and therefore, the Pearson's product moment correlation coefficient was used for analysis.

The Pearson's product moment correlation coefficient is a parametric (distribution dependant) statistic that measures linear dependencies, on an interval scale, between two variables (Hauke & Kossowski, 2011). It was first described by Karl Pearson in 1896 (Hauke & Kossowski, 2011) and it is the ratio of the covariance of two variables representing a set of numerical data, normalised to the square root of their variances (Hall, 2015). The Pearson's correlation coefficient was calculated using equation 16 (Hall, 2015):

$$r = \frac{C_{xy}}{\sqrt{C_{xx}C_{yy}}} = \frac{C_{xy}}{\sigma_x \sigma_y} \qquad (16)$$

Where C were the covariance of the variables and σ were the standard deviations (Hall, 2015).

The correlation analysis between soil moisture measurements and SMI were done for two soil moisture measurement depths; 5 and 10 centimetres. In each case, the data was checked for normality. Since the soil moisture datasets were all normally distributed, the Pearson's Product Moment Correlation Coefficient was used.

In each of the four cases, the null hypotheses (h_o) were that there were no significant correlations between the variables. The alternative hypotheses (h_a) were that there were significant correlations between the variables. The level of significance was 0.05 (95%) ($P<0.05$ to reject h_0) and the tests were two-tailed as there were no a priori assumption made on whether the relationships were negative or positive.

4.10 Drought Risk Mapping

Drought risk was the summation of hazard, exposure and vulnerability of an area. In order to map hazard, exposure and vulnerability, the Spatial Index Approach (CIESIN, 2015) was used to transform each to a comparable scale of 0 to 100. To map hazard, exposure and vulnerability, several datasets were used. Hazard was determined using calculated rainfall anomaly percentage, SPI, VCI and SMI.. Exposure was determined using the Zambia Land Cover Map Scheme I of 2014 (FD & FAO, 2016) and ward populations. Lastly, vulnerability was determined using the socioeconomic indicators (at ward level) extracted from de la Fuente et al. (2015), temporal and areal variations of rainfall and slope.

Drought hazards were meteorological and agricultural. Meteorological drought hazard was determined using rainfall anomaly percentage and SPI, whilst agricultural drought hazard was determined using VCI and SMI. To determine hazard, values of each data input had to be extracted to a point feature class. The attribute table of the feature class contained location information (coordinates) of each point, which meant each value to be extracted could be attributed to a specific location. To achieve extraction, a 1 kilometre by 1 kilometre grid polyline feature class covering the Southern Province was created. A point feature class was created at the centre of each square within the grid. Before the values were extracted, rainfall anomaly percentage and SPI were resampled to a spatial resolution of 1 kilometre by 1 kilometre from 5 kilometre by 5 kilometre resolution. After the two inputs were reclassified, the Extract Multiple Values to Point tool of the Spatial Analyst toolset was used to extract values of all the inputs at each point. After the extraction of values, the attribute table of the point feature class was exported as a table in Comma Separated Values (csv) format. Each

measure of drought hazard was rescaled to a range of 0 to 100 (where 100 was the most hazardous and 0 the least). For all the datasets, lower values represented a higher degree of a hazard. Therefore, equation 17 (CIESIN, 2015) was used to rescale all the inputs:

$$y = \left(\frac{x_i - x_{max}}{x_{min} - x_{max}}\right) * 100 \qquad (17)$$

Where y is the value of the input when rescaled to the range 0 to 100, x_i is the value of an input before rescaling, x_{max} is the maximum value of an input before rescaling and x_{min} is the maximum value of an input before rescaling.

Meteorological drought hazard was the summation of rescaled rainfall anomaly percentage and SPI. Agricultural drought hazard was the summation of rescaled VCI and SMI. Equation 18 (CIESIN, 2015) was used to calculate both types of hazard. Inputs were ranked the same and, therefore, had the same weights.

$$H = \frac{(x_1 a + x_2 b + x_3 c \ldots\ldots\ldots x_n z)}{n} \qquad (18)$$

Where H is hazard, x_1,x_2, x_3 and x_n are different months of drought for each input, a, b, c and z are weights of each drought month, and n is the number of drought months.

Exposure was calculated in a similar manner as hazard. However, the inputs used to determine exposure were ward level human populations (CSO, 2012) and the Zambia Land Cover Scheme I of 2014 (FD & FAO, 2016). The exposure was the extent to which the Southern Province was subject to drought hazards and the two elements of ward populations and land cover provided data of the numbers and locations of people and where agricultural activities were prominent. The ward populations constituted the human part of exposure whilst the land cover map provided information on possible agricultural activities in the province. The cropland (arable) and grassland (rangeland) could be used as elements to assess exposure of the livelihood of people within the province. Similar to hazard, the values of the two inputs (population and land cover) required to be extracted to point feature class, which had location information. However, two steps needed to be taken to enable extraction. The first step was the reclassification and resampling of the land cover map. The map was converted into an integer raster dataset using the Reclassify tool of the Spatial Analyst toolset in the ArcToolbox. Land cover classes were first ranked 1 to 6, where 1 was the most exposed and 6 the least. The ranks were based on the strength of the correlation between NDVI and rainfall in each land cover class. Where the NDVI-rainfall correlation was high,

exposure was deemed to be high. Where the correlation was lower, exposure was deemed to be lower. Using the ranks, the land cover map was reclassified into an integer raster dataset with each class represented by an integer equal to the class rank (Table 11). The land cover map was then resampled to a spatial resolution of 1 kilometre by 1 kilometre.

Table 11: Ranks of land cover based on the strenth of correlation between NDVI and rainfall

Soil Class	**Rank**
Grassland	1
Cropland	2
Forests	3
Wetlands	4
Settlements	5
Otherlands	6

The second step was the conversion of the ward population data into a long integer raster dataset. This was achieved by first attributing the populations of each ward to the Southern Province ward polygon shapefile. After the population attribute was included to the shapefile, the Polygon to Raster tool of the Conversion Tools of ArcToolbox was used to convert the shape file into a raster dataset, with values of the pixels being those of population. The selected spatial resolution of the raster dataset was 1 kilometre by 1 kilometre. However, pixel values over each ward were homogenous as only one population value could be attributed to each polygon. After the population and land cover data were converted to the desired formats and resolutions, the Extract Multiple Values to Point tool was used to attribute the values of each input to point feature class with location information. The attribute table of the point feature class was then formatted as a table and used for the determination of drought exposure. Each input was rescaled to a range of 0 to 100, where 0 was the lowest exposure and 100 the highest. In the case of population, high values entailed higher exposure, whilst low values meant lower exposure. Therefore, equation 19 (CIESIN, 2015) was used to rescale the ward populations:

$$y = \left(\frac{x_i - x_{min}}{x_{max} - x_{min}}\right) * 100 \qquad (19)$$

Where y is the value of the input when rescaled to the range 0 to 100, x_i is the value of a variable before rescaling, x_{max} is the maximum value of a variable before rescaling and x_{min} is the maximum value of a variable before rescaling.

With regards to land cover, the rank 1 was the most exposed whilst the rank 6 was the least, based on correlation results NDVI versus CHIRPS. Therefore equation 17 was used to transform the lower values to higher exposure on a scale of 1 to 100.

The two inputs were weighted depending on the order of importance. The weight of each input was determined by the rank sum method. Ranking was done in ascending order, where 1 was given the most importance (GITTA, 2013). In this case, population was deemed more important than land cover as exposure to drought would have direct impacts on the wellbeing of people. Therefore, population was given the most important rank of 1. Land cover was then given the less important rank of 2. The weight of each input was derived using equation 20 (GITTA, 2013):

$$w = \frac{k - r_i + 1}{\sum_{j=1}^{k} k - r_j + 1} \quad (20)$$

Where r_i is the rank of the ith input and k is the total number of inputs.

Therefore, the weights were 0.67 for population and 0.33 for land cover.

After the weights were determined, equation 21, as adopted from CIESIN (2015), was used to determine exposure:

$$E = \frac{(x_1 a + x_2 b)}{2} \quad (21)$$

Where E is exposure, x_1 is ward population, x_2 is land cover and a and b are the weights of ward population and land cover respectively.

Once exposure was determined, it was rescaled to a range of 1 to 100 using equation 17.

A similar approach was used to determine vulnerability. Values of each vulnerability input had to be extracted to a point feature class which had location information. The inputs of the drought vulnerability map were socioeconomic indicators, rainfall variability and slope. The available socioeconomic information was extracted from de la Fuente, et al. (2015) and these were poverty Head Count (HC) ratio and the number of the poor in each ward (Appendix 5), which required transformation into raster format. Like ward population, each HC value and number of poor were attributed to the appropriate polygon in the Southern Province ward shapefile. The shapefile was then converted to two 1 kilometre by 1 kilometre raster datasets,

with first having values of HC and the second the number of poor. The spatial and temporal variabilities of rainfall were resampled to a spatial resolution of 1 kilometre. Slope was derived from a 1 second arc Shuttle Radar Topography Model (SRTM) and was calculated using the Slope tool in the Surface Analysis toolset of Spatial Analyst of a GIS environment. Slope was expressed in degrees. The Extract Multiple Values tool was used to extract values of each input at each point, which resulted in a matrix of all the inputs. The matrix was exported as a csv file and used for vulnerability mapping of the Southern Province. Each input was rescaled to a range of 1 to 100, where 0 was the least vulnerable and 100 was the most. For HC, the number of poor, temporal rainfall variability and slope, lower values entailed lower vulnerability of an area, whilst higher values meant higher vulnerability. Therefore, equation 19 was used to rescale the four inputs. For spatial rainfall variability, equation 17 was used because higher values meant lower vulnerability and vice versa.

After each input was rescaled, the inputs were ranked in ascending order based on importance of the parameters. HC and the number of poor were deemed the most important and were both ranked equally at 1. This was because these provided information that was directly linked to human beings and their level of resilience to a drought. The two rainfall variability datasets were also ranked equally at 2. This was because these provided climatic information. Slope was deemed the least important and was ranked at 3 as it represented the topography of the area. The ranks were then used to determine the weights (Table 12).

Table 12: Ranks and weights of inputs in vulnerabilty determination used in this study

Input	**Rank**	**Weight**
HC	1	0.24
Number of poor	1	0.24
Spatial variability of rainfall	2	0.19
Temporal variability of rainfall	2	0.19
Slope	3	0.14
Total		**1.00**

Vulnerability Index was calculated using equation 22 as defined by CIESIN (2015):

$$V = \frac{(x_1 a + x_2 b + x_3 c + x_4 d)}{n} \quad (22)$$

Where V is vulnerability index, x_1,x_2, x_3 and x_4 are the different inputs, a, b, c and d are weights of each input and n is the number of inputs. In this case n was equal to 5.

Once the vulnerability index was calculated for each entry in the table, it was rescaled to a range of 0 to 100 using equation 19.

After each of hazard, exposure and vulnerability were calculated; the values were exported as a csv file and plotted. Each entry was plotted using the coordinates. The Point to Raster tool of the Conversion Tools in the ArcToolbox was used to create hazard, exposure and vulnerability maps of the Southern Province. These maps were also upscaled to district level using the Zonal Statistics tool in the Spatial Analyst toolset. The average hazard, exposure and vulnerability of each district was determined and mapped.

Hazard, exposure and vulnerability were summed using a raster calculator in order to create drought risk. Where the hazard was meteorological, the resultant drought risk was meteorological. Where hazard was agricultural, the resultant risk was agricultural. An integration of the two risks was also created by overlaying the two.

4.11 Limitations to Study

The following were the limitations faced as the study was undertaken:

(i) The unavailability of a comprehensive evapotranspiration dataset from meteorological stations and remote sensing sources resulted in the inability to calculate an adjusted version of Standardised Precipitation Index (SPI) called Standardised Precipitation and Evapotranspiration Index (SPEI). Therefore, the study relied on SPI;

(ii) Socioeconomic information such as population and poverty was only available at ward level. The data was not provided at enumeration area (EA) level. Nutrition information was only available at provincial level and was therefore not used. Income and irrigation information for small-scale farmers was not available, and this would have provided important data for determining resilience to droughts for different communities;

(iii) Maize production and yield information was only available at provincial level. The correlations between these and VCI could only be studied as a block at provincial level and the behaviour could not be explored in different agro-ecological zones and different livelihood zones;

(iv) Comprehensive data of surface air temperature, evapotranspiration and soil classes was unavailable. A detailed soil map would have improved the vulnerability profile created in the study. The behaviour of surface air temperature and evapotranspiration would have given an indication as to how much moisture the soil was losing during aggressive and regressive droughts, introducing a new dynamic in the characterisation of both droughts;

(v) MODIS NDVI and LST were only available from the year 2000. This limited the study in the sense that the severe droughts of the 1980s and 1990s could not be studied; and

(vi) Due to financial constraints, only two visits to the field were possible. Due to the vastness of the Southern Province, not many of the areas of interest could be visited. This was true for the northern parts of Kazungula, which the study revealed as low risk areas despite being located in agro-ecological Region I.

CHAPTER FIVE: RESULTS AND DISCUSSION

5.1 General Remarks

This chapter interprets the results and later discusses them following the objectives of the study set in Chapter 1.

5.2 The Changes in NDVI Due to Rainfall Variation

In this study, changes in the NDVI due to rainfall variability were observed using monthly NDVI and CHIRPS monthly rainfall. As indicated earlier, this was undertaken in order to assess the changes in NDVI due to rainfall variation at an intra-seasonal level. In each year, NDVI peaked during the months of January and February (Figure 17), which were two of the three months (December, January and February) described as the core rainfall months during the wet season of Zambia by Libanda et al. (2019). NDVI began to fall at the back end of each rainfall season (the month of March) and would drop to the lowest in the months of August and September. NDVI would continue to fall from March to August due to deciduous vegetation losing their leaves in the cold season (May to July), shrubs and grass drying and residual soil moisture depleting. Similarly, NDVI would rise quickly with rainfall because leaves would shoot quickly from deciduous trees and shrubs, and grass would also grow quickly.

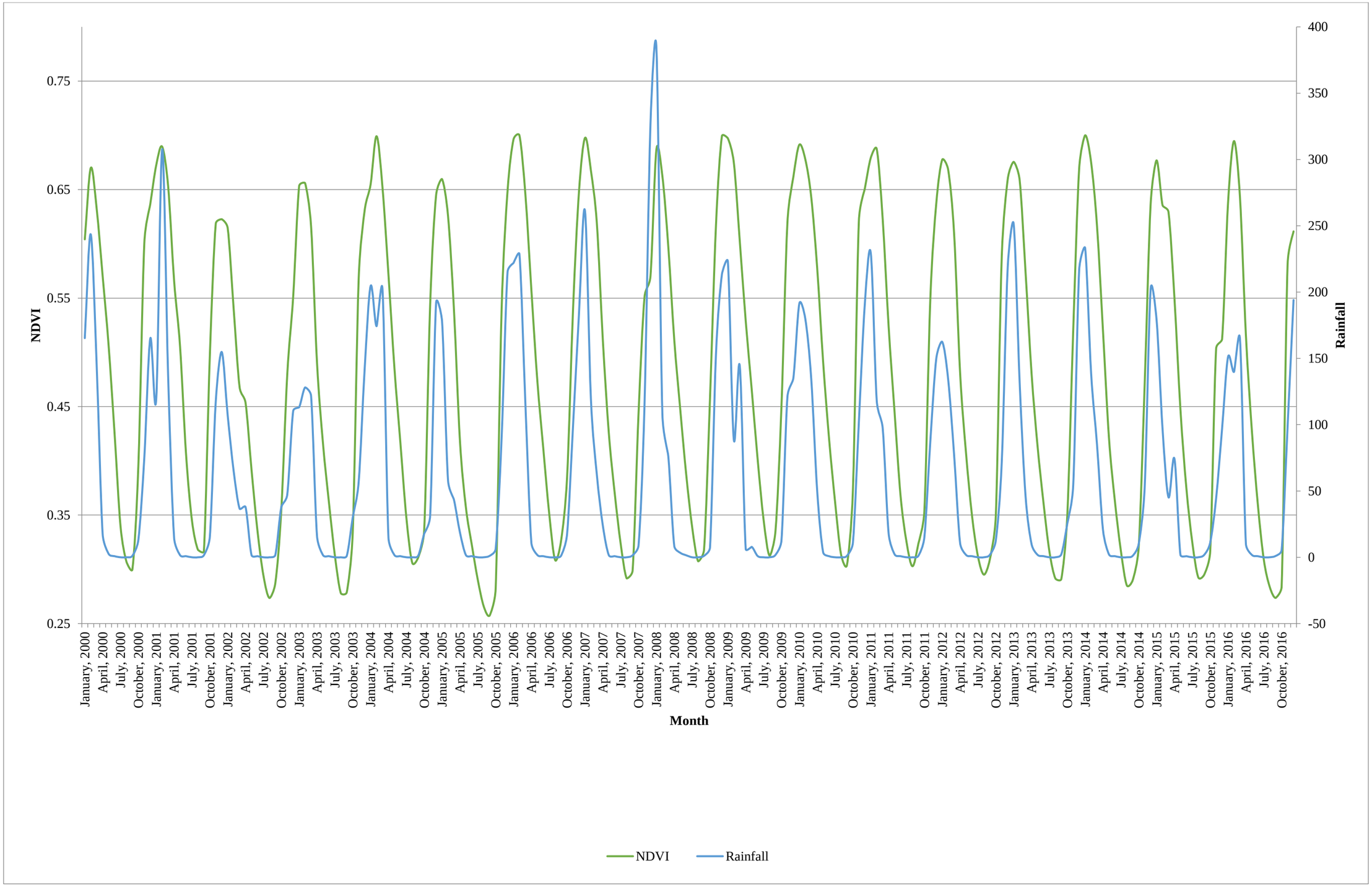

Figure 17: Changes in monthly NDVI and monthly CHIRPS rainfall estimates from January 2000 to October 2016 over the Southern Province of Zambia

The droughts of 2001/2002, 2002/2003, 2004/2005 and 2015/2016 were detected as rainfall and NDVI were well below average (Figures 18 and 19). During these rainfall seasons, rainfall and NDVI fell well below average in the high rainfall months of January and February. For instance, in the 2001/2002 rainfall season, the monthly rainfall of January and February were 107 millimetres and 65 millimetres, respectively. This was well below the average monthly rainfall values for January and February (for the study period), which were 199 millimetres and 145 millimetres, respectively. Correspondingly, NDVI was 0.61 for January, 2002 and 0.54 for February, 2002, both lower than the averages of 0.67 and 0.66 for January and February, respectively. The pattern was similar in all the other drought years, as rainfall and NDVI were below the averages of the study period. For this particular rainfall season (2001/2002), World Bank (2007) reported a 50% deficit of annual consumption requirements, which affected 2.9 million people.

At a monthly scale, NDVI responded quickly to increments in rainfall, peaking in the same months that rainfall peaked without any lag, which was similar to the findings of Rousvel et al. (2013). However, NDVI did drop slower than rainfall and at times lagged by a month. This was due to the availability of residual soil moisture to plants after the rain season had ended. Similarly, Thenkabail et al. (2004) asserted that NDVI had a delayed response to drought mainly because of lagged vegetation responses to developing rainfall deficits, which were as a result of residue soil moisture. Therefore, changes in NDVI during drought were not as drastic as the changes in rainfall. In general, NDVI responded to rainfall patterns, rising when the rainfall season begun and falling when rainfall amounts reduced towards the end of the season.

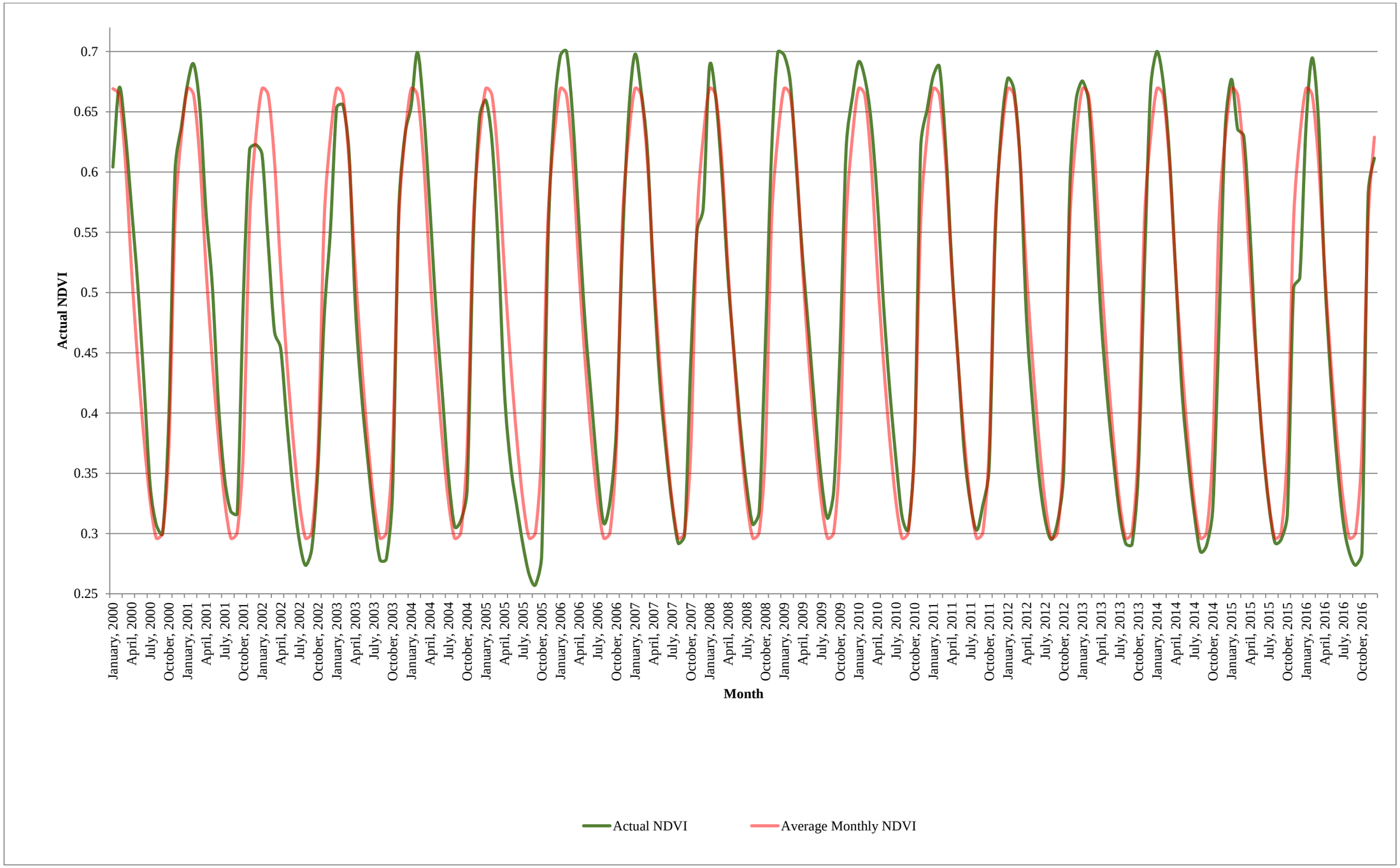

Figure 18: Average monthly NDVI from January 2000 to October 2016 for the Southern Province of Zambia

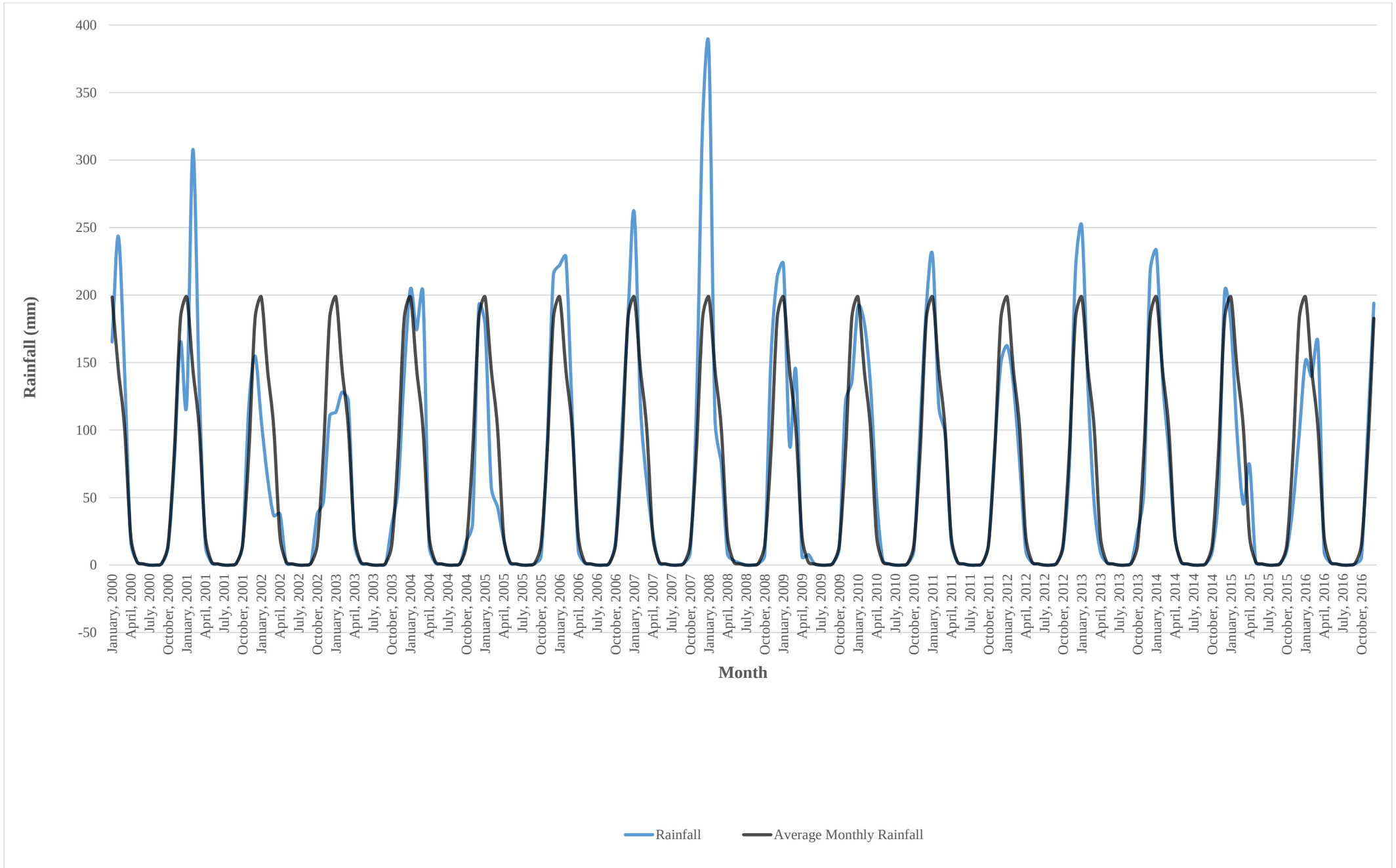

Figure 19: Average monthly rainfall versus actual monthly rainfall from January 2000 to October 2016 for the Southern Province of Zambia

A distinction was made between the patterns of rainfall and NDVI during El Niño events and regular droughts (Figure 20).

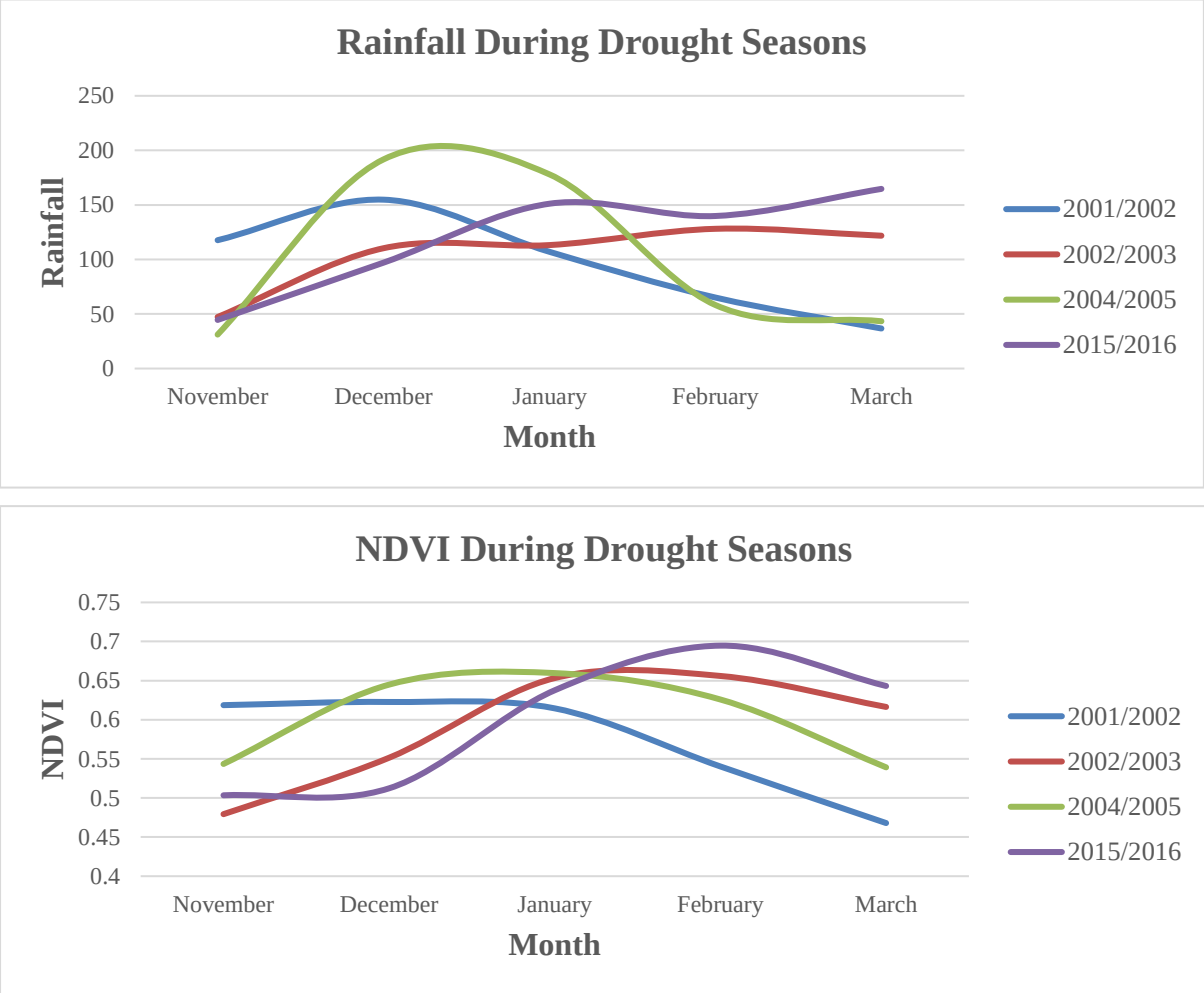

Figure 20: Pattern of rainfall and NDVI during drought seasons over the Southern Province of Zambia

As shown in Figure 20 above, where the El Niño conditions prevailed due to a strong or moderate El Niño signal, rainfall and NDVI were below average during the first months of the rainfall season (November and December, when El Niño signal tends to be strongest (WMO, 2014)). Rainfall and NDVI rose in January, February and March, the following year. This was evident during the seasons of 2002/2003 and 2015/2016, when moderate and strong El Niño events occurred. On the other hand, during regular droughts, rainfall and NDVI were normal in November and December, but dropped continuously then on to March the next year. This was observed during the drought season of 2001/2002. A particular drought year of interest was the 2004/2005 season, where a weak El Niño event occurred (WFP, 2016). In this season, rainfall and NDVI were below average in November, rose in December and peaked in January. This was similar to the droughts borne of prevailing El Niño conditions.

However, both rainfall and NDVI fell below average in the months of February (a core rainfall month (Libanda, et al., 2019)) and March, which was similar to a regular drought. Therefore, the rainfall and NDVI curves of the 2004/2005 season resembled a normal curve. Similarly, Lekprichakul (2008) reported that Zambia experienced late planting rain in the 2004/2005 rainfall season. He further reported that the rains were below average in quantity and were poor and erratic in distribution.

From the observed characteristics and the distinction made, droughts were classified to two categories; aggressive droughts and regressive droughts. The aggressive droughts were those in which drought conditions intensified as the season advanced. For such droughts, no or weak El Niño signals were detected. Conditions in these droughts worsened in the months of January to March, which included the two highest rainfall months (January and February). One such drought occurred in 2001/2002 season, which resulted in a national emergency. Regressive droughts were those where conditions were more intense at the onset, with intensity reducing as the season advanced. Such droughts were as a result of moderate or strong El Niño signal and were very dry in the months of November to January, which WMO (2014) have stated as the months in which El Niño phenomenon peaks. The 2002/2003 was such a drought.

5.3 Rainfall Anomaly and Variability

Monthly rainfall estimates from CHIRPS were used to calculate monthly rainfall anomaly percentage from the rainfall season 1999/2000 to the season 2015/2016. Rainfall variability was also determined over the Southern Province of Zambia. Similar to the observations in rainfall and NDVI trends, the seasons 2001/2002 and 2004/2005 displayed shortfalls in rainfall and, consequently, drought. The effects of El Niño in the seasons 2002/2003 and 2015/2016 rainfall seasons were also observed as negative rainfall anomaly percentages were recorded. In this case, the most severe condition were observed in the 2001/2002 rainfall season whilst the wettest condition were observed in the 2007/2008 season. NDVI corresponded with rainfall anomaly percentage as it dropped in the years 2002, 2005 and 2015, which were all drought years. This was another indication that rainfall highly affected vegetation. Dry conditions were also observed for the month of February, 2013. However, the 2012/2013 season was not considered a drought year in the country.

Intra-seasonal assessment reveals a similar pattern to that observed in rainfall and NDVI trends. Rainfall anomaly percentage assessment of the three wettest months (December, January and February) of a Zambian rainfall season reveals that the 2001/2002 drought was one in which drought intensity increased as the season progressed. Mostly normal conditions were observed in December 2001, which deteriorated to severely dry conditions over most of the province in January 2002. By February 2002, extremely dry conditions prevailed over the province (Figure 21). The drought was classified as aggressive in this study and the pattern was one where the early stages of the planting season received sufficient rainfall, but the rest of the growing season suffered major shortfalls in rainfall resulting in stunted and dry crops. CARE (2002) reported that planting in the 2001/2002 agricultural season, which began in September/October, was crippled by dry conditions. CARE (2002) carried out a rapid assessment in Choma, Kalomo, Kazungula, Monze, Senanga and Sesheke districts and found that all the districts received less overall rainfall compared to normal years. Precipitaion was found to have fallen on fewer days and with less consistent geographic distribution, which resulted in reduced crop planting and yields (CARE, 2002).

The 2002/2003 was a regressive drought. This was evident from the pattern of rainfall anomaly percentage. In this particular season, conditions progressed from moderately dry and severely dry in December 2002, to mostly severely dry in January 2003, and improved to mainly moderately dry conditions in February 2003. This period was one where moderate El Nino conditions prevailed over the region and in particular, Southern Zambia (WFP, 2016). Relief Web (2003) reported the southern and western parts of the country to be the most affected.

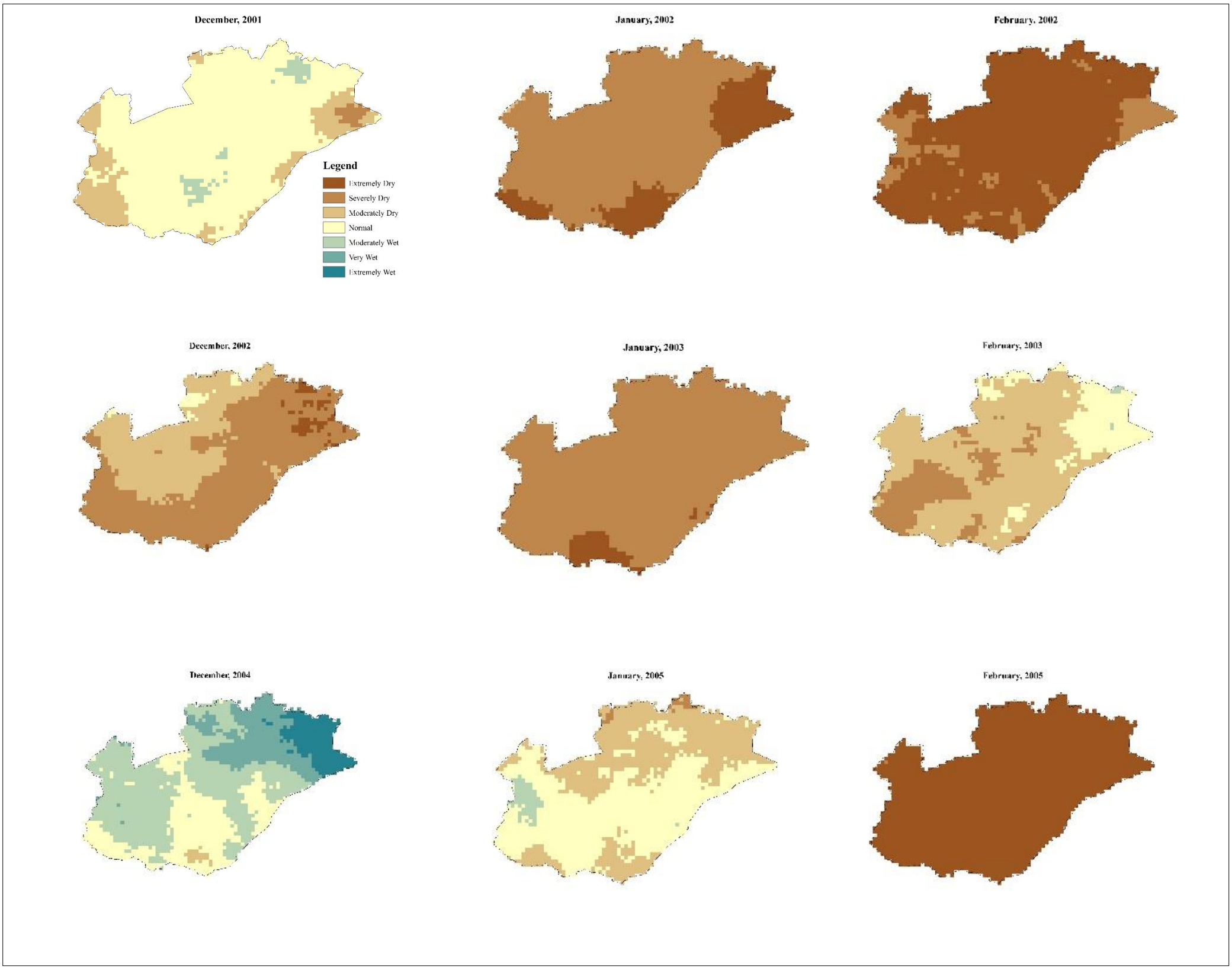

Figure 21: Rainfall anomaly percentage for the months of December, January and February during drought periods in the Southern Province of Zambia

Similar to the 2001/2002 drought season, the 2004/2005 drought season showed characteristics of an aggressive drought, as drought intensity increased as the season went on. The month of December 2004 faced wet conditions whereas in the month of February 2005, extremely dry conditions prevailed over the entire province. The 2004/2005 drought was one borne of weak El Niño conditions (World Bank, 2007). On the other hand, strong El Niño conditions prevailed over the region in the 2015/2016 season. In this period, the pattern of the drought was inverse to that of the drought of the 2001/2002 season as conditions moved from severely dry and extremely dry conditions in December 2015, to wet to normal conditions and dry conditions in February 2016. Therefore, the 2015/2016 drought was regressive. A distinction was defined between droughts borne purely of poor meteorological conditions (below normal rainfall and no El Niño signal) or weak El Niño events (weak signal) and those borne of moderate to strong El Niño events (strong signal). From the rainfall anomaly percentage, droughts that were not induced by El Niño or where a weak signal existed tended to increase in intensity as the season progressed, whilst droughts borne of moderate to strong El Niño events tended to be more severe at the onset and more moderate towards the end. As mentioned earlier, this supported WMO (2014) who stated that the phenomenon of El Niño peaked during the months of November to January, and began to decay the following months. Therefore, rainfall anomaly percentage was also used to categorise droughts as aggressive or regressive.

Spatial and temporal variabilities of rainfall were determined for the Southern Province. Spatial variability of the province was such that the southern parts received significantly less rainfall than those in the northern parts of the province (Figure 22). This followed the pattern of the agro-ecological regions of Zambia, with the exception of the northern part of Kazungula. Despite being in the low rainfall agro-ecological Region I, the northern part of Kazungula received significantly higher rainfall than the other areas in region. The districts of Livingstone, Sinazongwe and Zimba had low average rainfall, whilst the districts of Namwala, Monze and Chikankata received higher rainfall quantities. A different pattern was observed in temporal variability. The southern parts of the province experienced larger variations from the long term seasonal average than those in the northern parts. Temporal variability was especially higher in Zimba, Livingstone, Sinazongwe and the southern part of Kazungula. Rainfall varied as much as 30%, which entailed that rainfall was less reliable in these areas. Despite relatively higher average rainfall, the districts of Choma, Kalomo, Namwala and Pemba also had high temporal variability in rainfall, whilst the districts of

Mazabuka and Chikankata had low variability. Temporal variability of rainfall did not conform to the agro-ecological zones of the country, as was evidenced by the northern part of Kazungula, and by the districts of Choma, Kalomo, Namwala and Pemba (Figure 22).

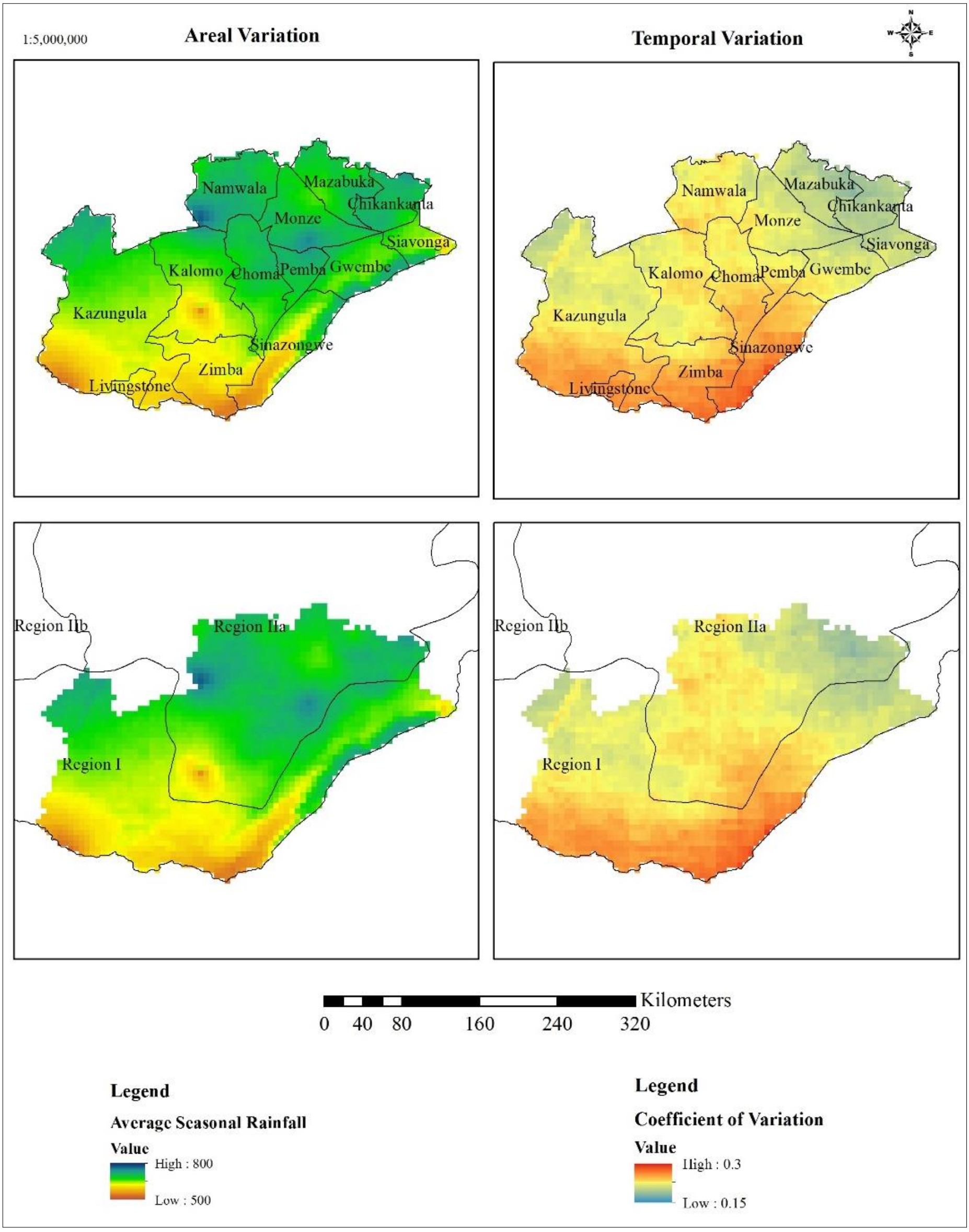

Figure 22: Areal and temporal rainfall variabilities of the Southern Province, Zambia

5.4 Standardised Precipitation Index (SPI) and Drought in the Southern Province

As indicated earlier, SPI was calculated at each of the five manual meteorological stations in the Southern Province. At each station, SPI was low in the seasons 2001/2002, 2002/2003 and 2004/2005 (Figure 23). For instance, for the month of January 2002, SPI was 0.43 (normal) at Chipepo, -1.38 (moderately dry) at Choma, -2.20 (extremely dry) at Kafue Polder, -0.67 (normal) at Livingstone and Magoye. This was a reflection of the droughts that occurred in those periods. Expectedly, drier conditions are observed in the months of November and March at each station, as these are, respectfully, the first and the last months of rainfall in a standard rainfall season.

SPI was plotted against time to establish a trend of drought severity (Figure 24). The same patterns of aggressive and regressive droughts were observed. For instance, the month of December 2001 was severely dry and was followed by the extremely dry month of January 2002. February, 2002 was moderately dry. This explains the food shortages that occurred during the year 2002 as the three high rainfall months of a Zambian rainy season were all dry. The moderate El Nino conditions of the 2002/2003 season were apparent as dry conditions only prevailed in the months of November (severely dry) and December (moderately dry). Conditions improved in the months of January and February. This patterns were identical to the patterns observed in rainfall anomaly percentage.

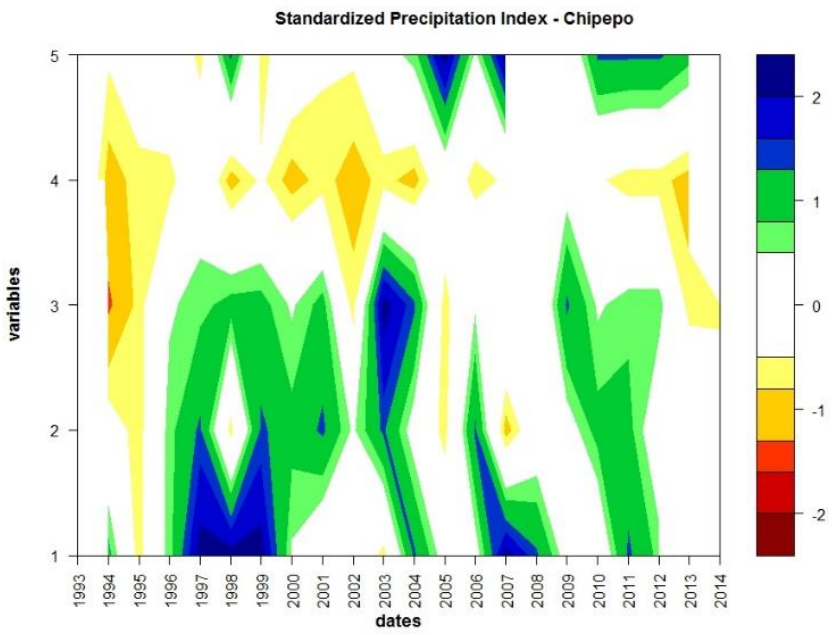

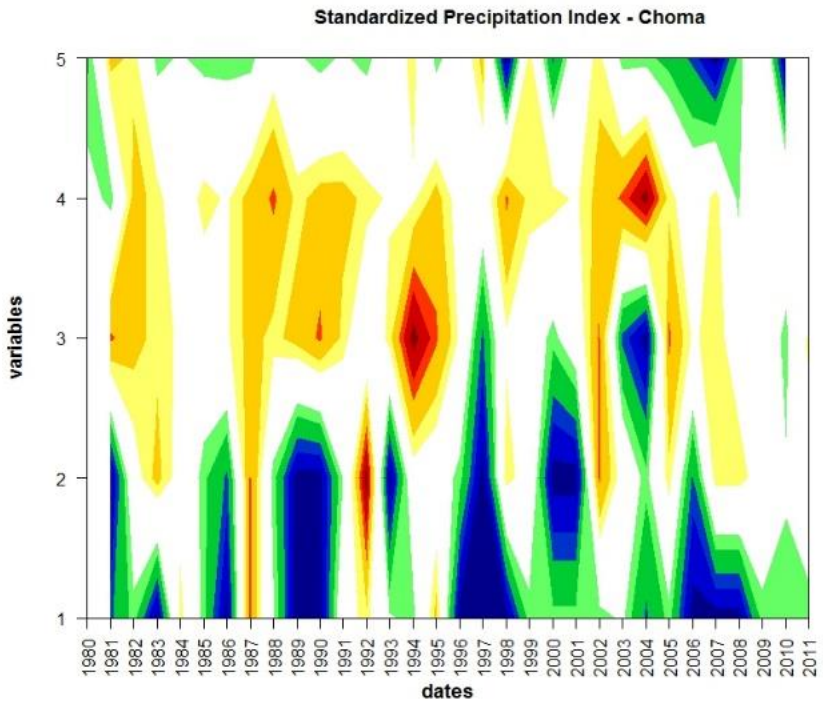

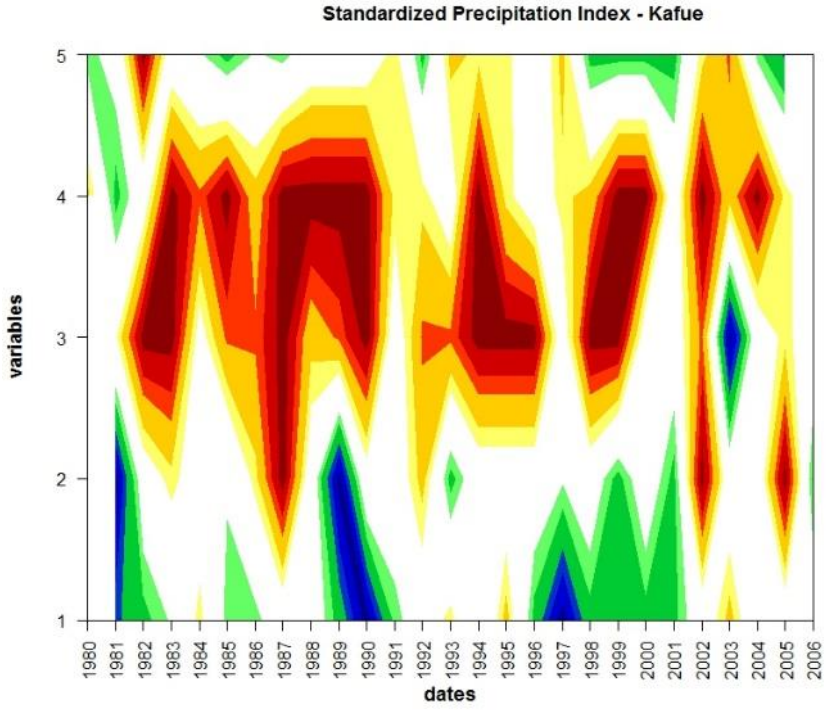

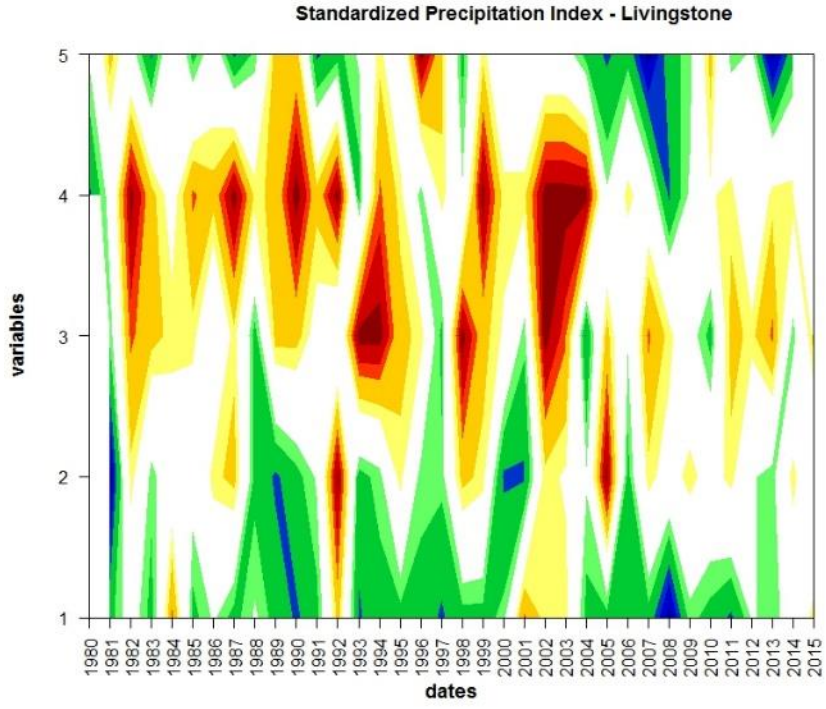

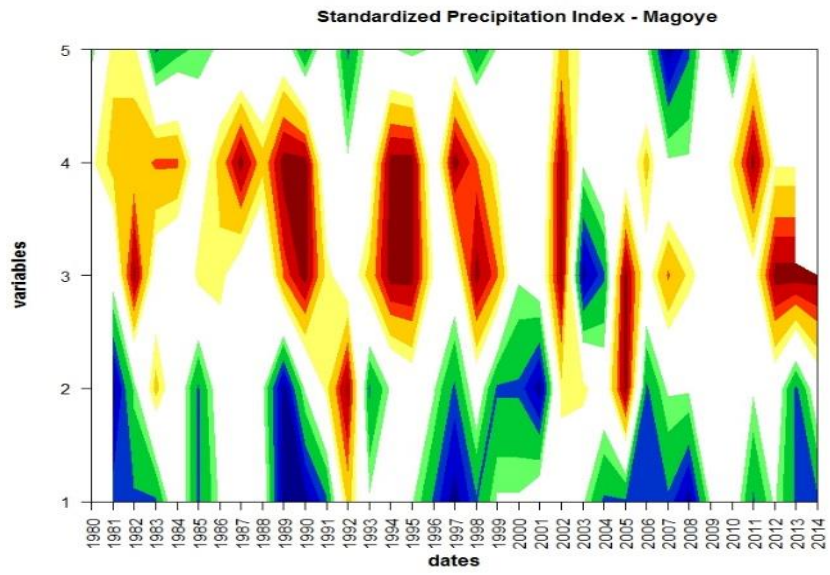

Key for months
1 = January
2 = February
3 = March
4 = November
5 = December

Figure 23: Standardised Precipitation Index (SPI) at the manual meteorological stations in Southern Province

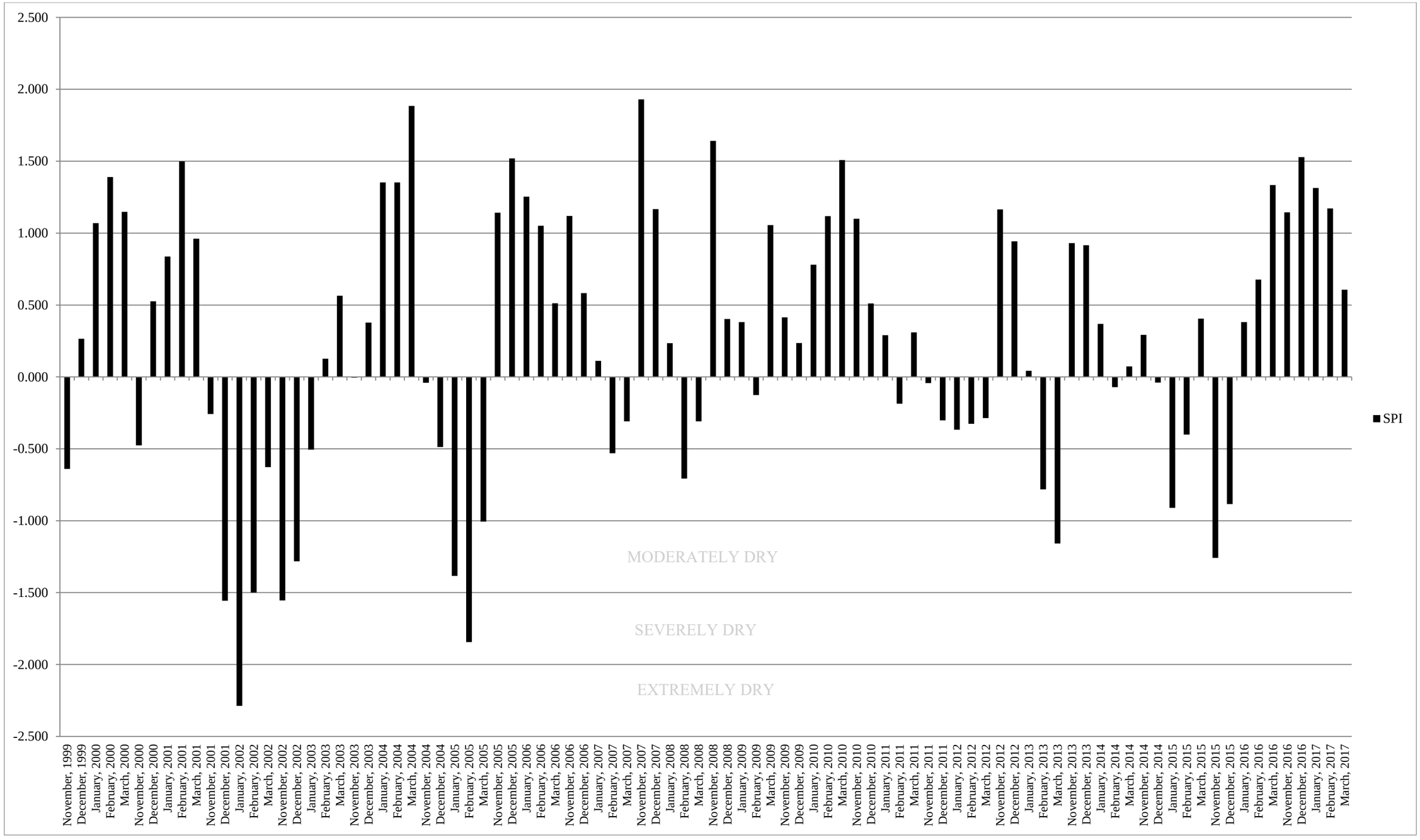

Figure 24: Temporal SPI of the Southern Province of Zambia

Based on the analysis of 36.25 years (January 1981 to March 2016) of CHIRPS monthly rainfall of the Southern Province, SPI indicated a moderate drought occurred 7.65% of the time, a severe drought 6.01% of the time and an extreme drought 1.09% of the time (Table 13). Therefore, moderate droughts were more likely to occur in the province than the other droughts. Furthermore, any kind of drought was expected to occur 14.75% of the time. These percentages are expected because SPI is standardized and normally distributed, and as such, 1.09% for an extreme drought was expected as it is typical for "extreme" events to occur at low frequencies and near normal events to occur the most frequently (WMO, 2012). The standardisation of SPI also allows for the determination of frequency of a drought as well as the probability of the rainfall necessary to end it (Mckee, et al., 1993).

Table 13: Probability of drought recurrence defined by this study

Category	**Frequency**	**Relative Frequency (%)**	**Drought Event Severity (Years)**
Extremely Dry	2	1.09	18.3
Severely Dry	11	6.01	3.3
Moderately Dry	14	7.65	2.6
Near Normal	124	67.76	0.3
Moderately Wet	26	14.21	1.4
Very Wet	6	3.28	6.1
Extremely Wet	0	0.00	0
Totals	183	100.00	

The results of this study indicate that moderate drought is expected to occur once in every 2.6 years, a severe drought once in 3.3 years and an extreme drought once in every 18 years. On the other hand, the wet conditions required to end a moderate drought (moderately wet conditions) will occur once in every 1.4 years and once in 6.1 years for a severe drought (very wet conditions) and 0 years for extreme droughts (extremely wet conditions). Whilst moderately wet events occur more frequently than moderate droughts, severely and extremely dry events occur more frequently than the wet conditions required to end them. Therefore, the study shows that the Southern Province is drier over a larger period of time than it is wet based on analysis of CHIRPS rainfall estimates from 1981 to March 2016. This was similar to the results of Libanda et al. (2019) who found that Zambia experienced more dry years (28) than wet years (27) during the period 1960 to 2016. Libanda et al. (2019) investigated the spatial temporal patterns of drought in Zambia using yearly SPI for the period 1960 to 2016. The study found that extremely dry conditions occurred the least, whilst moderately dry conditions occurred the most. Extremely dry years were years 1992 and 2015, a severely

dry year was 1995 and moderately dry years were 1972, 1980, 1987, 1999 and 2005 (Libanda, et al., 2019). Contrary to Libanda et al. (2019), the results of this study based on the analysis of 36.25 years (January 1981 to March 2016) showed that extremely dry seasons were 1991/1992 and 2001/2002, severely dry seasons were 1994/1995 and 2004/2005 and moderately dry seasons were 2002/2003 and 2015/2016. The main reasons for the differences between this study and Libanda et al. (2019) were the lengths of the study periods and the time step used to calculate SPI and that Libanda et al. (2019) considered annual rainfall whilst this study focuced on seasonal rainfall. Libanda et al. (2019) had a longer rainfall record, which meant there was more data to use in the calculation of SPI which yeilds better results. However, Libanda et al. (2019) focused on annual SPI, which was a larger time step than the monthly time step used in this study. This enabled intra-seasonal study of drought. Despite the differences, the results were similar in that the years in which Libanda et al (2019) detected droughts overlapped with the seasons in which this study detected drought.

A similar pattern was observed in SPI (derived from CHIRPS) as was in rainfall anomaly percentages with regards to the character of the meteorological drought. Drought intensity increased as the season progressed during aggressive droughts, whilst intensity reduced as the season progressed during regressive droughts. For instance, the 2001/2002 drought increased in intensity as the rainfall season progressed (based on SPI) whereas the drought intensity reduced towards the end of the season during the 2002/2003 drought. The same patterns of the meteorological drought were also observed in the assessment of station SPI derived from meteorological data from the Zambia Meteorological Department (ZMD). Considering the 2001/2002 and the 2002/2003 droughts, SPI at the five manual stations revealed an increase in intensity with time during the non El Nino periods, and a reduction during El Nino events. This was evident at the Kafue and Choma meteorological stations (Figure 25).

Spatially, moderately dry droughts occurred mainly in the northern parts of Kazungula and Mazabuka districts (Figure 26). The number of occurrences was also high in Zimba and the southern part of Kalomo. The occurrences were fewest over Namwala, Chikankata and the districts along the Zambezi Escarpment (Gwembe, Siavonga and Sinazongwe).

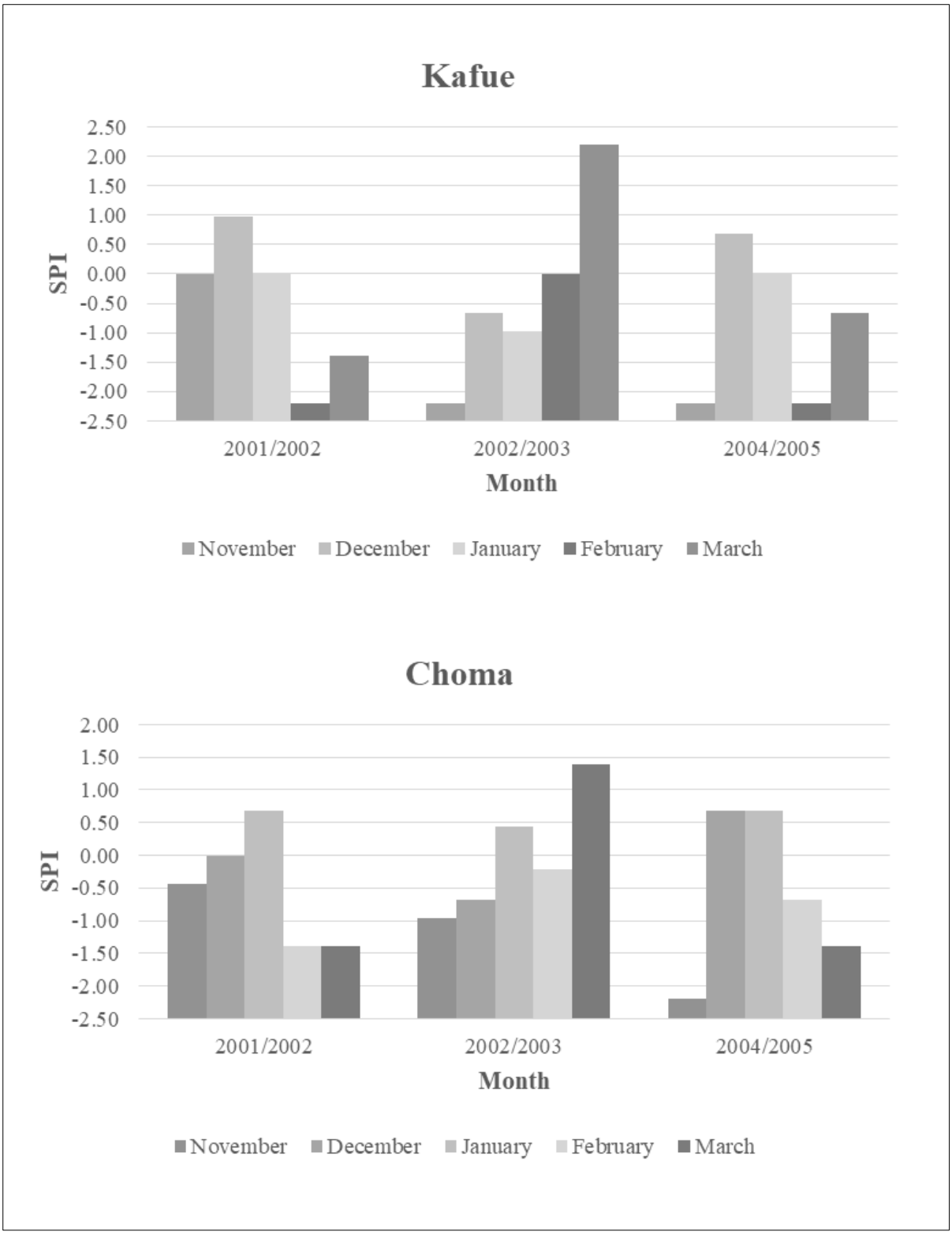

Figure 25: SPI at Kafue and Choma Meteorological stations for the 2001/2002, 2002/2003 ans 2004/2005 rainfall seasons

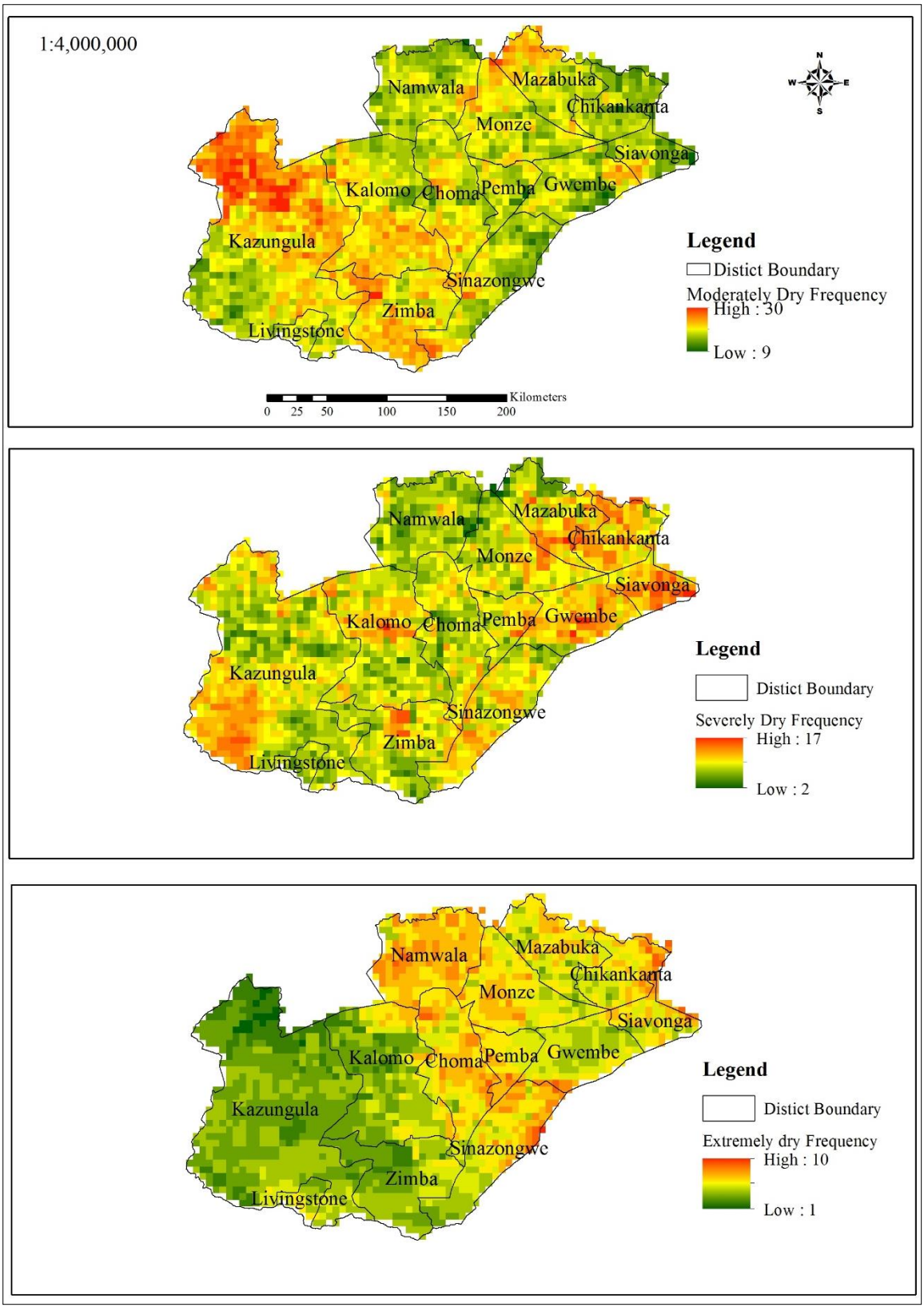

Figure 26: Spatial frequency of each drought severity occurrence for the Southern Province of Zambia

Severely dry droughts occurred mainly in Chikankata, Gwembe and Siavonga. Occurrences of severely dry droughts were also high in the southern part of Kazungula. The fewest occurrences were over Namwala. Extremely dry droughts showed an east to west gradient where occurrences reduced towards the west. The western districts of Kazungula, Kalomo, Livingstone and Zimba had few occurrences of extremely dry droughts whilst the eastern districts of Namwala, Choma, Monze and Pemba had high occurrences. In general, moderate droughts occurred the most over the province, with the frequency reaching as high as 30 in certain areas of the northern part of Kazungula. Extremely dry droughts occurred the least with the frequency only reaching a high of 10 (Namwala). This was similar to the conclusion of Mckee et al. (1993) who stated that extreme events expectedly occurred the least.

5.5 Drought Assessment Using Vegetation Condition Index (VCI)

Vegetation Condition Index (VCI) was used as an NDVI derived index for the study of agricultural drought. Similar to meteorological drought, VCI revealed that agricultural drought increased in intensity as the season progressed for drought periods where there was weak or no El Nino signal. For instance, the condition of vegetation deteriorated as the season progressed in the 2001/2002 season whilst conditions improved in the 2015/2016 drought seasons (Figure 27). Therefore, based on VCI, agricultural droughts were also aggressive or regressive in nature. This was because NDVI responded to reductions in rainfall (despite a lag) across the province. Shortfalls in rainfall entailed drops in NDVI and hence, worsening in conditions of vegetation.

The trend of VCI and maize production (CSO, 2016b) were similar (Figure 28). VCI dropped and rose with maize production for the Southern Province. A notable drop was that of 2002 where VCI was below 40 (35.8) and maize production at its lowest during the study period (63,092.6 mt). VCI was also below 50 (48.9) in 2005. A similar pattern was observed when comparing the trends of maize yield and VCI where both yield and VCI dropped in the years 2002, 2005, 2008 and 2013.

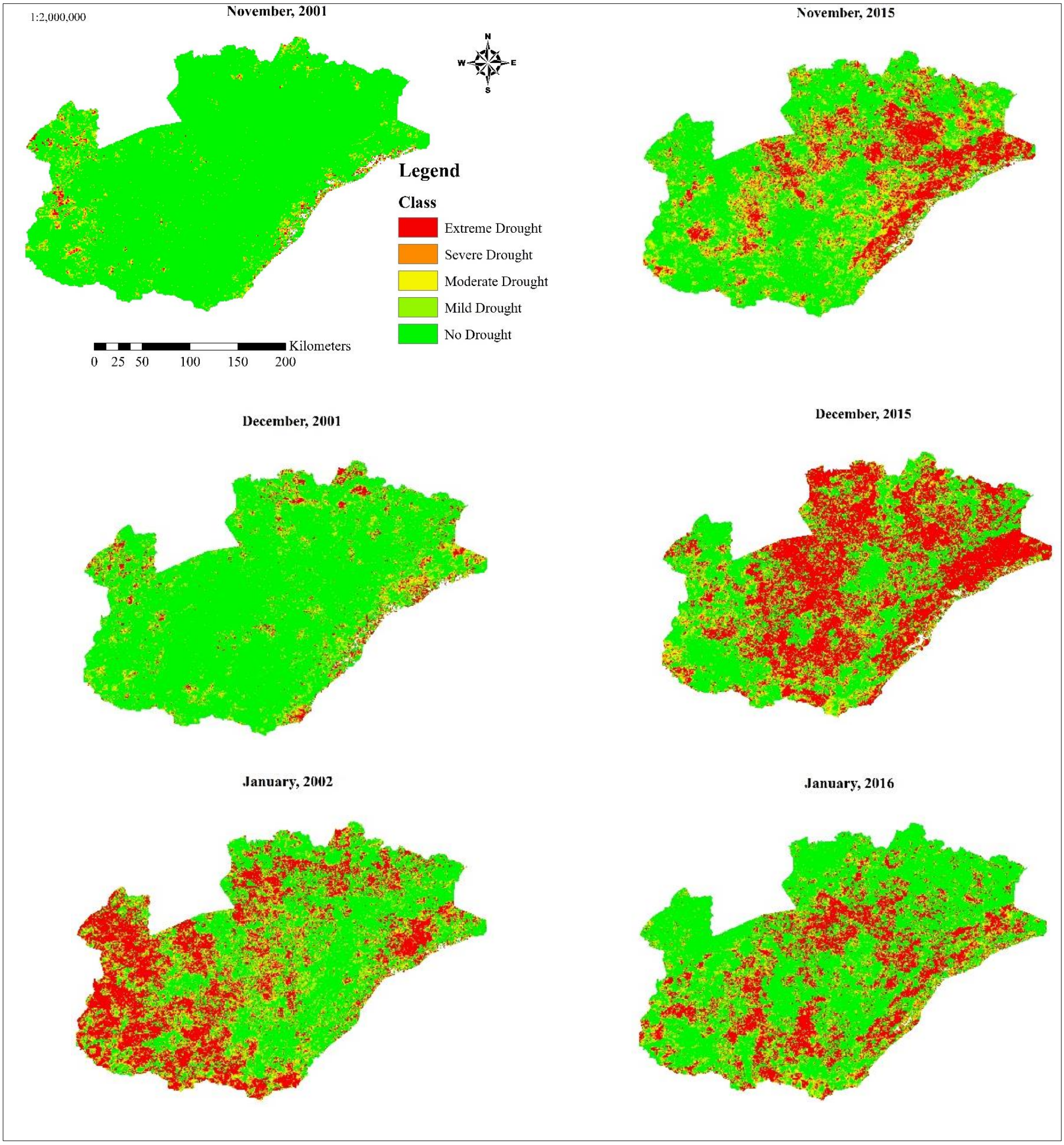

Figure 27: Changes in VCI across the seasons of 2001/2002 and 2015/2016 over the Southern Province of Zambia

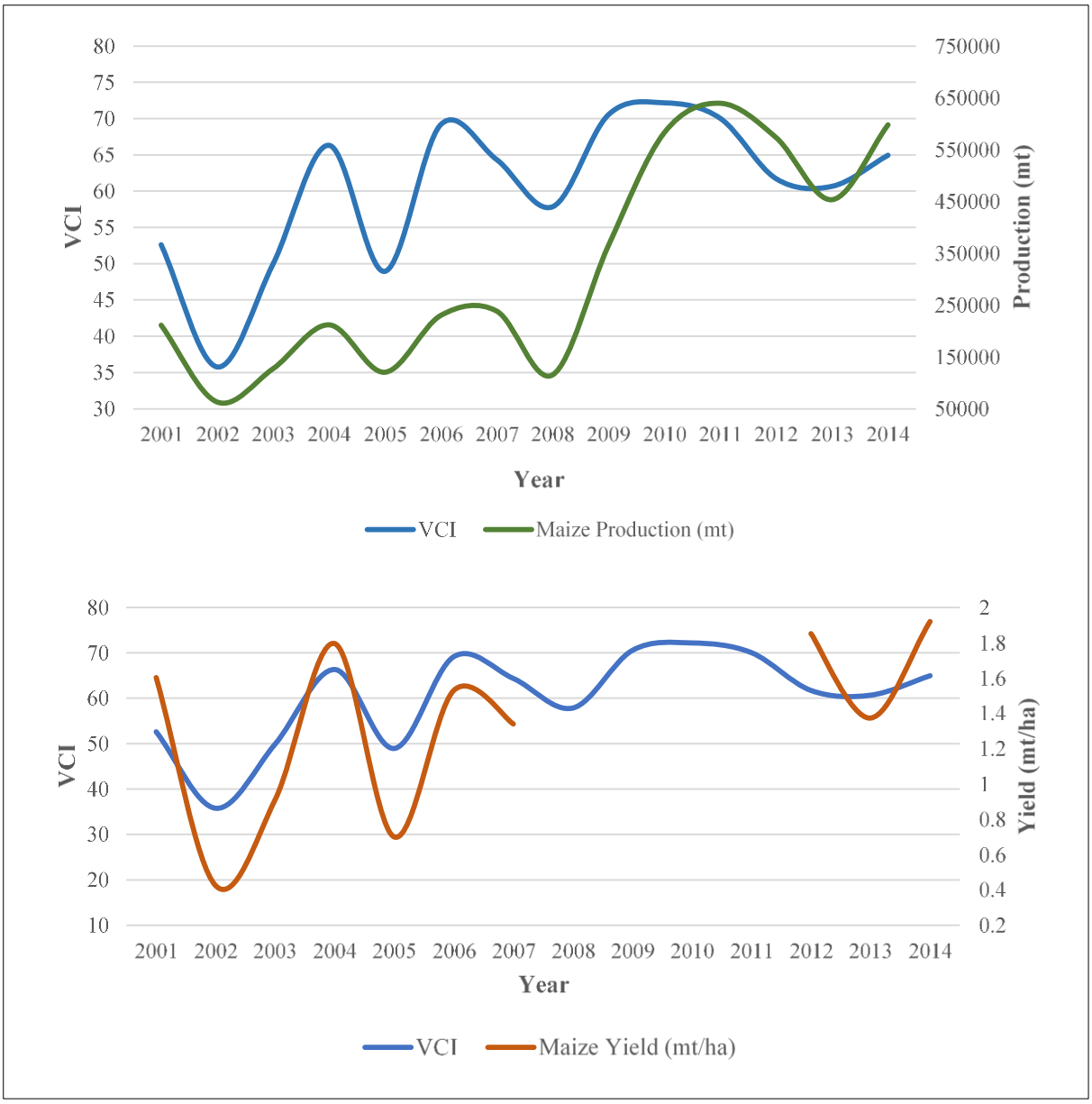

Figure 28: The trends of VCI, maize yield and maize production in the Southern Province of Zambia (note: gaps in yield are years with no data)

As mentioned earlier, the limitation of VCI is that it does not account for soil conditions and detects drought each time crops are stressed even though the cause is not a shortage of water (Kogan, 1997). This was observed for the years 2008 and 2013, which were not particularly drought years. Maize production and yield can fall due to other factors such as bad cultivation practices, pest outbreaks, lack of inputs and soil degradation. Therefore, drops in production and yield are not always results of droughts. For instance, the non-drought years were yield and production fell with VCI (2008 and 2013), VCI was still above 50. In 2008, the month of January received the most rainfall (384 millimetres, CHIRPS) of any month recorded during the study period, despite drops in maize production and yield. Mubanga (2014) conducted a

study in Choma District that assessed the seed breeders recommended maize varieties and how small-scale farmers had adapted to climate variability and change. He concluded that farmers in the district used maize seed varieties that were early maturing and drought tolerant. Mubanga (2014) also noted that farmers supplemented and complimented maize with crops such as okra, beans, soya beans, sorghum, finger millet and cassava in the event of poor maize yields. Furthermore, he concluded that the ZMS 616 from ZAMSEED was the preferred seed due to its drought tolerance, adaptability, stability, disease resistance and yield potential (Mubanga, 2014). This is an example of other factors that affect maize production and yield other than drought.

5.6 Surface Temperature and Soil Moisture Conditions during Drought

The NDVI value of soil was 0.1 and the maximum was 1, as depicted in Figure 29. These values were used to calculate Fractional Vegetation Cover (Fr). The maximum and minimum values of LST in each scene differed from month to month as temperature changed with time. Each T* scene was calculated using the maximum and minimum values of Land Surface Temperature (LST) of the specific months. The result was temperature rescaled to a range of 0 to 1 similar to that of Fr. Figure 30 was the result of the plotting Fr verses T*. Cloud and water pixels were well clustered and with linear fits for the wet and dry edges.

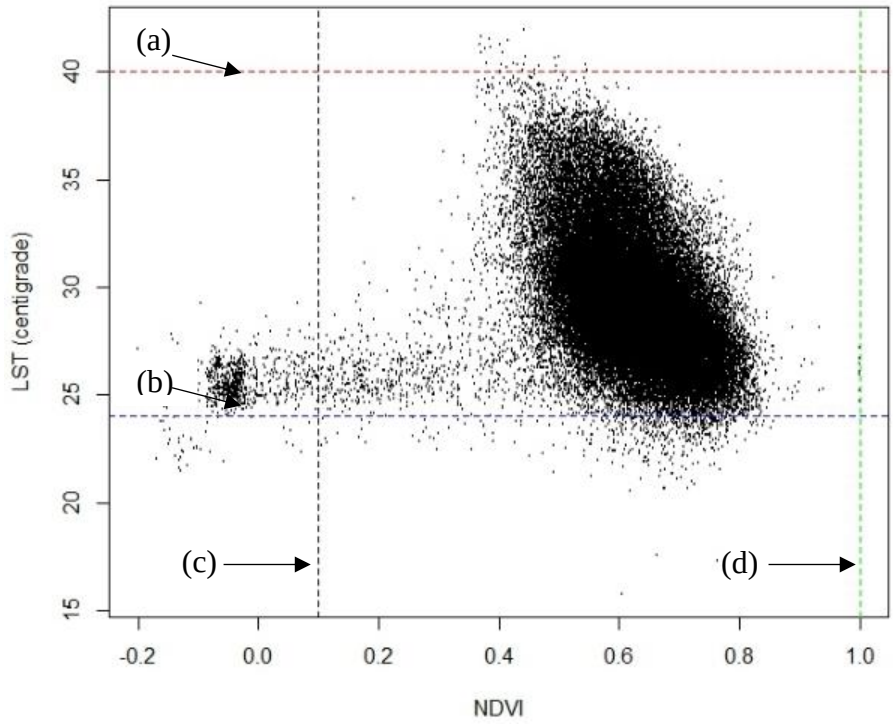

Figure 29: NDVI-LST space depicting (a) LST maximum (b) LST minimum (c) NDVI for bare soil, and (d) maximum NDVI of the Southern Province, Zambia

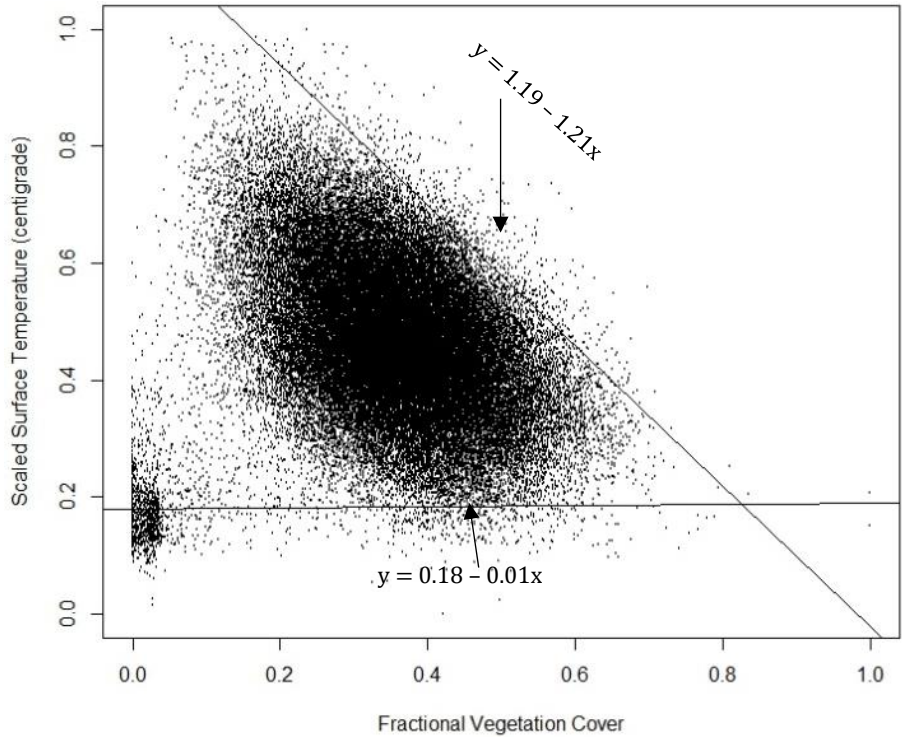

Figure 30: Fractional vegetation cover versus scaled land surface temperature in Southern Province of Zambia

Early rainfall months during seasons where El Niño conditions prevailed were characterised by higher than normal surface temperatures. For instance, in the months of November 2002

and November 2015, surface temperatures exceeded 50 ºc in some parts of the Southern Province (Figure 31). Surface temperatures dropped in December in both seasons despite being relatively higher than other seasons.

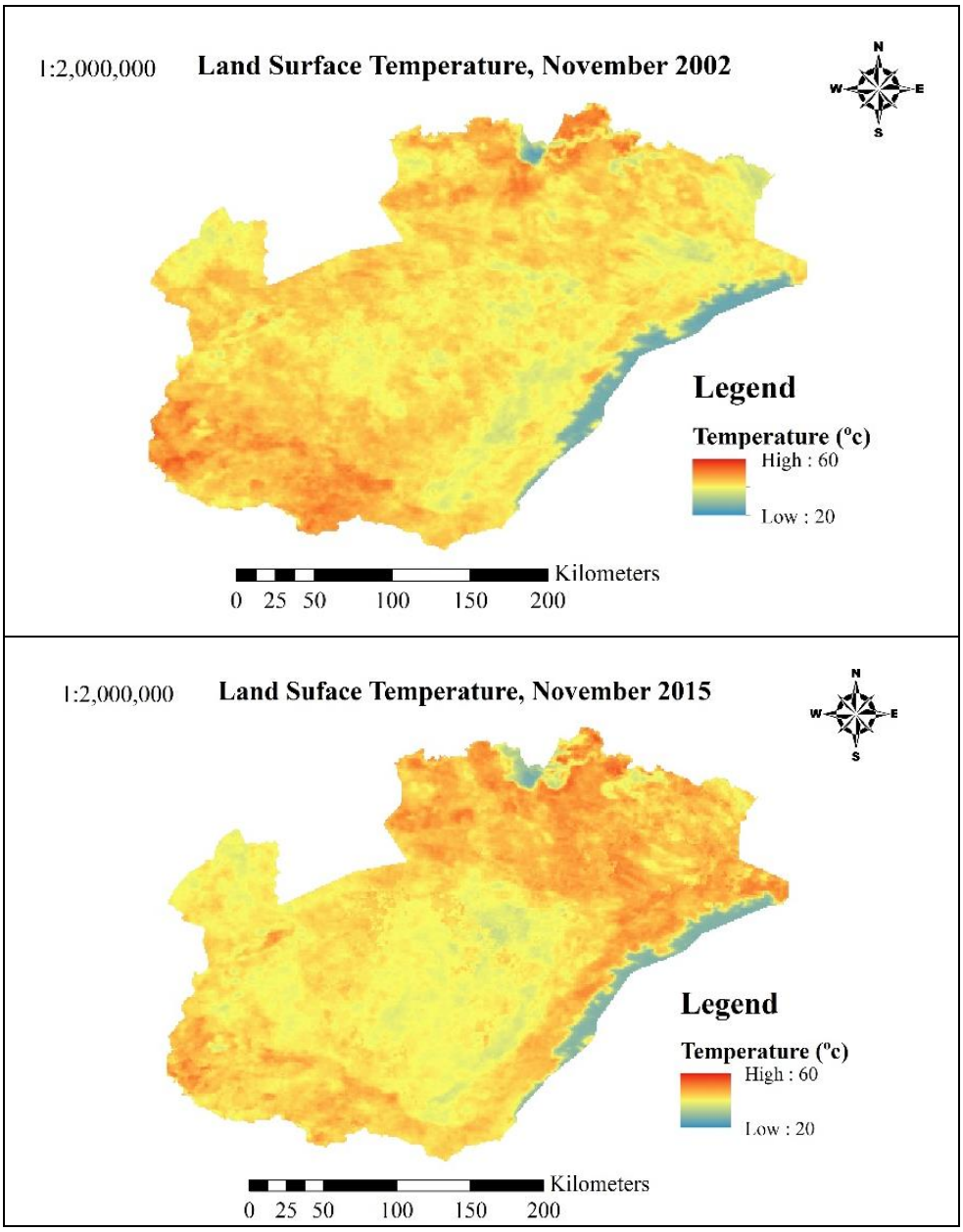

Figure 31: Land Surface Temperature (LST) during November for the drought seasons of 2002/2003 and 2015/2016 for the Southern Province of Zambia

In each season, the month of November was characterised by high LST. This resulted in the plots between Fr and T* to become less triangular and more irregular. However, during regressive droughts, the shape of the plot was trapezoid and not irregular. Figure 32 was a comparison between the two intense months of aggressive and regressive droughts (February and November, respectively) and their counterparts during a normal rain season. The figure

showed that the month of February 2002 (a regressive drought month) had a more distinct triangular shape than that of February 2003 (a normal rainfall month). Similarly, the regressive drought month of November 2015 had a more regular and trapezoid shape than the normal month of November 2003.

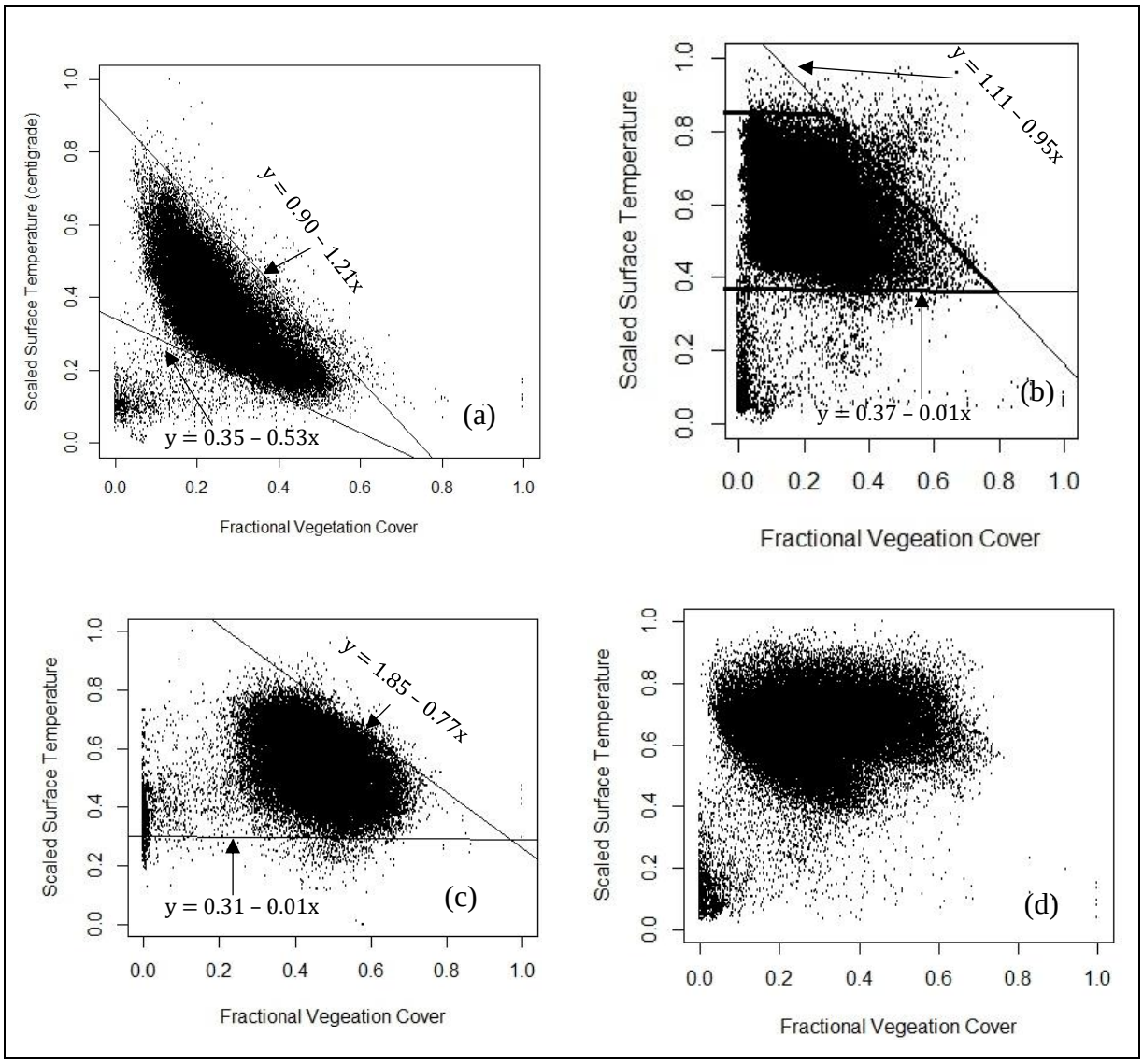

Figure 32: Fractional vegetation cover – scaled land surface temperature space (a) February 2002 drought month with triangular shaped (b) November 2015 drought month with trapezoid shape (c) February 2004 normal year with triangular shape (d) November 2003 normal, in the Southern Province of Zambia

Surface temperatures were higher during regressive droughts because El Niño events lead to increments in the average surface temperatures. Furthermore, the events are associated to a late start of the rainfall season (WFP, 2016), which meant the ground remained heated for longer periods of time before it was cooled by the moisture from precipitation. In general, the gradient at the warm edge (dry edge) tended to increase (line became steeper) as the season

carried on during both aggressive and regressive droughts. This was because more moisture accumulated in the soil with time, despite the characteristics of the drought occurring.

Soil Moisture Index (SMI) was calculated for the Southern Province of Zambia to assess the conditions of soil moisture during the drought months detected using SPI. Low SMI values were observed mainly in areas located in agro-ecological Region I. This was mainly due to low levels of rainfall (400 to 800 millimetres per annum) and high temperatures (35 to 40 ºc), which were even higher during El Niño events. Furthermore, areas along the Zambezi Escarpment had high slope resulting in more proportions of rain water running off than infiltrating the soil. Areas in agro-ecological Region IIa had more favourable soil moisture conditions than those in Region I. This is because Region IIa areas are in the central plateau area of the province, which is flatter, cooler, receives more rainfall and have soils more capable of retaining water. For instance, during the drought months of January and February 2005, the central agro-ecological Region IIa had more soil moisture than the surrounding Region I (Figure 33). However, despite most areas in Agro-ecological Region IIa having better soil moisture conditions, Namwala area had low soil moisture and, therefore, less favourable soil conditions than other areas in the agro-ecological region.

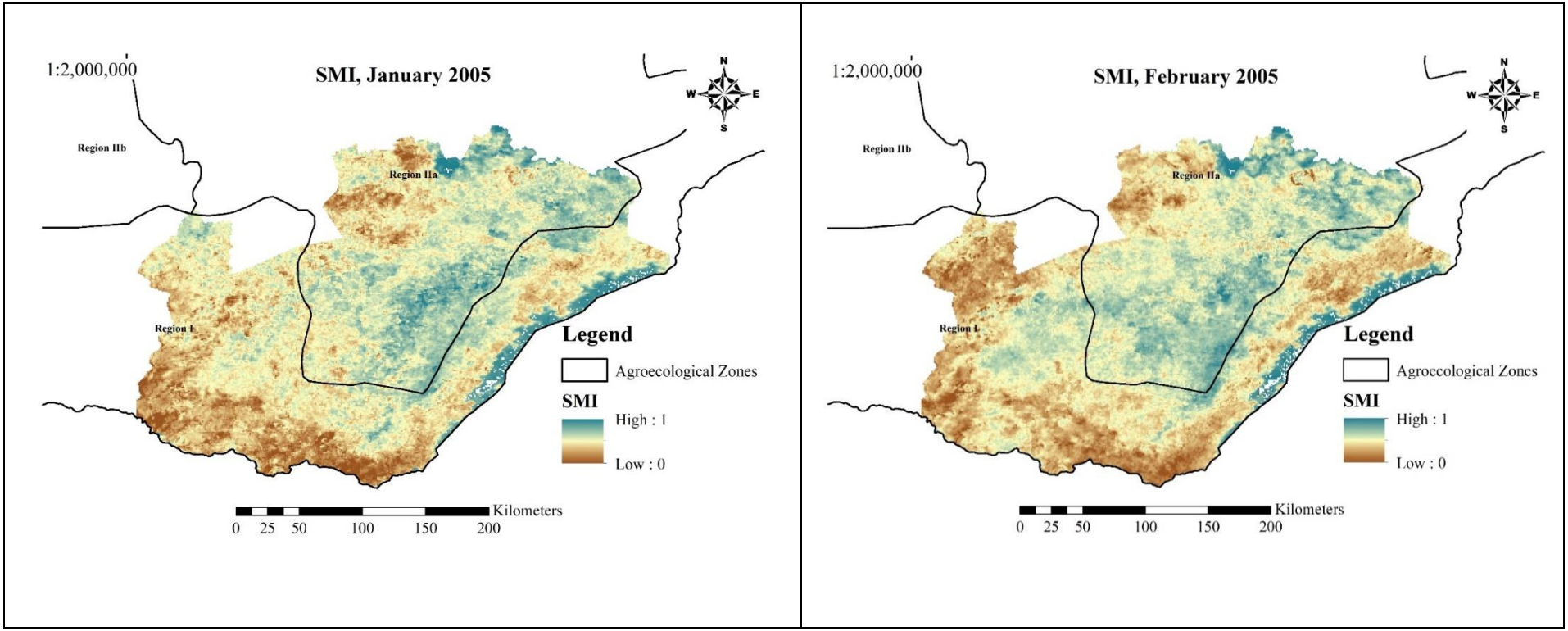

Figure 33: SMI during the months of January and February, 2005 in the Southern Province of Zambia

During El Niño events, soil moisture conditions were less favourable in the months of November and December, when the El Niño phenomenon was strongest and surface temperatures were higher than normal (WMO, 2014). As the phenomenon weakened at the opening of the next year, moisture conditions improved. During aggressive droughts, moisture conditions were more favourable in November and December compared to the years of El Niño. However, soil moisture conditions did not follow the normal patterns observed where conditions would worsen as the drought progressed. In this case soil moisture still accumulated as the season progressed even during aggressive droughts. This was because soil moisture accumulates over time, even though it might not be enough for a successful planting season. However, compared to normal rainfall seasons, soil moisture conditions would be unfavourable in drought seasons. Thenkabail et al. (2004) stated that residual moisture remains stored in the soil even as droughts develop. However, this soil moisture is not enough for the healthy growth of plants and resulted in a delayed response of NDVI to drought conditions.

5.7 Validation of NDVI Based Drought Indices

From the results of the Shapiro-Wilk normality test, monthly NDVI, monthly in situ rainfall measurements and CHIRPS rainfall estimates were not normally distributed as the p-values were less than the confidence interval of 0.05 (4.00E-16, < 2.2E-16 and < 2.2E-16, respectively). This was confirmed by the q-q plots as the distribution of these variables was not linear (Figure 34). Therefore, the Kendall tau correlation and the Spearman's rank correlation coefficients were used to test if any significant correlation existed between monthly NDVI and in situ rainfall. The Kendall tau and the Spearman's rank correlation coefficient were also used to assess whether a correlation existed between monthly NDVI and CHIRPS rainfall estimates.

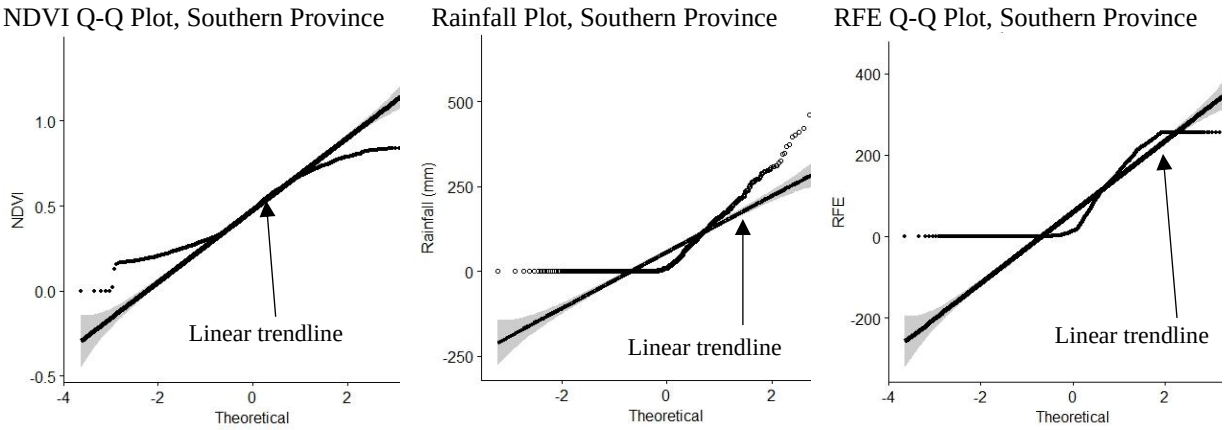

Figure 34: Q-Q plots for monthly NDVI, rainfall and CHIRPS rainfall estimates for the Southern Province of Zambia

The results of the correlation analysis carried out between NDVI and in situ rainfall measurements for the Southern Province showed that there was a significant correlation between monthly precipitation and monthly NDVI. The Kendall tau was 0.59 and the Spearman r_s was equal to 0.78. For both tests, the p-value was less than 2.2E-16. Therefore, the null hypothesis was rejected. NDVI increased with rainfall indicating a direct and positive relationship (Figure 35). This was similar to the findings of Wang et al. (2003), who found a strong and positive correlation between growing season NDVI (from NOAA-AVHRR) and in field rainfall measurements from 410 weather stations in the Great Plains of Kansas State. From the results of this study, the positive characteristic was evident in both aggressive and regressive droughts where NDVI increased as rainfall increased, or dropped as rainfall dropped.

Monthly NDVI was at optimum level when rainfall was at approximately 200 millimetres in a month. However, NDVI began to saturate when 250 millimetres of rainfall was exceeded. The rainfall-NDVI correlation was strongest at Choma Station and weakest at Magoye (Table 14).

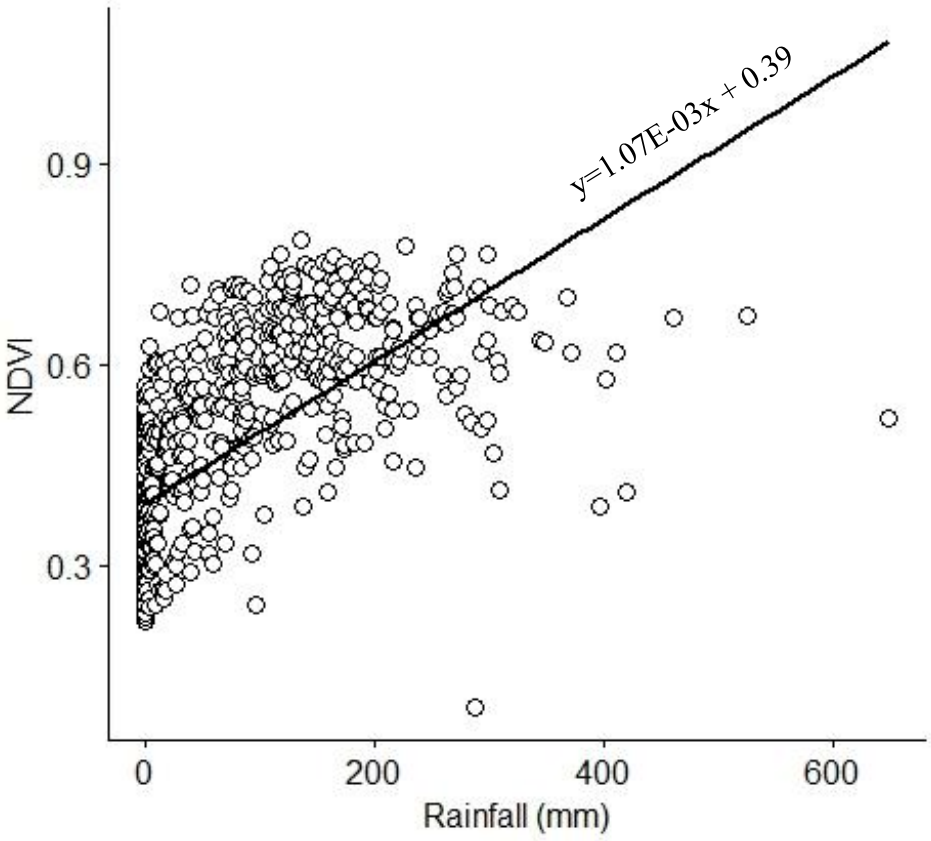

Figure 35: Rainfall-NDVI correlation of the Southern Province of Zambia

Table 14: Correlation at each station used in this study

Station	Kendall Tau	Spearman rho
All Stations	0.59	0.78
Chipepo	0.62	0.81
Choma	0.65	0.83
Kafue	0.61	0.78
Livingstone	0.64	0.82
Magoye	0.56	0.74

There was a significant correlation between monthly NDVI and monthly rainfall estimates from CHIRPS (Figure 36). The correlation was fairly strong at 0.54 (tau) and 0.74 (r_s). Similar to the monthly rainfall-NDVI correlation, NDVI rose steadily with the rainfall estimates indicating a positive relationship. Rousvel et al. (2013) carried out correlation analysis between monthly NDVI and gridded rainfall extracted from the Global Precipitation Climatology Project (GPCP) for Central Africa. The results of their study revealed that there was a relatively strong correlation between the two variables, especially in the brush-grass Savanna (0.90).

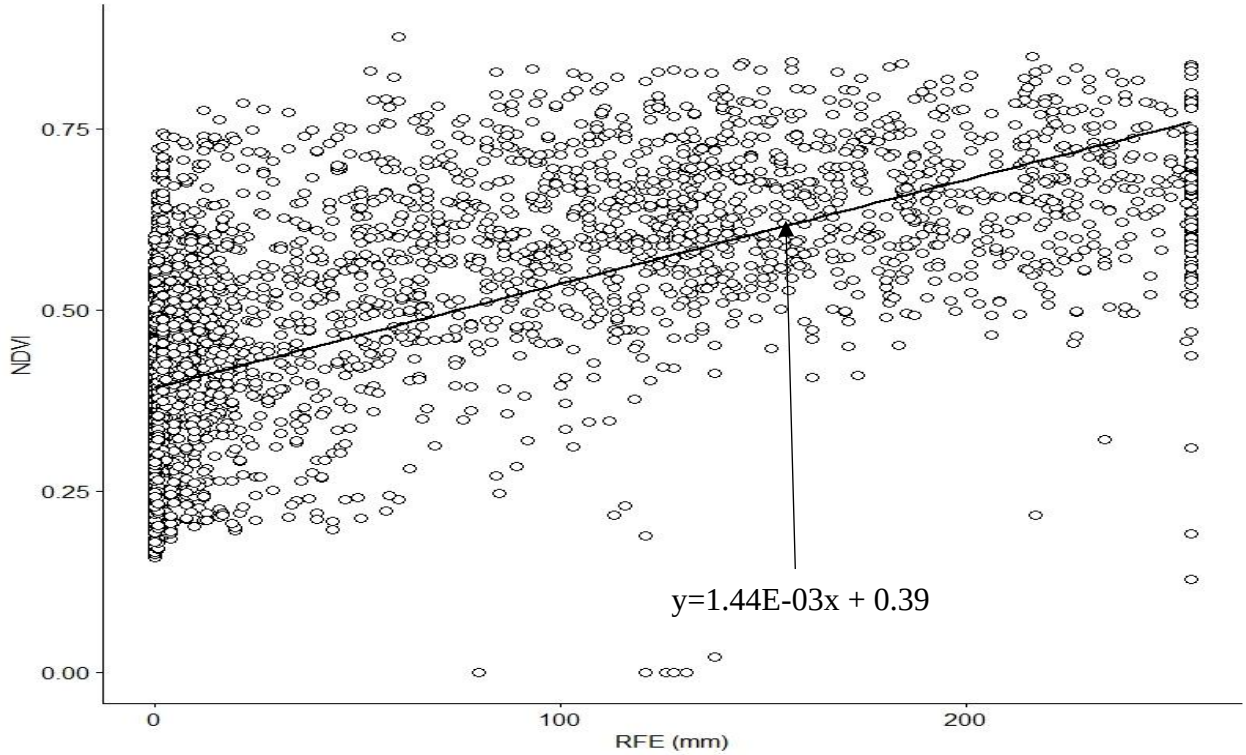

Figure 36: Monthly NDVI – RFE correlation of the Southern Province of Zambia

The correlation between NDVI and the two rainfall data sets showed that NDVI can be used to assess variations in rainfall and drought. The existence of correlation meant that temporal NDVI data was validated as an alternative or supplement in the assessment of drought, as NDVI has a direct relationship with rainfall. However, this relationship differed between different vegetation classes.

The correlation between NDVI and rainfall varied depending in the vegetation type. Using monthly NDVI and monthly CHIRPS data, correlation was determined in the four vegetation classes of the Zambia Land Cover Map Scheme I of 2014. The classes were forests, grasslands, croplands and wetlands (vegetated). Significant correlations existed in all four classes. The relationships were positive (Figure 37) and relatively high. However, certain classes revealed higher correlations than others. Using the Spearman's rank correlation coefficient, correlation between monthly NDVI and monthly CHIRPS rainfall data, it was determined that correlation was highest within the grasslands (0.81) and the croplands (0.80). The correlation reduced in the forests (0.77) and wetlands (0.76). This was an indication that grasslands responded the fastest to rainfall variations while wetlands were the slowest. The response in wetlands was slow because soil water was available for longer periods of time than in the other classes. Rousvel et al. (2013) had similar results where the correlation for a one month time step was highest (0.90) in the brush-grass Savanna Bioclimatic Ecoregion of

Central Africa. The other ecoregions were semi-desert and steppe (0.26), deciduous forest-woodland (0.42) and tropical forest (0.44). Wang, et al. (2003) aslo had similar results where correlation between two biweekly periods of NDVI and rainfall were high in grassland at 0.63, moderate in forests at 0.45 and weak in croplands at 0.30. In Wang, et al. (2003) , however, the correlation was higher in forests than in croplands. This was due to the study being carried out in the Great Prairie, an area with highly mechanised agriculture supported by irrigationof Kansas State. In this study, much of the cropland is rain fed, and therefore, more correlated to rainfall than forests. A study over Tropical Africa carried out by Camberlin et al (2007) found that correlations between NDVI and rainfall were distinctively higher in semi-arid open grasslands and croplands, which is similar to the findings of this study.

As indicated earlier, the differences in the correlation between NDVI and rainfall in the different classes (Appendix 6) were used as a basis of weighting land cover classes for vulnerability mapping which are further explained in the study.

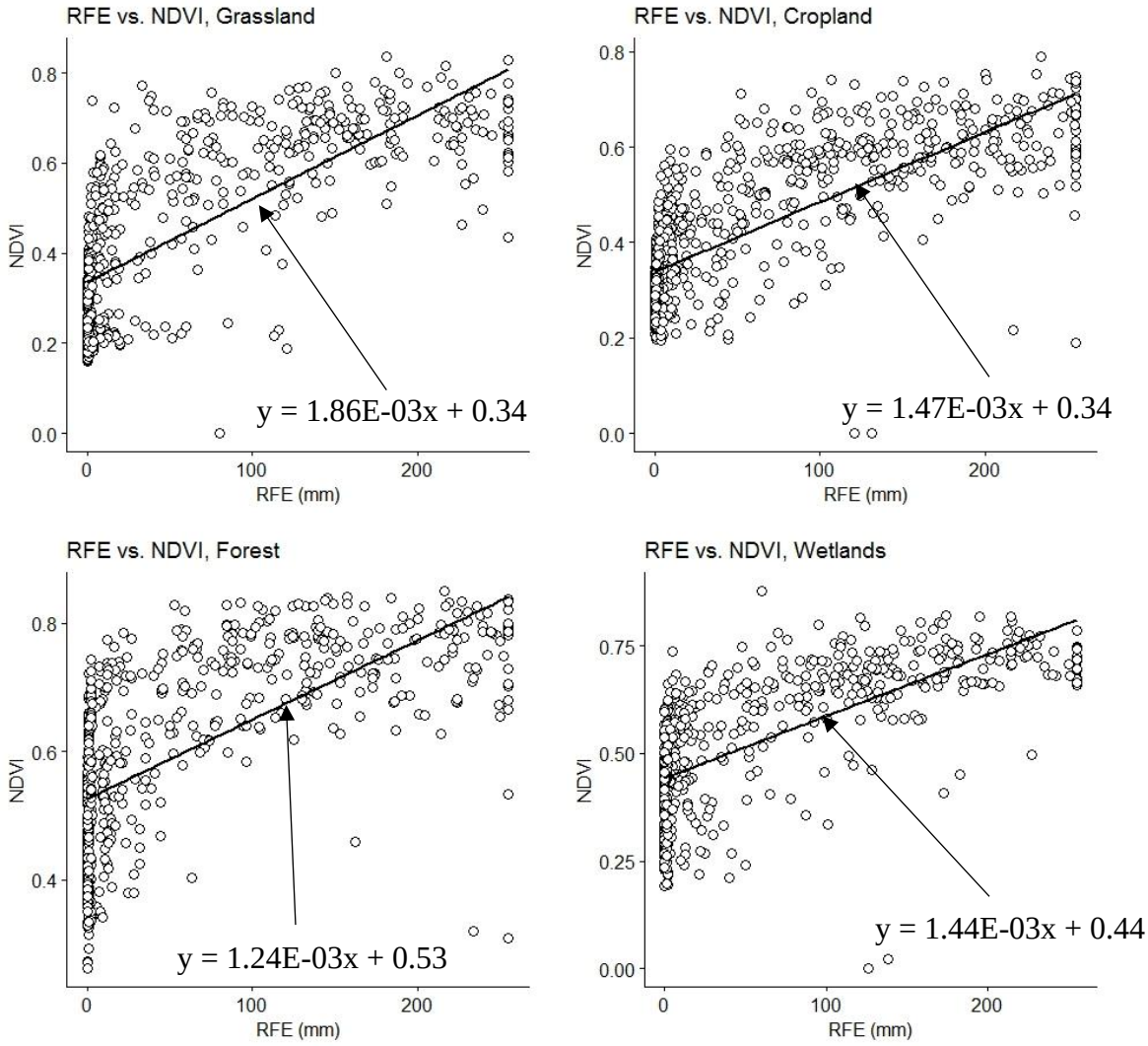

Figure 37: NDVI-Rainfall Correlation in different land cover classes, Southern Province, Zambia

Unlike the NDVI and rainfall datasets, seasonal average VCI, yearly maize production and yield were all normally distributed. The results of the Shapiro-Wilks tests showed p-values greater than 0.05 (0.15 for VCI, 0.06 for maize production and 0.33 for maize yield). The q-q plots displayed a linear distributions (Figure 38), which confirmed the normal distribution of data. Consequently, the Pearson's Product Moment Correlation Coefficient was used.

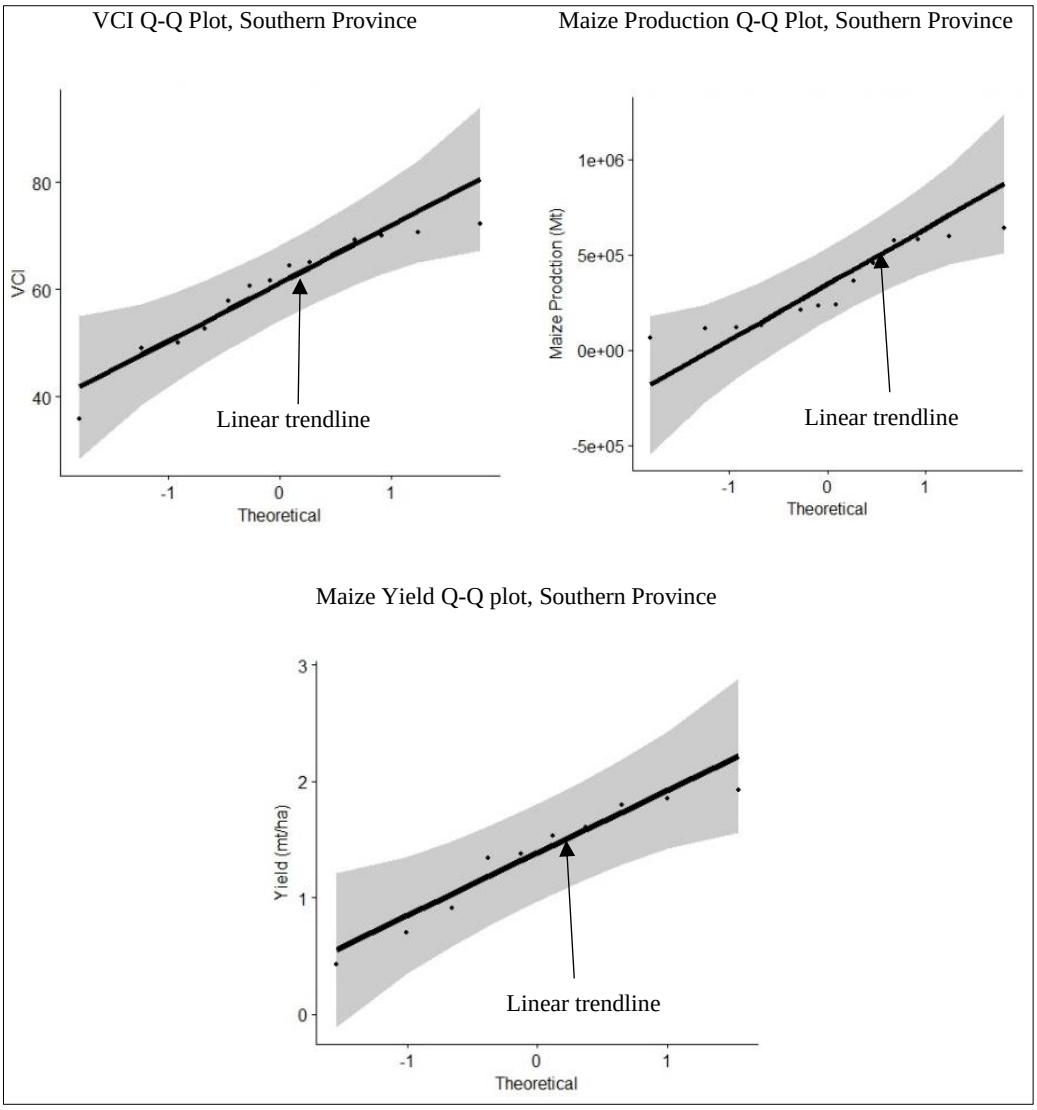

Figure 38: Q-Q plots of VCI, maize production and yield, Southern Province of Zambia

There was a significant correlation of 0.66 (p-value = 0.01) between maize production and VCI (Figure 39). A stronger correlation of 0.84 (p-value = 0.002) existed between maize yield and VCI. The correlation was stronger because yield was a measure of the mass of maize per unit hectare whereas production was the absolute total for the entire area. This meant that higher yields resulted in more pixels with higher NDVIs. On the other hand, production could be high in fewer areas (pixels) and NDVI would still rise whilst other areas were not as productive.

The relatively strong correlations between VCI and maize production and yield indicates that VCI can be used to assess agricultural drought for the Southern Province of Zambia. Unganai and Kogan (1998) used VCI and Temperature Condition Index (TCI) to estimate crop yield and to track drought in Southern Africa, mainly in Zimbabwe. They found that the VCI-corn

(maize) yield correlations ranged from 0.70 to 0.90 across the principal corn regions of Zimbabwe. The correlations reduced to a range of 0.30 to 0.50 in areas where tea and coffee were the major crops and corn was minor (Unganai & Kogan, 1998). Makaudze and Miranda (2008) assessed the feasibility of area-yield drought insurance in Zimbabwe. They found that VCI correlations reached a maximum at 0.64 and 0.73 for maize (corn) and cotton yields, respectively during the growing season.

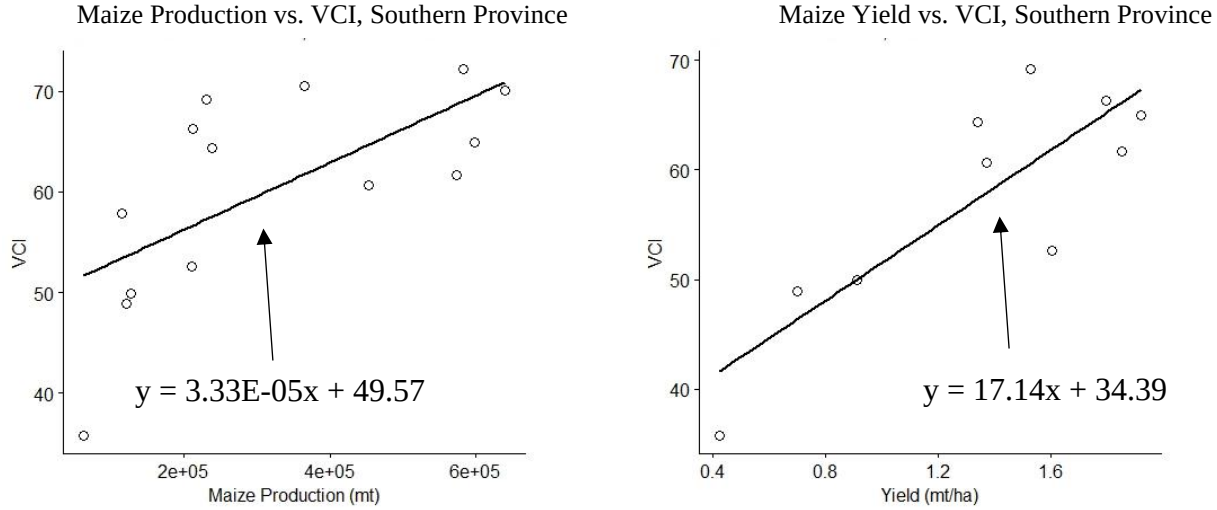

Figure 39: Maize production – VCI and Maize Yield – VCI correlations, Southern Province of Zambia

Monthly in situ soil moisture measurements at 5cm and 10cm, and SMI were normally distributed, as they displayed a linear scatter (Figure 40) on the q-q plots. This was confirmed using the Shapiro-Wilks tests where the p-values of both parameters were greater than 0.05 (0.11 for SMI, 0.18 for soil moisture measurements at 5 centimetres and 0.39 at 10 centimetres). Therefore, the Pearson's Product Moment Correlation Coefficient was used.

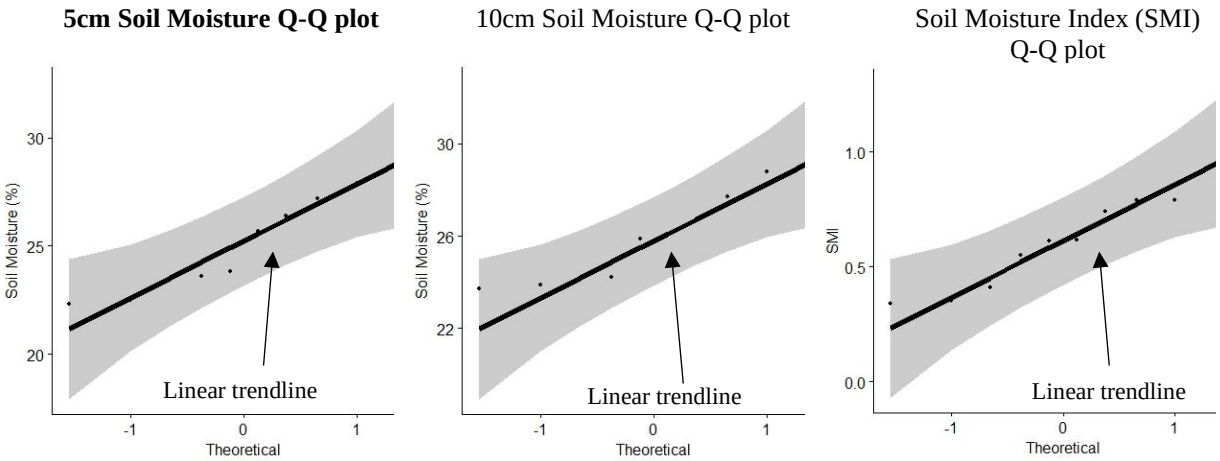

Figure 40: Q-Q plots for soil moisture at different depths and SMI, Southern Province of Zambia

At 5 centimetres, there was a significant correlation between soil moisture from in situ measurements obtained from ZMD and SMI (Figure 41). The correlation of 0.71 was positive. At 10 centimetres soil depth, the correlation reduced significantly to 0.40. The reduction in the correlation signified that SMI was best used for soil moisture evaluation at shallow depths and was not reliable at deeper soil depths. Similar results were reported by Wang, et al. (2007), who found that at a 10 centimetre depth, observation do not actually correspond to the surface parameters that are observed by the MODIS data. However, the results of Wang, et al. (2007) suggested that soil moisture estimation at shallow depths are feasible through combining ground measurements and MODIS land parameters. Therefore, the existence of a correlation between soil moisture measurements at 5 centimetre depths was validation that SMI could be used to assess soil moisture conditions at shallow depths in the Southern Province of Zambia. Therefore, SMI could be used to assess agricultural drought based on soil moisture conditions (Leeuwen, 2015).

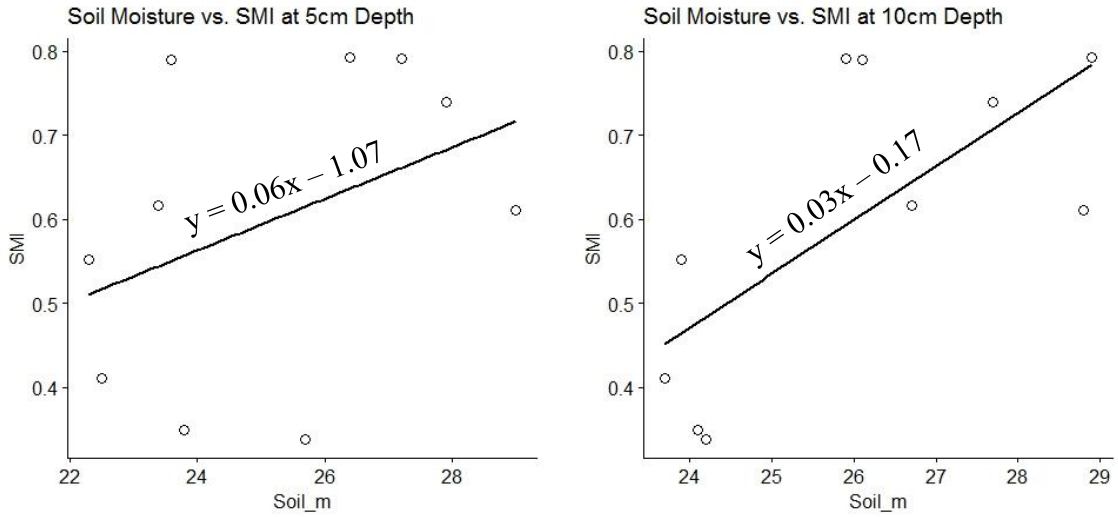

Figure 41: Soil Moisture-SMI Correlation for the Southern Province of Zambia

5.8 Drought Risk Mapping of the Southern Province, Zambia

As indicated in the study methods, the approach used to determine drought risk was the summation of hazard, exposure and vulnerability, which was in line with both the Cap-Net (2015) and Joint Research Centre (2018). Assessment of vulnerability, exposure and risk were done at pixel level and at district level for the Southern Province of Zambia.

5.8.1 Drought Hazard of the Southern Province of Zambia

Drought hazard was classified into two categories; meteorological and agricultural. The majority of the Southern Province faced high levels of meteorological drought hazard (Figure 42). The main hot spots were the south-western part of Kazungula and the adjoining area between Mazabuka and Monze. Hazard occurrences were also frequent in areas along the Zambezi Valley and the Kariba Lakeshore. The least hazardous areas to meteorological drought were the northern parts of Kazungula (despite high frequency of moderately dry droughts), the southern part of Kalomo and Namwala. Despite being in agro-ecological Region I, the northern part of Kazungula was in livelihood zone ZM02, which is the south-western cereal, livestock and timber zone (FEWS NET, 2014).

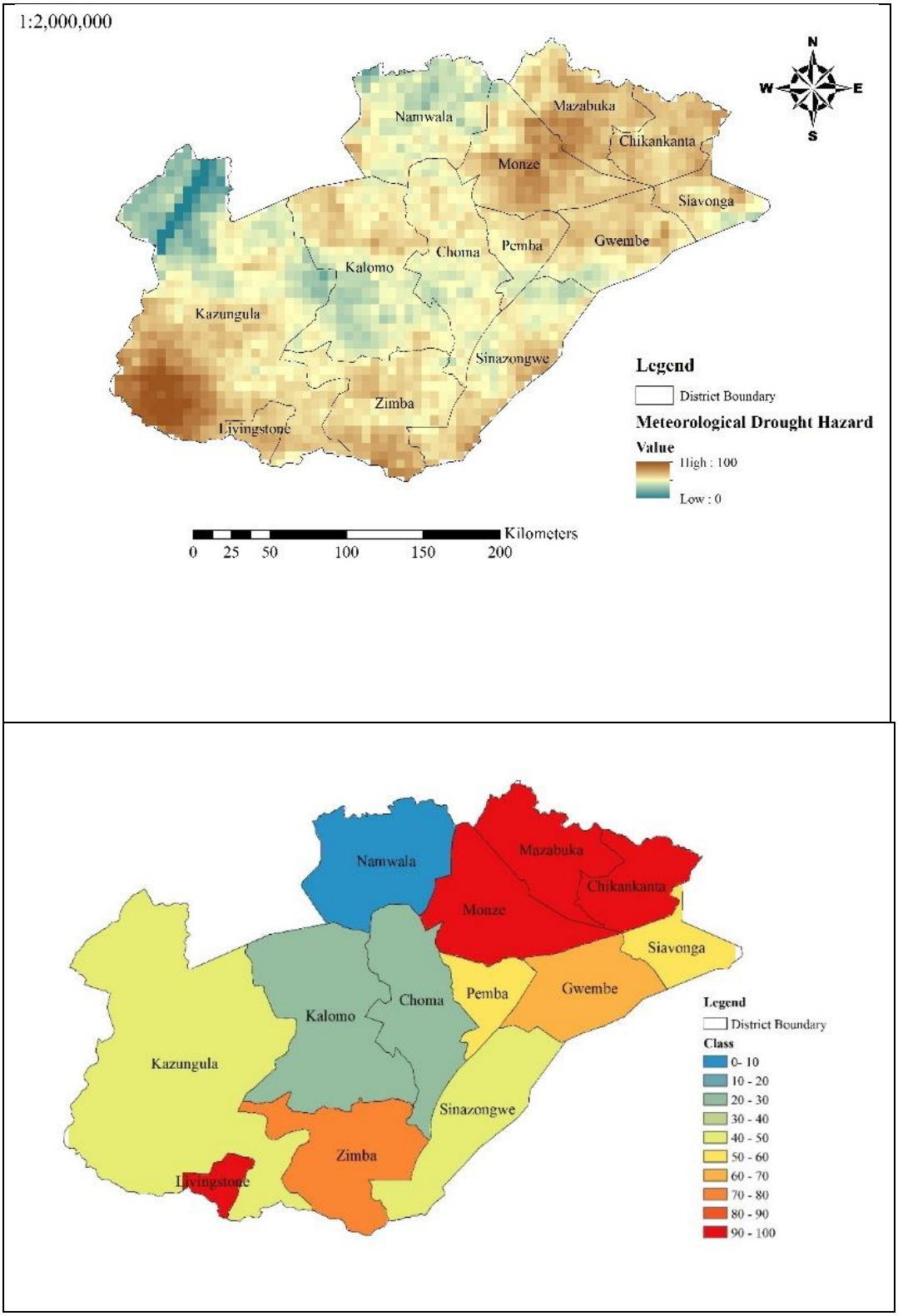

Figure 42: Meteorological drought hazard of the Southern Province of Zambia presented by district

In terms of meteorological drought hazard by district, Chikankata, Livingstone, Mazabuka and Monze all experienced high numbers of occurrences. All four districts were in the livelihood zone ZM08, where arable agriculture is prominent at small- and large-scales.

Hazard was moderate to moderately high in the districts of Gwembe, Siavonga, Sinazongwe and Zimba, all of which were in the Zambezi Valley along the Kariba Lakeshore. The livelihood zone in these districts is ZM10 (Zambezi Valley agro-fisheries zone), where fishing, livestock and cultivation of drought resistant crops (sorghum and pearl millet) are prominent (FEWS NET, 2014). This is an indication of adaptation in reaction to arid conditions.

Agricultural drought hazard occurred mainly along the Zambezi Escarpment and along the shores of Lake Kariba (Figure 43). The districts where agricultural drought hazard occurred the most were Gwembe, Siavonga and Sinazongwe, all of which are in the Zambezi Valley and along the shores of Lake Kariba. The livelihood zone is ZM10 where high frequency of droughts and floods over poor soils result in high food insecurity (FEWS NET, 2014). The nature of the terrain in this zone is mountainous slopes and cascading rocky terrain, which makes some parts of the zone highly erosive (FEWS NET, 2014). All the districts are located in agro-ecological Region I, which receives 400 to 800 millimetres of rainfall per annum, temperatures tend to be higher and the poor sandy soils limit agricultural production potential (FEWS NET, 2014). Agricultural drought hazard occurred the least in the district of Chikankata, whilst Zimba experienced mild drought hazard.

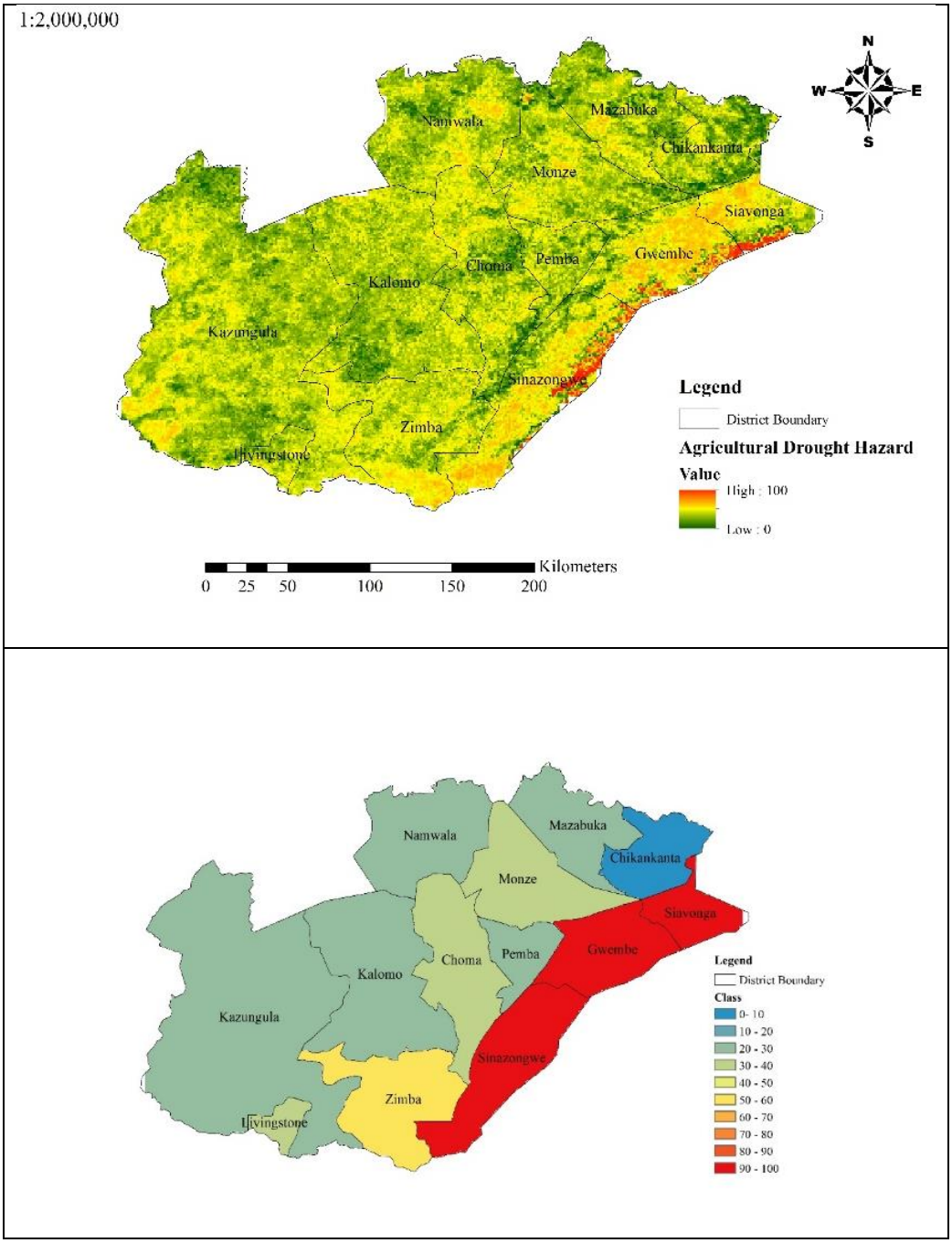

Figure 43: Agricultural drought hazard of the Southern Province of Zambia presented by district

5.8.2 Drought Exposure of the Southern Province, Zambia

As mentioned earlier, exposure was derived from human populations at ward level and land cover. The majority of the Southern Province was moderately exposed. The most exposed area in the province was Mazabuka Central Ward in Mazabuka District (Figure 44). The area was extremely exposed mainly due to a total population of 58,944 (CSO, 2012), the highest of all the wards in the province. The area was covered mainly by cropland and wetland (FD

& FAO, 2016), which were ranked 2 and 4 of the 6 classes. Manungu Ward in Monze was also highly exposed. The area had a population of 38,590 (CSO, 2012) and covered mainly by croplands (FD & FAO, 2016). Other notable areas with considerably high exposure were Chikanta, Chooma and Siachitema wards in Kalomo, and Lubombo and Chivuna wards in Mazabuka District. All the highly exposed areas are in agro-ecological Region II. The least exposed areas in the province were those in the Kafue flats and included Katengwa Ward of Namwala and Itebe Ward of Mazabuka. These wards had populations of 3,470 and 2,856, respectively (CSO, 2012). Notably, Moomba Ward in the northern part of Kazungula District was lowly exposed despite belonging to agro-ecological Region I.

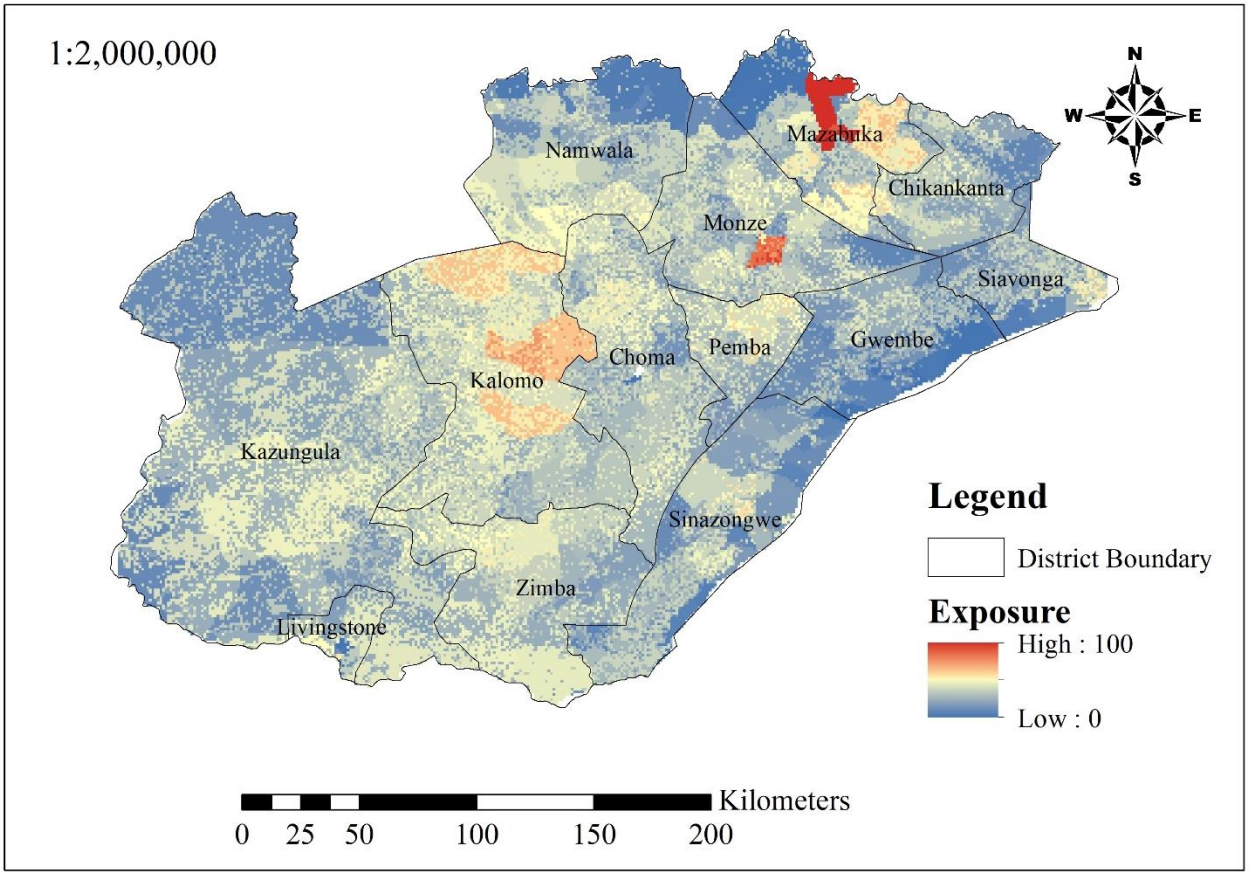

Figure 44: Drought exposure of the Southern Province, Zambia

At district level, the exposure was highest in Kalomo and Mazabuka districts (Figure 45), which were the two most populated with populations standing at 258,570 and 230,972, respectively (CSO, 2012). The two districts are predominantly farming areas, with Kalomo having the most area planted for maize (96,427.53 hectares) as of 2015 (CSO, 2015). Choma (which included Pemba in 2010 had a population of 247,860), and Zimba (formerly part of Kalomo, which had a population of 258,570) were also relatively highly exposed due to their high populations (CSO, 2012). The least exposed districts were Gwembe, Siavonga and

Sinazongwe despite belonging to agro-ecological Region I. This was due to the lower populations in the districts (CSO, 2012). Furthermore, the districts were covered mainly by forests along the Zambezi Escarpment and water over Lake Kariba (FD & FAO, 2016). The districts are also part of livelihood zone ZM 10, which is a fishing and livestock zone (FEWS NET, 2014).

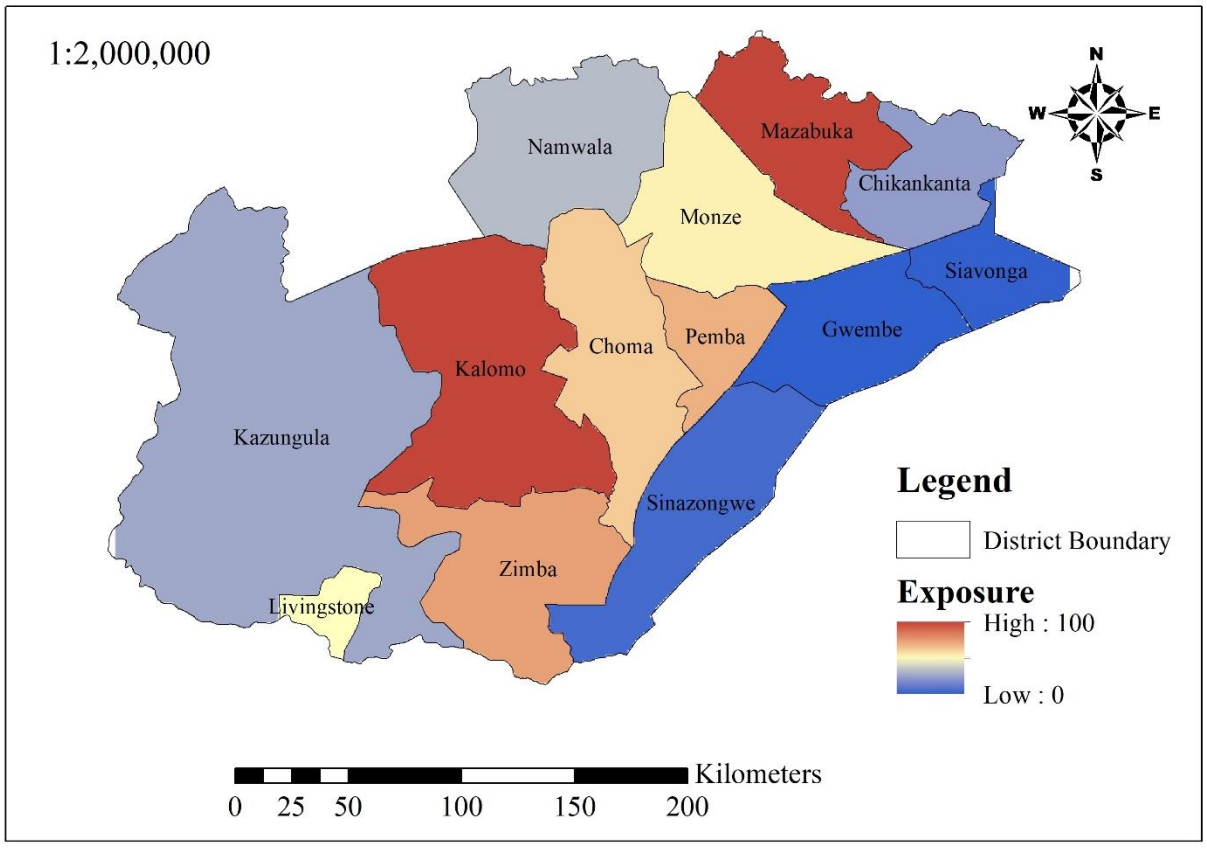

Figure 45: Drought exposure of each district of the Southern Province of Zambia

5.8.3 Drought Vulnerability of the Southern Province, Zambia

Vulnerability was based on poverty Head Count (HC) ratio, the number of poor, rainfall variability and slope. The southern region of the province was relatively more vulnerable than the northern counterpart (Figure 46). However, the most vulnerable area in the province was Siachitema Ward in Kalomo District. There were 21,068 people living under the poverty line and HC was 0.78 (De la Fuente, et al., 2015). The temporal variability of rainfall was moderately high despite a moderately high spatial variability (average rainfall). In general, the southern parts that lie in the Zambezi Valley, where rainfall is low and the land is not flat faced high vulnerability. However, the main form of livelihood in these areas is fishing and is classified as the Zambezi Valley agro-fisheries zone (ZM10) by FEWS NET (2014).

Vulnerability was low in the northern parts of the province, particularly in the Kafue Flats, which are wetlands (FD & FAO, 2016). Similarly, the northern parts of Kazangula had low vulnerability, even though the area fell in agro-ecological Region I, which was drought prone (FEWS NET, 2014).

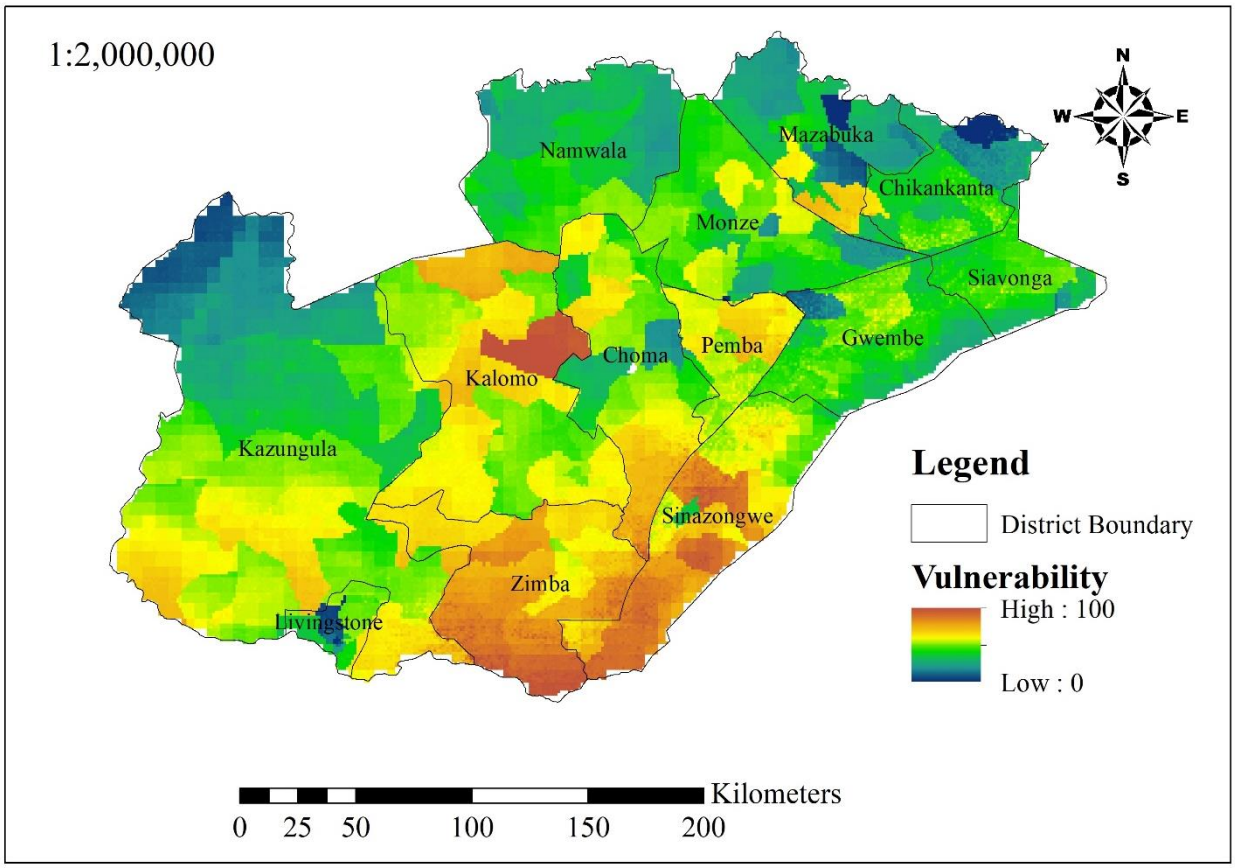

Figure 46: Drought Vulnerability of the Southern Province of Zambia

At district level, Zimba and Sinazongwe were the most vulnerable districts in the province (Figure 47). Both districts were in the southern parts of the province and mainly along the Zambezi River Valley and the Lake Kariba Shore. The districts are located in the livelihood zone ZM10, which is typical of areas that receive low rainfall (FEWS NET, 2014). The districts were also located in agro-ecological Region I, which is drought prone as it received only 400 to 800 millimetres of rainfall annually, with maximum temperatures of 35 to 40 ºC (FEWS NET, 2014). The least vulnerable districts were Chikankata, Mazabuka and Namwala where HC ratio were 0.63, 0.63 and 0.72, respectively (De la Fuente, et al., 2015). The livelihood zone was commercial rail line maize, livestock and cotton (ZM08) as zoned by FEWS NET (2014). Both rainfed and irrigated agriculture were prominent, with commercial and mechanized farms of maize and cotton dotted around the zone (FEWS NET, 2014). Notably, Choma, Kalomo and Pemba districts were fairly vulnerable despite being located in

livelihood zone ZM08 and agro-agricultural Region IIa. This was due to high numbers of people living under the poverty line (179,705 in Choma (of which Pemba was part of during the 2010 census, as it was the basis of the poverty estimations) and 197,306 in Kalomo) (De la Fuente, et al., 2015). Temporal variability of rainfall was also high in this areas.

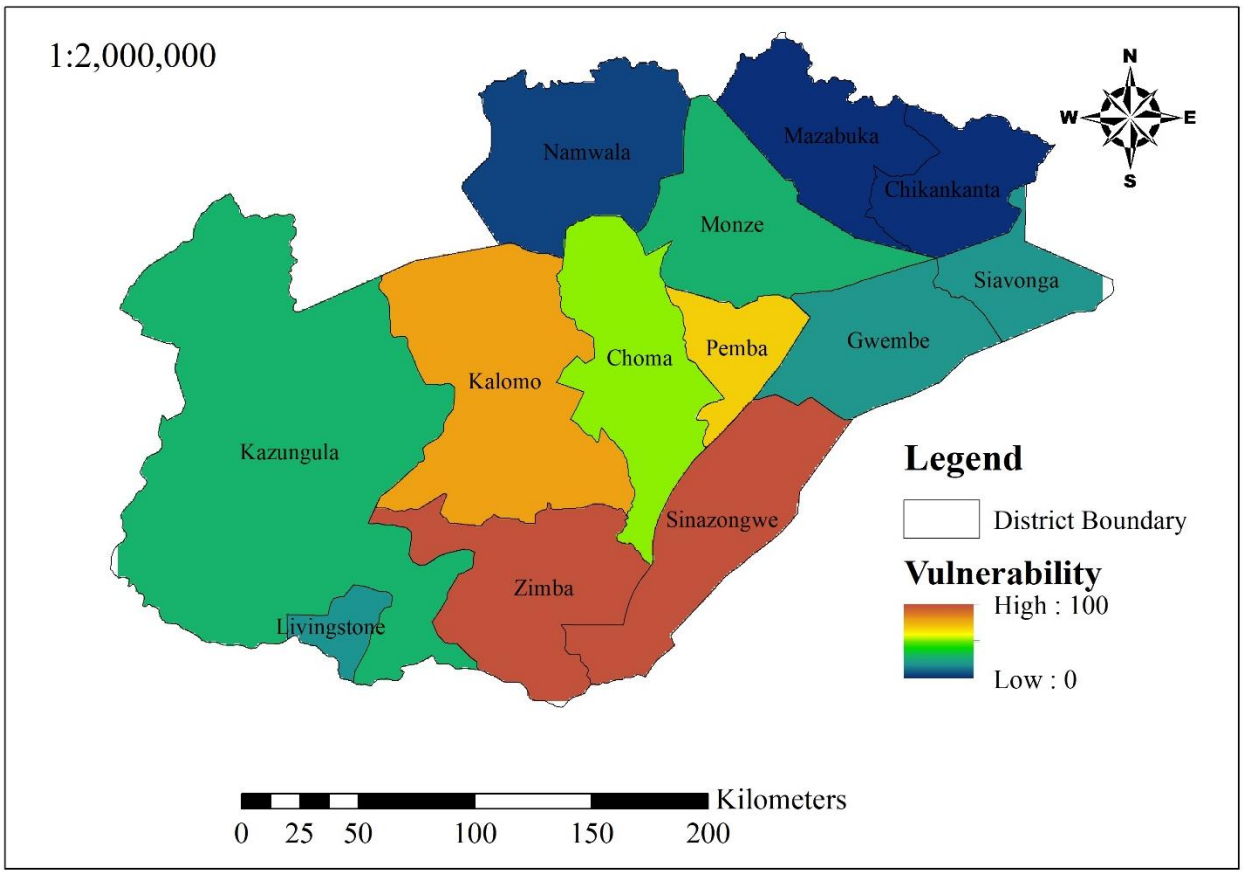

Figure 47: Average drought vulnerability of each district of the Southern Province, Zambia

5.8.4 Drought Risk of the Southern Province of Zambia

Drought risk was assessed for metorological and agricultural droughts. Meteorological drought risk was such that risk increased towards the south of the province (Figure 48). However, risk was the highest in Siachitema Ward in Kalomo and Mazabuka Central Ward in Mazabuka, which both had high populations of 26,725 and 58,944, respectively (CSO, 2012). This resulted in increased exposure. Siachitema Ward also had a high poverty Head Count (HC) ratio of 0.78, while Mazabuka Centrel had a low one of 0.32 (De la Fuente, et al., 2015). Manungu Ward in Monze also had high risk of 80 (out of 100) as it was highly exposed. All three wards are in ZM08, where arable agriculture is prominent (FEWS NET, 2014). By district, Kalomo, Pemba, Sinazongwe and Zimba were the most at risk with regards to meteorological drought. Notably, meteorological drought risk was also high in

Choma, Mazabuka and Monze districts. All these districts had high temporal variation of rainfall. In general, however, the southern lying regions of the province were at higher risk than those in the north. In general, meteorological drought risk did not follow the pattern of agro-ecological regions or livelihood zones.

The least risk areas with regards to meteorological drought were the northern part of Kazungula and the northern part of Namwala. By district, Namwala and Gwembe were the least at risk due to lower populations of 102,866 and 53,117, respectively (CSO, 2012). There was also less cropland cover in these two districts (FD & FAO, 2016).

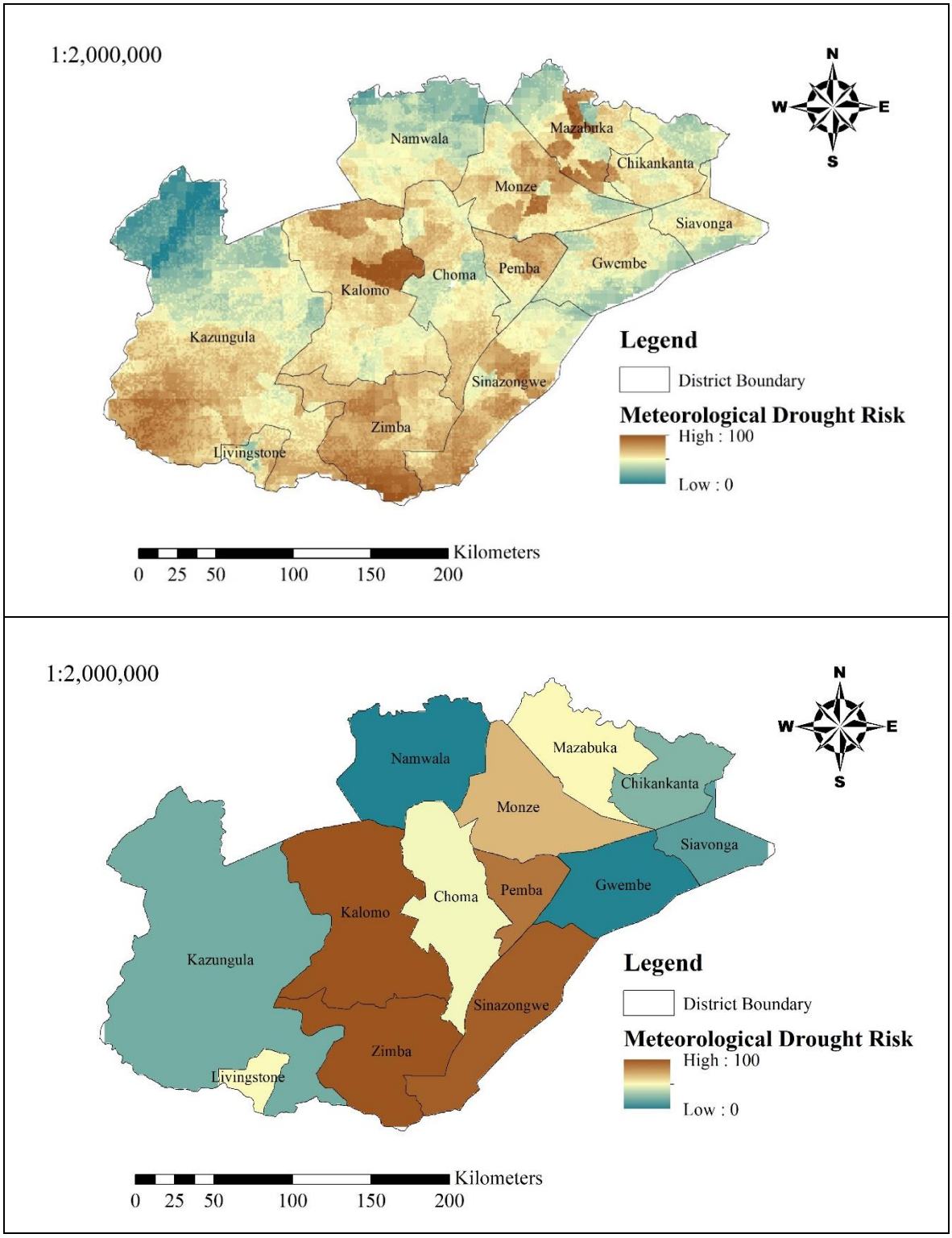

Figure 48: Meteorological drought risk of the Southern Province of Zambia

Agricultural drought risk was similar to meteorological drought risk in that the highest risk was in Saichiteme Ward of Kalomo District (Figure 49). Mazabuka Central Ward was high risk for agricultural drought as it was for meteorological drought. The other similarity was that the northern parts of Kazungula and Namwala had low risk. This was due to lower populations (CSO, 2012) and less croplands (FD & FAO, 2016), which meant less assets

were exposed. The main difference was that meteorological drought risk was more intense and covered more of the province than agricultural drought risk. With regards to the districts, Zimba and Sinazongwe were the most at risk.

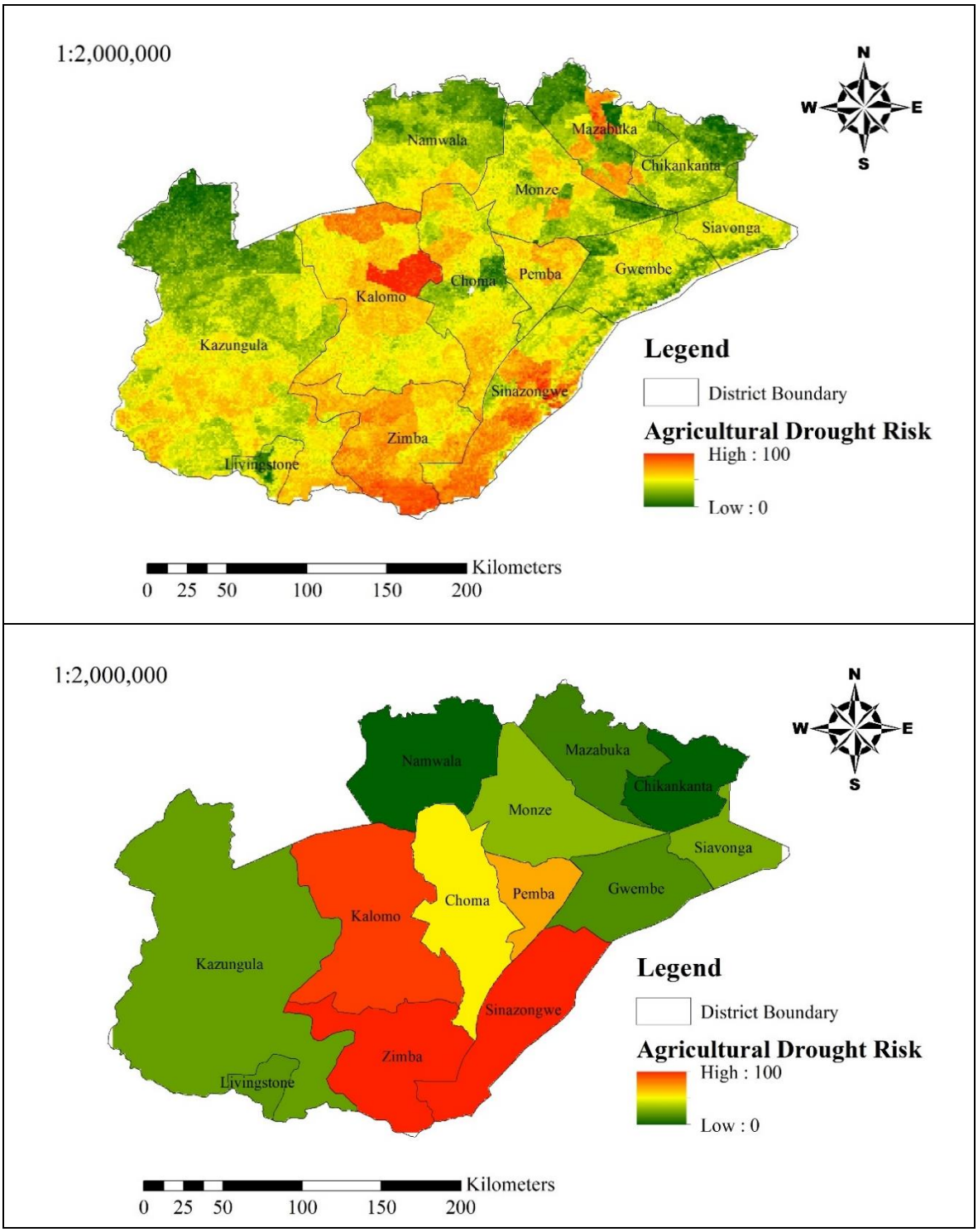

Figure 49: Agricultural drought risk of the Southern Province, Zambia

Integrated drought risk is a combination of meteorological and agricultural drought risk. Similar to the two risks, integrated risk did not follow the pattern of the agro-ecological

regions as high risk areas were present in both Region I and Region II. The areas that were most at risk in the Southern Province were Siachitema and Mazabuka Central wards (Figure 50), which both had high populations (CSO, 2011) as mention earlier. Other hot spots were the southern parts of the province in Sinazongwe and Zimba and the south western part of Kazungula. These are found in agro-ecological Region I, which has low rainfall, high temperatures and poor sandy soils (FEWS NET, 2014).

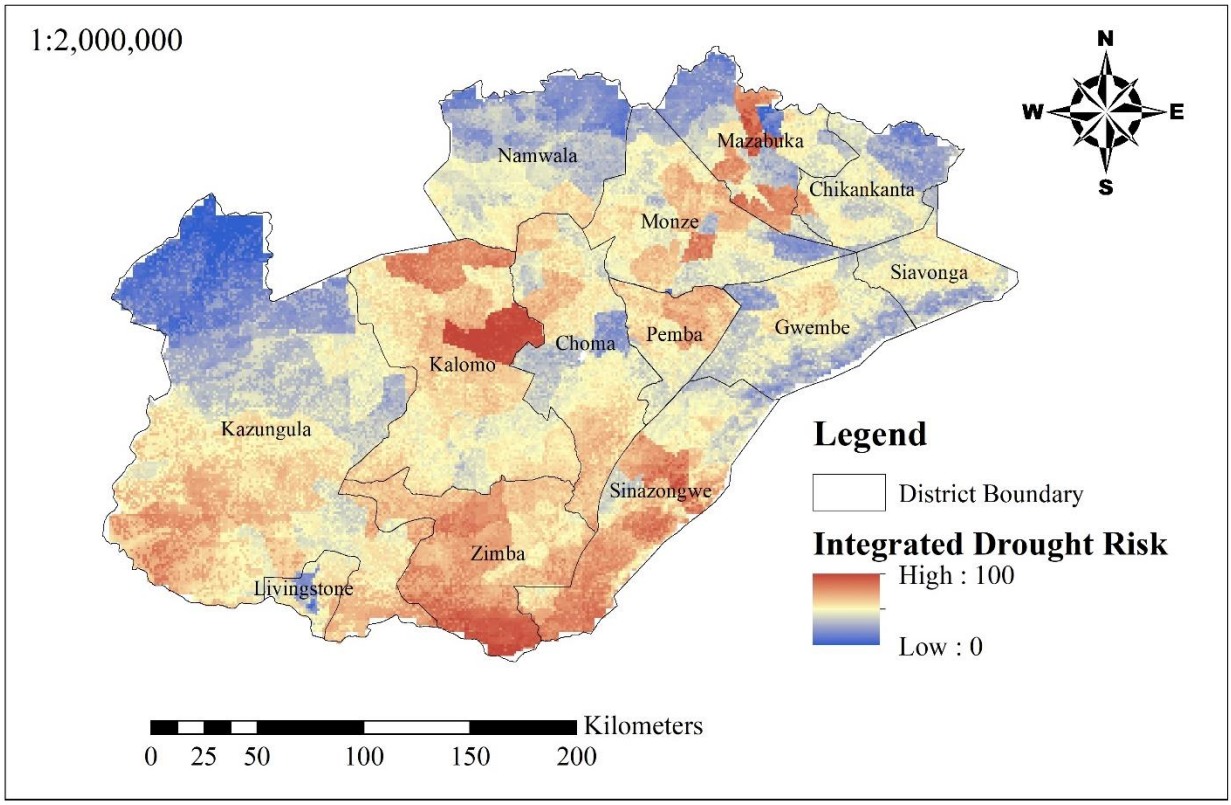

Figure 50: Integrated drought risk of the Southern Province of Zambia derived by the combining meteorological and agricultural drought

The district which was most at risk with regards to integrated drought risk was Zimba, located in the Zambezi Valley (Figure 51). Sinazongwe was also at relatively high risk, although not as high as Livingstone and Zimba. Risk was also high in Kalomo, Pemba and Sinazongwe. The districts where integrated risk was low were Chikankata, Gwembe and Namwala. Kazungula and Siavonga also faced low risk.

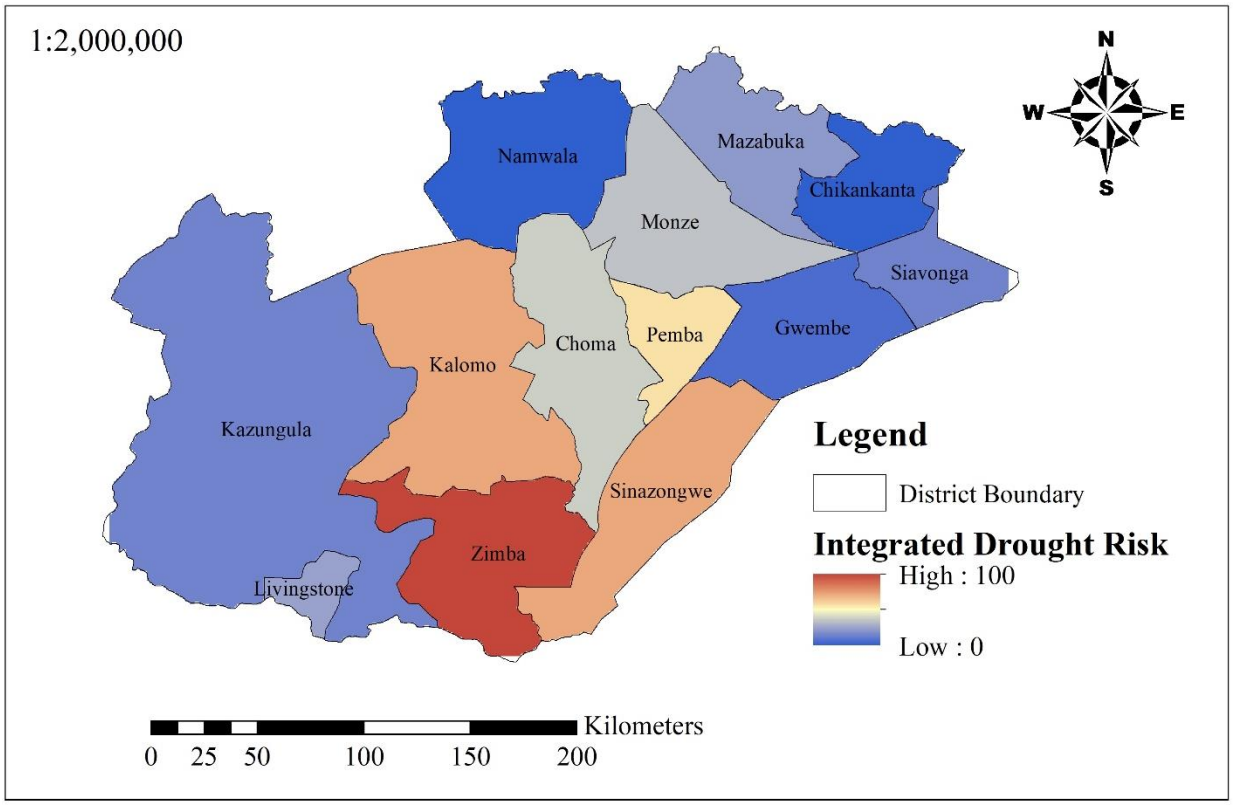

Figure 51: Average integrated drought risk of each district in the Southern Province of Zambia

Of particular interest, Kalomo and Zimba (were one district and formerly called Kalomo before being split) were the districts that planted the most maize (Appendix 7) with regards to small- and medium-scale farmers in the Southern Province (Figure 52) (CSO, 2016b). This was also an area were population was high (CSO, 2012) and croplands covered the majority of the land (FD & FAO, 2016) translating to high exposure and vulnerability and high risk. The presence of extensive agricultural activities in the area further justified the high risk of the area as there were more people exposed and more cropland stood to be lost during droughts. The area was mainly in ZM09 livelihood zone, which is the southern plateau cattle, maize and tobacco zone (FEWS NET, 2014). The zone is characterised by highly fertile sandy loams that are well-drained soils, with rainfall of 800 to 1000 millimetres per annum (FEWS NET, 2014). The high productin of crops and livestock in the area means that more elements and assets are exposed to drought, which Joint Research Centre (2018) noted that could raise drought risk. In Kalomo, sensistivity to drought (vulnerabilty) is high due to a high number of people living under the poverty line (De la Fuente, et al., 2015). Joint Research Centre (2018) also discussed how high sensitivity to drought would raise risk. Based on this, the area has high risk because more elements and assets are exposed and the

vulnerability to drought is high. Despite this, FEWS NET (2014) classified the area as having low food insecurity due to high production of crops and livestock.

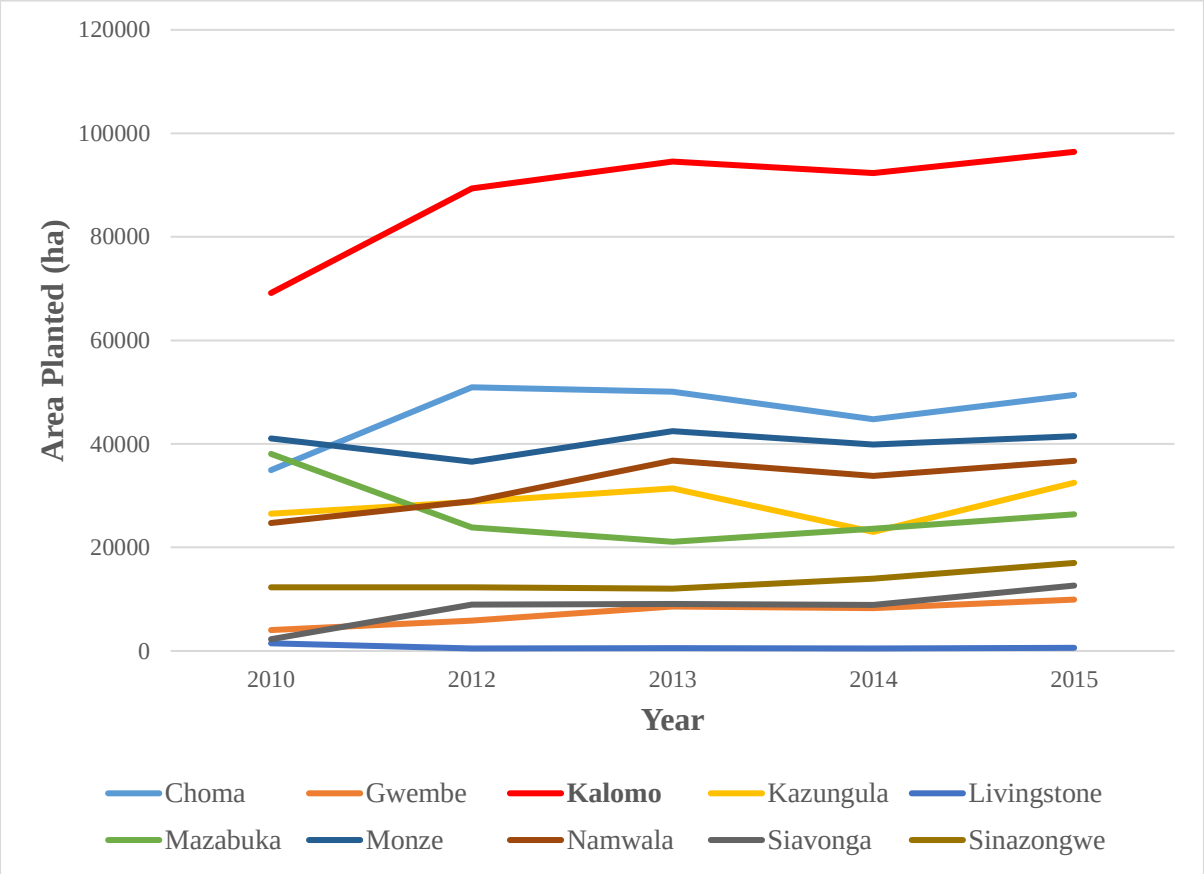

Figure 52: Area Planted for Maize in the Southern Province of Zambia (CSO, 2015)

Across the province, a notable rise in maize production was observed from the year 2010. This is a result of linear increase in area planted (CSO, 2015). However, area harvested dropped despite an increase in area planted. This is demonstrated by a bar plot of area planted and area harvested for the Southern Province (Figure 53). A drop in the area harvested but a rise in production was a sign of adaptation, as discussed by Mubanga (2014), as small- and medium-scale farmers used seeds that have higher yield potential and were drought resistant. However, a reduction in area harvested despite an increase in area planted suggested that crop failure had increased, despite the use of better seeds. This failure could be attributed, among other reasons, to longer, more frequent and more intensive dry periods.

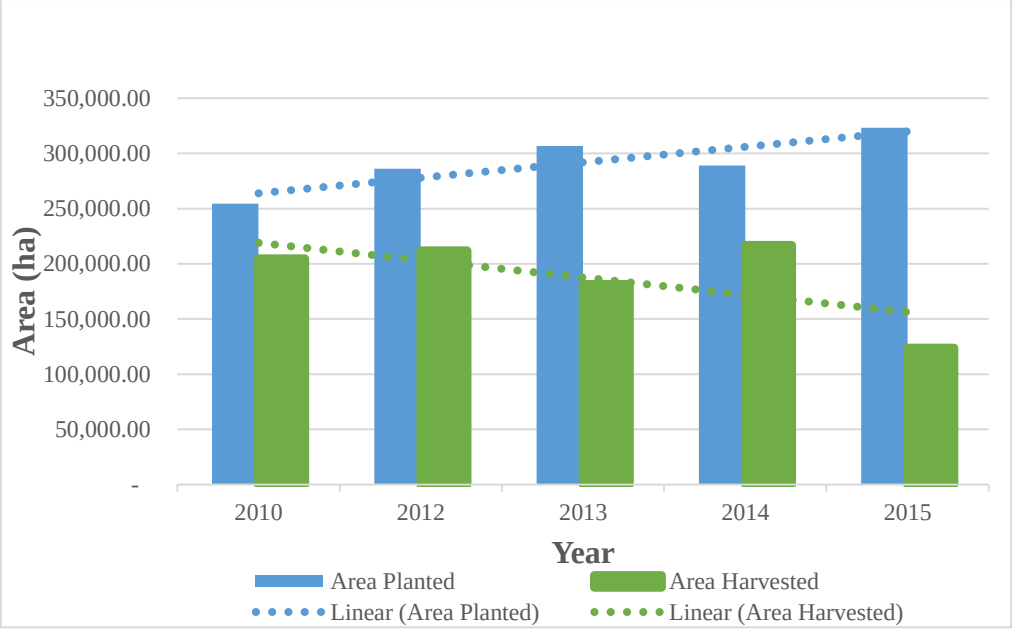

Figure 53: Area Planted and area harvested of maize in the Sothern Province of Zambia from 2010 to 2015

5.9 Discussion of Results

This section gives a summary discussion of the results following the objectives of this study.

5.9.1 Calculation of Remotely Sensed to Determine Meteorological and Agricultural Drought Indices Drought Hazard for the Southern Province of Zambia

As indicated earlier, meteorological drought hazard was determined using rainfall anomaly percentage and Standardised Precipitation Index (SPI) whilst agricultural drought hazard was determined and assessed using Vegetation Condition Index (VCI) and Soil Moisture Index (SMI). From the results, meteorological drought hazard was classified into two categories, which were aggressive droughts and regressive droughts. Aggressive droughts were those where the intensity of a drought increased as the season progressed. Conditions would be normal or near normal in November and December but worsen in the core rainfall months of January and February. One such drought occurred in the season of 2001/2002 where early stages of the planting season received sufficient rainfall, but the later stages suffered shortfalls in rainfall resulting in stunted and dry drops. It was reported by CARE (2002) that in the 2001/2002 planting season, rainfall fell on less days with an inconsistent spatial distribution. In this study, this was reflected in rainfall anomaly percentage of the Southern Province in 2001/2002 which dropped from an average - 4% (normal) in December 2001 to averages of - 42 % (severely dry) and - 61% (extremely dry) in January and February 2002,

respectively. Similarly, SPI in November 2001 was - 0.26 (normal) but reduced sharply to - 1.56 (severely dry) and - 2.29 (extremely dry) in the core rainfall months of December 2001 and January 2002, respectively. Regressive drought were those where the intensity of drought reduced as the season progressed. These droughts occurred during times of moderate or strong El Niño events. One such drought occurred during the 2015/2016 rainfall season were strong El Niño was detected. During this season, the average rainfall anomaly percentage of the Southern Province of Zambia in December 2015 was - 48% (severely dry) but rose to - 9% (normal) in February 2016. Average SPI for the province was - 1.23 in November 2015 but rose to 1.33 by March 2016.

Based on the standardised nature of SPI, it was possible to determine the frequency of occurrence for meteorological drought (Mckee, et al., 1993). SPI revealed that the most frequent meteorological drought hazard were the moderately dry droughts which occurred 7.65% of the time whilst the least frequent were the extremely dry droughts which occurred 1.09% of the time. These frequencies of droughts were expected as it is typical for extreme events to occur at lower frequencies and near normal events to occur most frequently as observed in other studies (WMO, 2012).

Agricultural drought hazard was assessed using VCI and SMI. Similar to rainfall anomaly percentage and SPI, VCI showed that during times of El Niño, agricultural droughts would begin with greater intensity that would subside later in the season. However, during droughts that were not influenced by El Niño, agricultural droughts would increase in intensity. This was similar to the meteorological droughts, and therefore, agricultural droughts were also categorised as aggressive or regressive. VCI displayed a similar pattern to maize yield and production, where VCI dropped as maize production and yield reduced. For instance, the average VCI for the Southern Province was as low as 35.8 for the year 2002, which was also the year that saw the lowest maize production (for the province for the period 2000 to 2016) of 63,092.6 metric tonnes (CSO, 2016b). VCI was not without any limitation. Kogan (1997) asserted that VCI was unable to account for soil conditions and would detect drought whenever a crop was under stress although the cause was not a shortfall of water. Maize production can decrease for a number of reasons such as bad cultivation practices, pest infestations and floods. In this study, Kogan (1997)'s assertion was observed in the years 2008 and 2013 which were not drought years. For instance, in 2008, the Southern Province received the most rainfall (within the study period) with the monthly value reaching as high

as 384 millimetres (CHIRPS) in January. Despite this, maize production was only 115,421 tonnes (CSO, 2016b). Kodamaya (2011) attributed the drop in maize production in the season 2008/2009 to too much rain which damaged crops. The reduction in production was also attributed to a decrease in significance of maize to small-scale farmers whereas production from dambo gardens and petty trade such as vegetable trade increased significantly (Kodamaya, 2011). Mubanga (2014) also noted that farmers supplimented maize with beans, cassava, finger millet, okra, sorghum and soya beans within the event of poor maize yields. Soil Moisture Index (SMI) values were observed to be low in the southern parts of the province, which were mainly areas located in agro-ecological Region I. These were due to these areas receiving low levels of rainfall that were between 400 and 800 millimetres per annum and high temperatures that range from 35 to 40 ºC (FEWS NET, 2014). Areas with high slopes, such as the Zambezi Escarpment, also had low SMI due to higher run off and less infiltration. Higher SMI was observed in agro-ecological Region IIa which covered the central part of the province. These areas were relatively flat and received rainfall between 800 and 1000 millimetres. The high SMI meant that these areas were suitable for arable agriculture and FEWS NET (2014) described these areas as the central plateau of the Southern Province where maize and tobacco cultivation were popular. SMI did not show any aggressive or regressive characteristics that rainfall anomaly percentage, SPI and VCI displayed. This was due to soil moisture still accumulating despite drought conditions.

5.9.2 Relationship between Normalised Vegetation Index (NDVI) and in situ Rainfall, NDVI and Remotely Sensed Rainfall Estimates, Maize Production and Yield versus Vegetation Condition Index (VCI), and Soil Moisture and Soil Moisture Index (SMI)

To achieve this specific objective, correlation analysis was carried out between monthly Normalised Difference Vegetation Index (NDVI) and monthly rainfall values received from the Zambia Meteorological Department (ZMD), seasonal VCI and maize production and yield, and in field soil moisture measurements at 5 and 10 centimetre depths (from ZMD) and SMI. The results show that monthly NDVI and monthly rainfall values received from ZMD were strongly correlated (0.78). Monthly NDVI was at optimum when rainfall was approximately 200 millimetres, but saturated when 250 millimetres of rainfall was exceeded. Similarly, monthly NDVI and monthly rainfall estimates from CHIRPS were also highly correlated. The correlation was 0.74 and indicated that NDVI rose and fell with rainfall.

Wang et al. (2003) found a strong and positive correlation between growing season NDVI (from NOAA-AVHRR) and in field rainfall for 410 weather stations in the Great Plains of Kansas State. Similarly, Rousvel et al. (2013) carried out correlation analysis between monthly NDVI and gridded rainfall extracted from the Global Precipitation Climatology Project (GPCP) for Central Africa and the results revealed that there was a relatively strong correlation between the two variables, especially in the brush-grass savanna (0.90). In this study, correlation was highest in grasslands (0.81). Similar to the findings of Rousvel et al. (2013), the strong correlation displayed between NDVI with both in field rainfall measurements from ZMD and rainfall estimates from CHIRPS validated the use of NDVI based indices in the assessment of drought in the Southern Province of Zambia.

A significant correlation of 0.66 existed between maize production and VCI while a correlation of 0.84 existed between maize yield and VCI. Similarly, a correlation of 0.71 existed between soil moisture measurements at 5 centimetres depth and SMI. The correlation reduced at 10 centimetre depth to 0.40. Unganai and Kogan (1998) found that the VCI-corn (maize) yield correlations ranged from 0.70 to 0.90 across the principal corn regions of Zimbabwe. The correlations reduced to a range of 0.30 to 0.50 in areas where tea and coffee were the primary crops. They concluded that similar results can be obtained in the rest of Southern Africa. Wang, et al. (2007) reported that at a 10 centimetre soil depth, observations do not correspond to the surface parameters that are observed by the MODIS but suggested that soil moisture estimation at shallow depths (5 centimetres) are feasible through combining ground measurements and MODIS land parameters. The strong correlation between VCI and maize production and yield validated the use of VCI to assess agricultural drought in the Southern Province of Zambia. SMI can also be used to assess soil moisture conditions during agricultural drought. However, this is only feasible at shallow depths (Leeuwen, 2015).

5.9.3 Identification of Drought Hotspots in the Southern Province of Zambia using Drought Hazard, Exposure and Vulnerability

This objective was achieved through the combination of drought hazard, exposure and vulnerability of the Southern Province of Zambia. Results showed that integrated drought risk was highest (score of 100) in Zimba, Kalomo (80) and Sinazongwe (80) districts. As of 2010, Zimba and Kalomo had a combined population (the two districts were one at the time) of 258,570 people (CSO, 2012), of which 197,306 (75% of the population and poverty headcount (HC) of 0.75) of them lived under the poverty line (De la Fuente, et al., 2015).

Furthermore, the two districts led in the area of maize planted in the province, with 96,427.53 hectares planted in 2015 (CSO, 2016b). The two districts were highly exposed to drought as they had the largest population in the province and the most agricultural activity with regards to maize. The districts were also highly vulnerable due to the high number of people living under the poverty line. The high exposure and vulnerability to drought resulted in the two districts being at high risk of drought. The risk and effects of these droughts were reflected in 2015 where only 36,271.23 hectares of the 96,427.53 hectares planted of maize were harvested (CSO, 2016b). The districts least at risk of drought were Chikankata, Gwembe, Kazungula, Namwala and Siavonga. In this study, these districts had low risk due to low exposure of populations and crops. The populations of these districts in 2010 were 59,909 in Chikankata, 53,117 in Gwembe, 104,731 in Kazungula, 102,866 in Namwala and 90,213 in Siavonga (CSO, 2012). In addition, the area of maize planted was much lower in these districts. For instance, Gwembe and Siavonga districts planted a combined area of 22,563.92 hectares (CSO, 2016b). When the poverty HC derived by De la Fuente, et al. (2015) is considered, only Gwembe had a higher poverty HC than Kalomo and Zimba which stood at 0.82. However, the number of people living under the poverty line in Gwembe was 44,103, which was much less than those in Kalomo and Zimba (De la Fuente, et al., 2015). The low risk of these districts could, therefore, be attributed to the low exposure due to lower populations (CSO, 2012) and crop production (CSO, 2016b), and the lower number of people leaving under the poverty line (De la Fuente, et al., 2015).

CHAPTER SIX: CONCLUSION AND RECOMMENDATIONS

This chapter gives the conclusions and recommendations of the study following the objectives outlined in Chapter 1.

6.1 Conclusions

The following were the conclusions of the study:

(i) Based on the trend of NDVI, the changes of vegetation due to rainfall variation were such that vegetation followed the pattern of rainfall. During drought years, NDVI dropped below average (as low as 0.54 in February, 2002) due to lower levels of rainfall (as low as 65 millimetres in February, 2002). On a monthly timescale, NDVI responded quickly to increments in rainfall. However, NDVI response lagged to drops in rainfall. This was due to residual soil moisture that remained after the rainfall season. Therefore, changes in NDVI were not as drastic as those in rainfall;

(ii) From the assessment of intra-seasonal patterns of rainfall and NDVI, droughts of the Southern Province were categorised into two types: those that increased in intensity from mild to severe as the season progressed (aggressive droughts); and those that reduced in intensity from severe to mild as the season advanced (regressive droughts). For instance, during the 2001/2002 season, SPI fell from -0.26 (normal) in November 2001 to -2.29 (extremely dry) by January 2002, which indicated an aggressive drought. On the other hand, in the season of 2002/2003, SPI rose from -1.55 (severely dry) in November 2002 to 0.57 (normal) by March 2003, which indicated a regressive drought. Aggressive droughts occurred without the influence of El Niño events and tended to intensify during the months of January to March. Regressive droughts occurred during times of moderate or strong El Niño signals were detected and tended to be more intensive during the months of November to January. Regressive droughts subsided during the months of January to March as rainfall begun to return to normal. This characteristic was borne from the fact that El Niño peaks in November to January, and begins to decay in the first half of the next year;

(iii) Spatial variability of rainfall across the Southern Province was such that the areas in the northern parts received more rainfall (averaged as high as 800 millimetres per season for the period 1981 to 2016) than those in the south (averaged as low as 500 millimetres per season for the period 1981 to 2016). This pattern followed the distribution of agro-ecological regions in the province, with the northern parts belonging to Region IIa and the southern parts to the low rainfall Region I. However, the northern part of Kazungula District indicated an anomaly, as it belonged to agro-ecological Region I but received more rainfall than the other areas in the region. Temporal rainfall variability was similar to spatial variability in that the southern parts of the province experienced larger rainfall variations (as much as 30%) than the northern areas (as low as 15%). However, the central parts of the province also experienced high rainfall variation despite being in agro-ecological Region IIa which receives more rainfall than Region I;

(iv) Analysis of SPI revealed that the Southern Province experienced a drought 14.75% of time from January 1981 to March 2016. During this period, a moderate drought occurred 7.65% of the time, a severe drought 6.01% and an extreme drought 1.09%. Therefore, in the Southern Province, a moderate drought is expected to occur once every 2.6 years, a severe drought once every 3.3 years and an extreme drought once every 18.3 years. Spatially, extremely dry droughts displayed an east to west gradient with occurrences reducing towards the west. Severely dry droughts were more frequent in the districts along the Zambezi Escarpment and moderate droughts occurred mainly in the northern part of Kazungula;

(v) The aggressive and regressive nature of droughts was true for both meteorological droughts and agricultural droughts, as was revealed by rainfall anomaly percentage, SPI and VCI. VCI also revealed that an aggressive agricultural drought was preceded by an aggressive meteorological drought. Similarly, a regressive agricultural drought was preceded by a regressive meteorological drought;

(vi) VCI showed a similar trend to maize production and maize yield. The trend was similar in that VCI dropped each time maize production and maize yield fell. In fact, the lowest VCI recorded in 2002 (35.77) for the province was also the lowest record of maize production and yield (63,092.60 mt and 0.42, respectively). This was the

year in which a national crisis was declared due to a very severe drought. A statistically significant correlations existed between maize production and VCI and maize yield and VCI. The correlation between maize production and VCI was 0.66 and was weaker than that between maize yield and VCI which was 0.84. This meant that VCI was more directly affected with an increase in yield than an increase in production;

(vii) During aggressive droughts, surface temperatures (~40ºC) did not deviate from the normal. However, these droughts were drier as they intensified mainly in the high rainfall months of January and February. Because of their nature to occur due to El Nino, regressive droughts were characterised by higher surface temperatures (above 50ºC) during the months of November and December. During these droughts, surface temperatures were as high as 55ºC for pixels in which NDVI was also high (wet pixels). This resulted in trapezoid shaped plots of Fractional Vegetation Cover (Fr) and Scaled Land Surface Temperature (T*). Therefore, trapezoid shaped Fr-T* plots in the months of November and December indicated the onset of regressive droughts;

(viii) There was a significant correlation between NDVI and in situ rainfall measurements. The Kendall tau was 0.59 while the Spearman's rho was 0.78 (p value < 2.2E-16, in both cases). Similarly, a significant correlation between NDVI and CHIRPS rainfall estimates existed. The Kendall tau was 0.54 and the Spearman's rho was 0.74. The existence of these correlations indicated that NDVI based indices could be used to assess variations in rainfall, therefore, be used as a proxy or supplement to in situ rainfall measurements during the assessment of drought;

(ix) The relationship between NDVI and rainfall differed within different vegetation covers. The correlation was higher in grasslands and croplands (0.81 and 0.80. respectively) and lower in forests and wetlands (0.77 and 0.76, respectively). This meant that grasslands and croplands responded faster to changes in rainfall. Wetlands response was slow due higher soil moisture levels throughout the year;

(x) There was a significant correlation 0.71 (p-value = 0.02) between soil moisture at 5 centimetre depth and SMI. However, the correlation 0.40 was not significant at 10cm

as the p-value was 0.25 (>0.05). Therefore, SMI could be reliably used to assess soil moisture conditions across the Southern Province during periods of drought. However, this was only true for the top layers of soil (<= 5 centimetres) as no correlation existed at deeper levels;

(xi) Meteorological drought hazard was highest to the south of Kazungula. However, the north of the district had low hazard. This was in line with rainfall variability were the north of Kazungula was classed as an anomaly due to the fact that it was located in the low rainfall agro=ecological Region I. Meteorological drought hazard was also high at the border between Mazabuka and Monze. By district, hazard was high in the districts of Chikankata, Livingstone, Mazabuka and Monze. Hazard was the lowest in Namwala. Agricultural drought hazard was high along the Zambezi Escarpment and the most affected districts were Gwembe, Siavonga and Sinazongwe. The least affected district was Chikankata;

(xii) Based on ward populations and land cover, the most exposed area to drought in the Southern Province was Mazabuka Central Ward in Mazabuka District. The area was extremely exposed mainly due to a total population of 58,944 (the highest of all the wards in the province) and agricultural activities (cropfield land cover). The least exposed area in the province was the Kafue flats and this included Katengwa Ward of Namwala and Itebe Ward of Mazabuka. By district, Kalomo and Mazabuka were the most exposed whereas the least exposed were Gwembe and Siavonga. The determinant of exposure was human population, which was highest in Kalomo and Mazabuka, and lowest in Gwembe and Siavonga;

(xiii) Based on socioeconomic indicators, rainfall variability and slope, Siachitema Ward in Kalomo District was the most vulnerable area in the province as there were 21,068 people living under the poverty line and HC was 0.78. The most vulnerable districts were Kalomo, Pemba, Sinazongwe and Zimba. The least vulnerable districts were Namwala, Mazabuka and Chikankata, which are located in Region II;

(xiv) The northern part of Kazungula and areas in the Kafue Flats faced the least risk to drought. On the other hand, the southern parts of Kazungula were high risk. Kalomo, Sinazongwe and Zimba were at the highest risk to meteorological drought, whilst

Gwembe and Namwala were at the lowest. In terms of agricultural drought, Zimba, Sinazongwe and Kalomo faced the highest risk. Kalomo was high risk despite having the highest area of maize planted (69,162.63 to 96,427.53 hectares between 2010 and 2015) and area of maize harvested (36,271.23 to 66,526.22 hectares between 2010 and 2015). Namwala and Chikankata faced the least agricultural drought risk; and

Perhaps the most interesting area in the province was the northern part of Kazungula. Despite being in agro-ecological Region I, the area had the little hazard, exposure, vulnerability and risk with values of less than 20 out of 100 for each.

6.2 Recommendations

Based on the conclusions of the study, the following recommendations are made to the appropriate stakeholders:

(i) The Disaster Management and Mitigation Unit (DMMU) should integrate remote sensing drought indices and GIS work flows to the drought early warning systems. The inclusion of soil moisture conditions, LST and VCI to early warning systems can prove cardinal in improving early warning systems. Fr-T* plots can also be used with the system with trapezoid plots indicating a possible regressive drought;

(ii) The National Remote Sensing Centre (NRSC) should extend the study to the rest of the country and develop a national framework of drought monitoring using remote sensing and GIS;

(iii) NRSC should increase the temporal resolution of the study from one month to a 10 day time-step in order to detect changes in NDVI, VCI, LST, SMI and rainfall quicker and hence improve early warning systems;

(iv) During aggressive droughts, DMMU and the Ministry of Agriculture (MoA) should focus mitigation measures during the drought intense months of January, February and March and advise farmers to grow more drought resistant crop varieties;

(v) During regressive droughts, DMMU should focus mitigation measures during the intense months of November, December and January and advise the farmers to plant late. The MoA should advise farmers to plant fast growing varieties of grain;

(vi) A detailed study of the high drought risk areas of Kalomo, Sinazongwe and Zimba should be carried out by the NRSC and the University of Zambia Integrated Water Resources Management (UNZA IWRM) Centre to determine other factors contributing to high risk;

(vii) The MoA, NRSC and ZMD should carry out further research in the northern part of Kazungula to determine the reasons why the area is low risk despite being located in agro-ecological Region I; and

(viii) The University of Zambia (UNZA), CSO and the NRSC should include other socioeconomic and health information, such as income from agricultural and livestock dependency ratios and nutrition to the study to improve the vulnerability profile of the Southern Province.

REFERENCES

Abdi, H., 2010. *Coefficient of Variation.* [Online]
Available at: https://www.utdallas.edu/~herve/abdi-cv2010-pretty.pdf
[Accessed 12 June 2017].

Amalo, L. F., Hidayat, R. & Haris, 2017. Comparison Between Remote-Sensing-Based Drought Indices in East Java. *IOP Conf. Series: Earth and Environmental Science,* Volume 54, pp. 1 – 7.

Busetto, L. & Ranghetti, L., 2018. *MODIStsp: A Tool for Automatic Preprocessing of MODIS Time Series* [Online] Available at: https://cran.rproject.org/web/packages/MODIStsp/vignettes/MODIStsp.pdf

Camberlin, P., Martiny, N., Philippon, N. & Richard, Y., 2007. Determinants of the Interannual Relationships Between Remote Sensed Photosynthetic Activity and Rainfall in Tropical Africa. *Remote Sensing of Environment,* Volume 106, pp. 199 – 216.

Cap-Net, 2015. *Drought risk reduction training manual.* New York: United Nations Develoment Programme, pp. 1 – 106.

CARE, 2002. *The Hungry Months: A report on drought, crop failure and food shortages in Zambia.* Lusaka: Care International, pp 1 – 11.

Carlson, T., 2007. An Overview of the "Traingle Method" for Estimating Surface Evapotranspiration and Soil Moisture from Satellite Imagery. *Sensors,* Volume 7, pp. 1612 – 1629.

Chok, N. S., 2008. *Pearson's versus Spearman's and Kendall's Correlation,* Pittsburgh: University of Pittsburgh (Master of Science Thesis), pp. 1 – 30.

Chopra, P., 2006. *Drought Risk Assessment using Remote Sensing and GIS : A case study of Gujarat.,* Enschede: University of Twente (Master of Science Thesis), pp. 1 – 77.

CIESIN, 2015. *Step-by-Step Guide to Vulnerability Hotspots Mapping: Implementing the Spatial Index Approach.* New York: Columbia University, pp. 68 – 117.

CSO, 2011. *Zambia 2010 Census of Population and Housing: Preliminary Population Figures.,* Lusaka: Government of the republic of Zambia (GRZ), pp. 75 – 78.

CSO, 2012. *Zambia 2010 Census of Population and Housing: Population Summary Report.* Lusaka: Government of the republic of Zambia (GRZ), pp. 54 – 81.

CSO, 2015. *Agriculture Statistics - Zambia Data Portal.* [Online] Available at: http://zambia.opendataforafrica.org/ionawve/agriculture-statistics [Accessed 20 September 2017].

CSO, 2016a. *2015 Living Conditions Monitoring Survey Report,* Lusaka: GRZ, pp. 4 – 121.

CSO, 2016b. *Crop Forecast Survey Data of Zambia, 2015.* [Online] Available at: http://zambia.opendataforafrica.org/ZMCRFCSD2016/crop-forecast-survey-data-of-zambia-2015?action=download [Accessed 11 March 2019].

Dabanli, I., 2018. Drought Risk Assessment by Using Drought Hazard and Vulnerability Indexes. *Natural Hazards and Earth System Sciences Discussions,* pp. 1 – 15.

Damizadeh, M., Bahram, S. & Gieske, A., 2001. *Studying Vegetation Responses and Rainfal Relationship Based-On NOAA/AVHRR Images.* Singapore, Centre for Remote Imaging, Sensing and Processing (CRISP), pp. 1 – 11.

Davenport, M. L. & Nicholson, S. E., 1993. On the Relation Between Rainfall and the Normalized Difference Vegetation Index for Diverse Vegetation Types in East Africa. *International Journal of Remote Sensing,* 14(12), pp. 2369 – 2389.

De la Fuente, A., Murr, A. & Rascón, E., 2015. *Mapping Subnational Poverty in Zambia,* Washington D.C: World Bank Group, pp. 1 – 98.

Development Initiatives, 2016. *Definitions and Measures of Poverty.* [Online] Available at: http://devinit.org/wp-content/uploads/2016/07/Definitions-and-measures-of-poverty.pdf [Accessed 7 March 2019], pp. 1 – 8.

Didan, K., Munoz, A. B., Solano, . R. & Huete, A., 2015. *MODIS Vegetation Index User's Guide.* [Online] Available at: https://vip.arizona.edu/documents/MODIS/MODIS_VI_UsersGuide_June_2015_C6.pdf [Accessed 21 January 2017], pp. 21 – 24.

Doesken, N. J., Mckee, T. B. & Kleist, J., 1991. *Development of a Surface Water supply Index for the Western United States: Climate Report #91-3,* Fort Collins: Colorado State University, pp. 7 – 22.

FAO, 2016. *Southern Africa El Niño Response Plan (2016/17).* Rome: FAO, pp 1 – 16.

FD & FAO, 2016. *Integrated Land Use Assessment Phase II (2011-2016) - Final Report,* Lusaka: GRZ, 13 – 94.

FEWS NET, 2014. *Zambia Livelihood Zones and Descriptions.* Lusaka: USAID, pp. 1 – 53.

FEWS NET, 2017. *Early Warning and Environmental Monitoring Program.* [Online] Available at: https://earlywarning.usgs.gov/fews [Accessed 6th October 2017].

Funk, C. et al., 2015. The Climate Hazards Infrared Precipiatation with Stations - A New Environmental Record for Monitoring Extremes. *Scientific Data,* Volume 2.

Ganesh, S., 2013. *Investigation of the Utility of the Vegetation Condition Index (VCI) As an Indicator of Drought,* College Station: Texas A&M University (Master of Science Thesis), pp. 1 – 50.

Gibbs, W. J. & Maher, J. V., 1967. *Rainfall Deciles as Drought Indicators.* Melbourne: Bureau of Meteorology, pp. 1 – 23.

GITTA, 2013. *Weighting by Ranking.* [Online]
Available at:
http://www.gitta.info/Suitability/en/html/Normalisatio_learningObject1.html
[Accessed Febraury 2018].

Govaerts, B. & Verhulst, N., 2010. *The Normalized Difference Vegetation I(NDVI) GreenSeekerTM Handheld Sensor: Toward the Integrated Evaluation of Crop Management. Part A: Concepts and Case Studies.* Mexico: CIMMYT, pp. 1 – 12.

Guenang, G. M. & Kamga, F. M., 2014. Computation of the Standardized Precipitation Index(SPI) and Its Use to Assess Drought Occurrences in Cameroon over Recent Decades. *Journal of Applied Meteorology and Climatology,* Volume 53, pp. 2310 – 2324.

Hall, G., 2015. [Online]
Available at: http://www.hep.ph.ic.ac.uk/~hallg/UG_2015/Pearsons.pdf
[Accessed 13 December 2016].

Hauke, J. & Kossowski, T., 2011. Comparison of Values of Pearson's and Spearman's Correlation Coefficients on the Same Sets of Data. *Quaestions Geagraphicae,* 30(2), pp. 87 – 93.

Hunt, E. D. et al., 2008. The Development and Evaluation of Soil Moisture Index. *International Journal of Climatology,* Volume 29, pp. 747 – 759.

Joint Research Centre, 2018. *Drought Risk Assessment and Management: A Conceptual Framework,* Brussels: European Commision, pp. 1 – 48.

Kodamaya, S., 2011. Agricultural Policies and Food Security of Smallholder Farmers in Zambia. *African Study Monographs,* Volume 42, pp 19 – 39.

Kasim, A. A. & Usman, A. A., 2016. Triangle Method for Estimating Soil Surface Wetness from Satellite Imagery in Allahabad District, Uttar Pradesh, India. *Journal of Geoscience and Environment Protection,* Volume 4, pp. 84 – 92.

Kogan, F. N. , 1997. Global Drought Watch from Space. *Bulletin of the American Meteorological Society*, 78(4), pp. 621 – 636.

Kogan, F. N., 2001. Operational Space Technology for Global Vegetation Assessment. *Bulletin of the American Meteorological Society*, 82(9), pp. 1949 – 1964.

Kundzewicz, Z. W. & Matczak, P., 2015. *Hydrological extremes and security.* Göttingen, Copernicus Publishers, pp. 44 – 53.

Leeuwen, B., 2015. *GIS Workflow for Continuous Soil Moisture Estimation Based on Medium Resolution Satellite Data.* Lisbon, AGILE.

Lekprichakul, T., 2008. *Impact of 2004/2005 Drought on Zambia's Agricultural Production.* Kyoto: Research Institute for Humanity and Nature (RIHN). pp. 1 – 21.

Libanda, B., Zheng, M., & Ngonga, C., 2019. Spatial and temporal patterns of drought in Zambia. *Journal of Arid Land*, 11(2), pp. 180 – 191.

Makaudze, E. M. & Miranda, M., 2008. *Using Remotely-Sensed Vegetation Condition Index to Investigate the Feasibility of Drought Insurance for Smallholder Farmers in Zimbabwe.* Cape Town, University of Western Cape, pp. 5 – 46.

Mckee, T. B., Doesken,, N. J. & Kleist, J., 1993. The Relationship of Drought Frequency and Duration to Time Scales. *AMS 8th Conference on Applied Climatology,* pp. 179 – 184.

MESA SADC-THEMA, 2014. *Drought Service Manual.* [Online]
Available at:
http://www.mesasadc.org/sites/default/files/manuals/Service%20Product%20Manual%20-%20Drought.pdf [Accessed 26th September 20117], pp. 1 – 32.

MESA SADC-THEMA, 2017. *Drought.* [Online]
Available at: http://www.mesasadc.org/drought [Accessed 28th September 2017].

Meshu, T. & Berhan, G., 2013. Interactive Drought Monitoring Information System: A Case Study on Standardized Precipitation Index for Ethiopia. *HiLCoE Journal of Computer Science and Technology,* 1(2), pp. 125 – 131.

Mishra, A. K. & Singh, V. P., 2012. Simulating Hydrological Drought Properties at Different Spatial Units in the United States Based on Wavelet–Bayesian Regression Approach. *Earth Interactions,* 16(17), pp. 1 – 23.

Mishra, M. M. & Nagarajan, R., 2013. Hydrological Drought Assessment in Tel River Basin Using Standardized Water Level Index (SWI) and GIS Based Interpolation Techniques. *International Journal of Conceptions on Mechanical and Civil Engineering,* 1(1), pp. 3 – 6.

Mubanga, K. H., 2014. Assessing Seed Breeders Recommended Maize Varieties for Southern Zambia: How Small-Scale Farmers Have Adapted. *International Conference on Agricultural, Environmental and Biological Sciences,* pp. 29 – 35.

Mu, Q. et al., 2013. A Remotely Sensed Global Terrestrial Drought Severity Index. *Bulletin of American Meteorological Society,* 94(1), pp. 83 – 98.

Narasimhan, B. & Srinivasan, R., 2005. Development and Evaluation of Soil Moisture Deficit Index (SMDI) and Evapotranspiration Deficit Index (ETDI) for Agricultural Drought Monitoring. *Agricultural and Forest Meteorology,* 133(1-4), pp. 69 – 68.

National Drought Mitigation Centre, 2019. *How Does Drought Affect Our Lives.* [Online] Available at: https://drought.unl.edu/Education/DroughtforKids/DroughtEffects.aspx [Accessed 28 January 2019].

National Weather Service, 2012. *Drought Fact Sheet.* Silver Spring: National Oceanic and Atmospheric Administration, pp. 1.

NDMC, 2006. *Types of Drought.* [Online] Available at: http://drought.unl.edu/DroughtBasics/TypesofDrought.aspx [Accessed 22 August 2016].

NIST, 2016. *Gamma Distribution.* [Online] Available at: http://www.itl.nist.gov/div898/handbook/eda/section3/eda366b.htm [Accessed 10 March 2017].

Palmer, W. C., 1965. *Meteorological Drought,* Washinton D.C: US Weather Bureau, pp. 1 – 58.

Potic, I., Burgarski, M. & Matic-Verenica, J., 2017. Soil Moisture Determination Using Remote Sensing Data for the Property Protection and Increase of Agricultural Drought. *Annual World Bank Conference on Land and Poverty*, pp. 1 – 12.

Relief Web, 2003. *Drought relief in Zambia (2002-2003).* [Online] Available at: https://reliefweb.int/report/zambia/drought-relief-zambia-2002-2003 [Accessed 14th November 2018].

RisCura, 2017. *The effect of El Niño on key Southern African countries.* [Online] Available at: http://www.riscura.com/brightafrica/el-nino/effect-southern-african-countries/ [Accessed 13th November 2017].

Rousvel, S. et al., 2013. Comparison between Vegetation and Rainfall of Bioclimatic Ecoregions in Central Africa. *Atmosphere,* Volume 4, pp. 411 – 427.

Shahid, S., 2008. Drought Risk Assessment in the Western Part of Bangladesh. *Natural Hazards,* Volume 46, pp. 391 – 413.

Sivakumar, M. V., Wilhite, D.A., Svoboda, M.D., Hayes, M., & Motha, R., 2010. *Global Assessment Report on Disaster Risk Reduction:Drought Risk and Meteorological Drought,* Geneva: UNISDR, pp. 1 – 26.

Statistics Solutions, 2018. *Kendall's Tau and Spearman's Rank Correlation Coefficient.* [Online]
Available at: https://www.statisticssolutions.com/kendalls-tau-and-spearmans-rank-correlation-coefficient/ [Accessed 22 November 2018].

Tempfli, K., Kerle, N., Huurneman, G. C. & Janssen, L. L., (eds.), 2009. *Principles of Remote Sensing: An introductory textbook.* Fourth ed. Enschede: International Institute for Geo-Information Science and Earth Observation (ITC), pp. 124 – 128.

The Climate Reality Project, 2016. *The Facts About Climate Change and Drought.* [Online]
Available at: https://www.climaterealityproject.org/blog/facts-about-climate-change-and-drought [Accessed 28 January 2019].

Thenkabail, P. S., Gamage, M. S. & Smakhtin, V. U., 2004. *The Use of Remote-Sensing Data for Drought Assessment and Monitoring in Southwest Asia,* Colombo: International Water Management Institute (IWMI), pp. 1 – 24.

U.N.I.S (2007). *Drought Risk Reduction Framework and Practices: Contribution to the Implementation of Hyogo Framework.* s.l.:ISDR, pp. 1 – 5.

Unganai, L. S. & Kogan, F. N. (1998). Drought Monitoring and Corn Yield Estimation in Southern Africa From AVHRR Data. *Remote Sensing of Environment,* 63(3), pp. 219 – 232.

UNOCHA, 2017. *El Niño in Southern Africa.* [Online]
Available at: http://www.unocha.org/legacy/el-nino-southern-africa
[Accessed 13th November 2017].

Venables, W. N., Smith, D. M. & R Core Team, 2018. *An Introduction to R.* Los Angelas: R Core Team, 1 – 81.

Wang, J., Rich, P. M. & Price, K. P., 2003. Temporal Responses of NDVI to Precipitation and Temperature in the Central Great Plains, USA. *International Journal of Remote Sensing,* 24(11), pp. 2345 – 2364.

Wang, L., Qu J. J., Zhang, S., Hao X. & Dasgupta S., 2007 Soil moisture Estimation using MODIS and Ground Measurements in Eastern China. *International Journal of Remote Sensing,* 28(6), pp. 1413 – 1418.

Wan, Z., 2013. *MODIS Land Surface Temperature Products Users' Guide.* [Online] Available at: https://lpdaac.usgs.gov/sites/default/files/public/product_documentation/mod11_user_guide.pdf [Accessed 21 January 2017], pp. 11 – 17.

WFP, 2016. *El Niño: Undermining Resilience . Implications of El Niño in Southern Africa from a Food and Nutrition Security Perspective,* Rome: World Food Programme (WFP), pp. 1 – 53.

WMO and GWP, 2016. *Handbook of Drought Indicators and Indices.* Geneva: WMO, pp. 1 – 41.

WMO, 2012. *Standardized Precipitation Index User Guide.* Geneva: World Meteorological Organisation (WMO), pp. 1 – 16.

WMO, 2014. *El Niño/Southern Oscillation.* Geneva: World Meteorological Organisation (WMO), pp. 2 – 8.

World Bank, 2007. *Project Performance Assessment Report: Republic of Zambia Emergency Drought Recovery Project,* Washingtone D.C: World Bank Group, pp. 1 – 25.

Zoungrana, B. J. et al. (2015). Land Use/Cover Response to Rainfall Variability: A Comparing Analysis between NDVI and EVI in the Southwest of Burkina Faso. *Climate,* Volume 3, pp. 63 – 77.

APPENDICES

Appendix 1: Coordinates of meteorological stations in the Southern Province, Zambia

Name	Latitude	Longitude	Type
Chipepo	-16.79	27.88	Manual
Choma	-16.84	27.07	Manual
Choma	-16.836	27.07	Automatic
Gwembe	-16.629	27.772	Automatic
Kafue Polder	-15.78	27.92	Manual
Kalomo	-16.96	26.478	Automatic
Livingstone	-17.82	25.82	Manual
Maamba	-17.34	27.187	Automatic
Magoye	-16	27.62	Manual
Pemba Cheelo	-16.686	27.289	Automatic
Pemba kanchomba	-16.594	27.494	Automatic

Appendix 2: Livelihood zones of Zambia (FEWS NET, 2014)

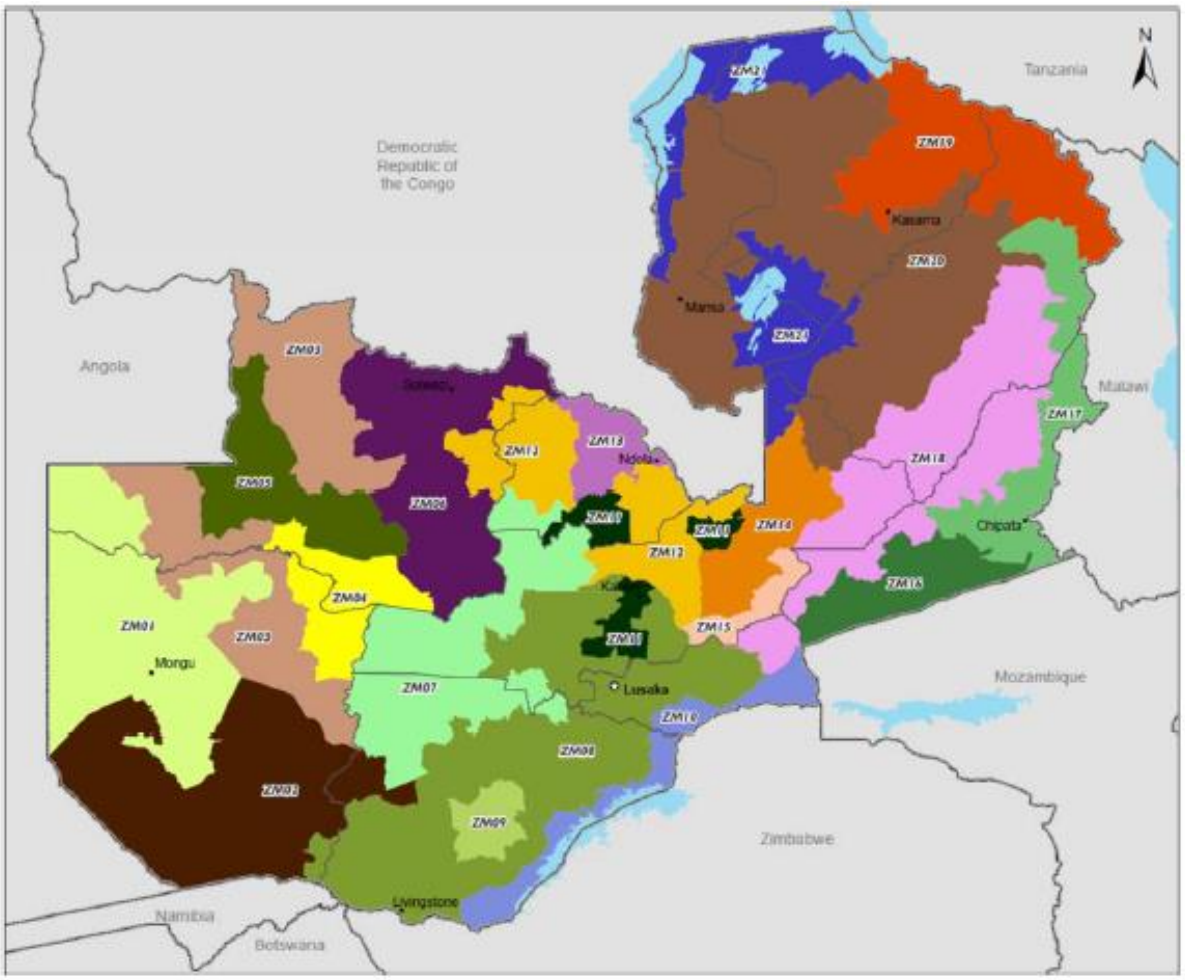

Appendix 3: Coordinates of sample points used for correlation analysis for the Southern Province of Zambia

Name	Longitude	Latitude	Land Cover
SP1	27.10	-15.72	Wetlands
SP2	27.36	-15.75	Wetlands
SP3	26.77	-16.03	Grassland
SP4	26.47	-16.02	Grassland
SP5	25.10	-17.57	Wetland
SP6	26.69	-17.94	Grassland
SP7	26.97	-16.82	Settlement
SP8	27.47	-16.28	Settlement
SP9	25.86	-17.85	Settlement
SP10	27.26	-17.25	Forests
SP11	27.47	-16.92	Forests
SP12	25.36	-16.21	Forests
SP13	25.19	-16.59	Otherlands
SP14	25.17	-16.65	Otherlands
SP15	26.79	-17.25	Cropland
SP16	27.61	-15.91	Cropland
SP17	28.04	-16.19	Cropland
SP18	26.72	-16.66	Cropland

Appendix 4: Maize production and yield of the Southern Province, Zambia (CSO, 2016b)

Year	Maize Production (mt)	Maize Yield (mt/ha)
2001	211,281.39	1.60
2002	63,092.60	0.42
2003	127,277.00	0.91
2004	211,976.00	1.79
2005	120,518.00	0.70
2006	230,105.00	1.53
2007	238,570.00	1.34
2008	115,421.00	unavailable
2009	365,225.77	unavailable
2010	582,984.00	unavailable
2011	639,540.90	unavailable
2012	573,175.97	1.85
2013	453,532.00	1.37
2014	597,999.41	1.92

Appendix 5: Ward Population, Number of Poor and Poverty Headcount of Southern Province Zambia (De la Fuente, et al. 2015) and (CSO 2012)

District	Constituency	Ward	Population	Number of Poor	HC
Choma	Choma	Moomba	3,300	2,292	0.68
Choma	Mbabala	Mbabala	14,759	12,032	0.81
Choma	Pemba	Hamaundu	18,408	14,904	0.80
Choma	Mbabala	Simaubi	11,991	10,344	0.86
Choma	Mbabala	Mapanza	5,998	4,878	0.80
Choma	Mbabala	Mangunza	6,132	5,273	0.85
Choma	Mbabala	Chilalantambo	9,521	8,140	0.84
Choma	Mbabala	Macha	7,501	5,588	0.73
Choma	Mbabala	Kabimba	2,035	1,732	0.84
Choma	Choma	Simamvwa	11,505	8,948	0.77
Choma	Choma	Stateland	6,544	4,296	0.65
Choma	Choma	Nakeempa	5,595	4,848	0.85
Choma	Choma	Namuswa	11,517	9,626	0.82
Choma	Choma	Siasikabole	8,421	7,209	0.85
Choma	Choma	Singani	8,927	7,219	0.80
Choma	Choma	Sikalongo	8,111	6,652	0.81
Choma	Choma	Batoka	6,974	5,344	0.74
Choma	Pemba	Pemba	2,328	1,078	0.46
Choma	Pemba	Kasiya	12,861	10,991	0.84
Choma	Pemba	Habunkululu	4,388	3,854	0.86
Choma	Pemba	Kauba	7,232	6,106	0.84
Choma	Pemba	Nachibanga	9,254	7,853	0.84
Choma	Pemba	Maambo	12,716	11,171	0.87
Gwembe	Gwembe	Chisanga	2,862	2,457	0.86
Gwembe	Gwembe	Lukonde	4,231	2,707	0.63
Gwembe	Gwembe	Jongola	660	594	0.90
Gwembe	Gwembe	Fumbo	9,029	7,292	0.80
Gwembe	Gwembe	Bbondo	8,682	7,575	0.86
Gwembe	Gwembe	Chaamwe	2,894	2,498	0.86
Gwembe	Gwembe	Kkole	2,743	2,404	0.87
Gwembe	Gwembe	Luumbo	3,668	3,203	0.86
Gwembe	Gwembe	Kota Kota	1,113	1,023	0.88
Gwembe	Gwembe	Siampande	1,450	1,268	0.87
Gwembe	Gwembe	Chibuwe	5,420	4,434	0.81
Gwembe	Gwembe	Kkoma	5,880	4,936	0.82
Gwembe	Gwembe	Sinafala	2,060	1,780	0.85
Gwembe	Gwembe	Jumbo	2,425	2,088	0.87
Kalomo	Dundumwezi	Chikanta	20,836	16,549	0.79
Kalomo	Kalomo Central	Mayoba	11,337	8,681	0.76
Kalomo	Mapatizya	Mbwiko	9,161	7,321	0.79

Kalomo	Kalomo Central	Siachitema	26,725	21,068	0.78
Kalomo	Kalomo Central	Kalonda	13,562	10,188	0.74
Kalomo	Kalomo Central	Choonga	21,559	10,872	0.50
Kalomo	Kalomo Central	Namwianga	9,785	6,471	0.65
Kalomo	Kalomo Central	Simayakwe	5,034	4,036	0.79
Kalomo	Kalomo Central	Nachikungu	8,399	6,680	0.79
Kalomo	Kalomo Central	Chawila	8,063	6,335	0.78
Kalomo	Kalomo Central	Sipatunyana	3,814	3,028	0.78
Kalomo	Mapatizya	Luyaba	15,165	12,194	0.79
Kalomo	Mapatizya	Zimba	13,185	9,696	0.73
Kalomo	Mapatizya	Siamafumba	10,413	8,327	0.79
Kalomo	Mapatizya	Chidi	10,347	8,221	0.79
Kalomo	Mapatizya	Mulamfu	6,549	5,390	0.81
Kalomo	Mapatizya	Simwatachela	5,057	3,943	0.77
Kalomo	Dundumwezi	Naluja	13,707	10,943	0.79
Kalomo	Dundumwezi	Bbilili	9,990	8,086	0.80
Kalomo	Dundumwezi	Omba	10,676	8,510	0.79
Kalomo	Dundumwezi	Kasukwe	15,141	11,710	0.77
Kalomo	Dundumwezi	Chamuka	10,065	7,753	0.77
Kazungula	Katombola	Ngwezi	10,182	7,252	0.71
Kazungula	Katombola	Moomba	2,425	1,786	0.73
Kazungula	Katombola	Nguba	11,393	8,193	0.71
Kazungula	Katombola	Kauwe	6,539	4,279	0.65
Kazungula	Katombola	Chooma	7,264	4,900	0.67
Kazungula	Katombola	Sikaunzwe	7,542	5,142	0.68
Kazungula	Katombola	Mandia	9,246	4,991	0.53
Kazungula	Katombola	Sekute	3,228	2,317	0.71
Kazungula	Katombola	Mukuni	8,862	5,913	0.66
Kazungula	Katombola	Simango	4,745	3,255	0.68
Kazungula	Katombola	Musokotwane	4,960	3,466	0.69
Kazungula	Katombola	Kanchele	10,860	7,815	0.72
Kazungula	Katombola	Nyawa	11,075	7,688	0.69
Kazungula	Katombola	Katapazi	6,410	4,169	0.65
Livingstone	Livingstone	Kasiya	9,165	5,013	0.54
Livingstone	Livingstone	Simonga	12,926	4,969	0.38
Livingstone	Livingstone	Freedom	11,974	2,230	0.18
Livingstone	Livingstone	Lizuma	2,761	312	0.11
Livingstone	Livingstone	Dambwa Central	6,329	1,198	0.19
Livingstone	Livingstone	Zambezi	16,098	3,662	0.23
Livingstone	Livingstone	Nansanzu	7,194	2,058	0.29
Livingstone	Livingstone	Kariba	4,521	1,006	0.22
Livingstone	Livingstone	Maramba	9,590	1,410	0.14
Livingstone	Livingstone	Libuyu	7,817	2,657	0.34
Livingstone	Livingstone	Mulungushi	8,263	2,669	0.32

Livingstone	Livingstone	Mwalibonena	9,886	2,704	0.27
Livingstone	Livingstone	Namatama	11,606	4,179	0.36
Livingstone	Livingstone	Musi o Tunya	8,213	606	0.07
Livingstone	Livingstone	Dr Mubitana	6,543	1,123	0.17
Livingstone	Livingstone	Akapelwa	3,058	237	0.08
Livingstone	Livingstone	Shungu	3,565	1,922	0.53
Mazabuka	Magoye	Chivuna	19,508	16,140	0.82
Mazabuka	Mazabuka	Lubombo	21,496	11,891	0.55
Mazabuka	Chikankanta	Mabwetuba	12,974	10,496	0.81
Mazabuka	Magoye	Itebe	2,856	2,323	0.80
Mazabuka	Magoye	Kalama	3,351	2,857	0.84
Mazabuka	Magoye	Munenga	2,713	2,321	0.85
Mazabuka	Magoye	Mwanachingwala	11,742	8,726	0.73
Mazabuka	Magoye	Ngwezi	16,557	13,031	0.78
Mazabuka	Magoye	Munjile	2,508	2,193	0.86
Mazabuka	Magoye	Musuma	5,534	4,722	0.85
Mazabuka	Magoye	Nkonkola	6,462	5,601	0.86
Mazabuka	Mazabuka	Chizobo	6,040	3,928	0.64
Mazabuka	Mazabuka	Mazabuka Central	58,944	18,725	0.32
Mazabuka	Mazabuka	Nakambala	8,565	3,128	0.36
Mazabuka	Mazabuka	Nega Nega	4,787	3,796	0.79
Mazabuka	Chikankanta	Kasengo	6,787	5,829	0.85
Mazabuka	Chikankanta	Namalundu	7,989	4,223	0.52
Mazabuka	Chikankanta	Musaya	1,133	1,006	0.86
Mazabuka	Chikankanta	Nansenga	2,701	2,257	0.83
Mazabuka	Chikankanta	Upper Kaleya	11,340	9,076	0.79
Mazabuka	Chikankanta	Chitete	10,531	8,672	0.82
Mazabuka	Chikankanta	Malala	6,454	5,521	0.85
Monze	Bweengwa	Hamangaba	8,461	7,266	0.85
Monze	Monze	Ufwenuka	9,601	7,539	0.78
Monze	Moomba	Moomba	1,010	881	0.85
Monze	Bweengwa	Kaila	7,405	6,370	0.85
Monze	Bweengwa	Keemba	12,513	10,700	0.85
Monze	Bweengwa	Malundu	8,291	6,759	0.80
Monze	Bweengwa	Choongo East	12,798	9,711	0.75
Monze	Bweengwa	Choongo West	3,668	3,023	0.81
Monze	Monze	Monze Urban	1,502	1,110	0.73
Monze	Monze	Manungu	38,590	17,535	0.45
Monze	Monze	Mayaba	4,685	3,812	0.81
Monze	Monze	Hufwa / Hamapande	3,589	3,080	0.85
Monze	Monze	Hamamvwa	4,290	3,773	0.87
Monze	Monze	Katimba	7,051	6,115	0.86
Monze	Monze	Hantotola	11,960	10,421	0.86
Monze	Monze	Bbombo	5,787	4,979	0.86

Monze	Monze	Chisekesi	7,206	5,678	0.78
Monze	Moomba	Mwanza West	13,041	10,931	0.83
Monze	Moomba	Mwanza East	6,286	5,162	0.82
Monze	Moomba	Chona	9,716	8,221	0.84
Monze	Monze	Chipembele	7,141	6,097	0.84
Monze	Bweengwa	Bweengwa	7,281	6,125	0.84
Namwala	Namwala	Mandondo	4,474	3,383	0.75
Namwala	Namwala	Namakube	10,943	8,153	0.74
Namwala	Namwala	Itapa	7,117	5,462	0.76
Namwala	Namwala	Moobola	12,748	9,317	0.72
Namwala	Namwala	Ndema	9,308	7,294	0.77
Namwala	Namwala	Ngabo	2,729	2,228	0.80
Namwala	Namwala	Namwala Central	10,300	5,719	0.55
Namwala	Namwala	Baambwe	4,069	3,180	0.77
Namwala	Namwala	Maala	5,776	4,156	0.72
Namwala	Namwala	Kantengwa	4,506	3,470	0.76
Namwala	Namwala	Mbeza	5,122	3,710	0.71
Namwala	Namwala	Nakamboma	13,614	10,356	0.75
Namwala	Namwala	Chitongo	4,939	4,018	0.80
Namwala	Namwala	Kabulamwanda	7,221	5,563	0.76
Siavonga	Siavonga	Simamba	6,304	5,251	0.83
Siavonga	Siavonga	Lusangazi	3,075	2,822	0.91
Siavonga	Siavonga	Sinadambwe	4,325	3,905	0.90
Siavonga	Siavonga	Manchanvwa	4,723	4,105	0.86
Siavonga	Siavonga	Mulima	6,162	4,822	0.88
Siavonga	Siavonga	Ibwe Munyama	3,376	2,936	0.88
Siavonga	Siavonga	Sikoongo	3,905	3,407	0.87
Siavonga	Siavonga	Nanyanga	2,588	2,241	0.85
Siavonga	Siavonga	Kariba	16,415	7,702	0.46
Sinazongwe	Sinazongwe	Namazambwe	5,120	4,370	0.84
Sinazongwe	Sinazongwe	Malima	6,162	5,210	0.84
Sinazongwe	Sinazongwe	Sinenge	8274	6,643	0.80
Sinazongwe	Sinazongwe	Nangombe	6,384	5,242	0.82
Sinazongwe	Sinazongwe	Nkandabwe	6,490	5,046	0.77
Sinazongwe	Sinazongwe	Sinazongwe	10,698	8,136	0.76
Sinazongwe	Sinazongwe	Mweezya	17,200	13,030	0.75
Sinazongwe	Sinazongwe	Maamba	10,249	4,379	0.42
Sinazongwe	Sinazongwe	Muchekwa	6,791	5,286	0.77
Sinazongwe	Sinazongwe	Mweemba	11,331	9,400	0.82
Sinazongwe	Sinazongwe	Tekelo	1,923	1,686	0.87
Sinazongwe	Sinazongwe	Muuka	4,819	4,226	0.86
Sinazongwe	Sinazongwe	Mweenda	5,398	4,749	0.87
Sinazongwe	Sinazongwe	Mabinga	778	653	0.84

Appendix 6: Correlations in different land cover classes of the Zambia Scheme II Land Cover Map

Land Cover Class	Kendall Tau	P-value	Spearman rho	P-value
All Classes	0.54	< 2.2E-16	0.74	< 2.2E-16
Forest	0.57	< 2.2E-16	0.77	< 2.2E-16
Grassland	0.62	< 2.2E-16	0.81	< 2.2E-16
Cropland	0.63	< 2.2E-16	0.81	< 2.2E-16
Wetland	0.57	< 2.2E-16	0.77	< 2.2E-16

Appendix 7: District area planted and harvested for Maize in the Southern Province, Zambia (CSO, 2015)

District	Indicator Name (ha)	Year				
		2010	2012	2013	2014	2015
Choma	Area planted	34,937.29	50,943.43	50,095.39	44,785.55	49,487.12
	Area Harvested	29,114.90	42,282.31	31,175.38	33,980.19	25,554.82
Gwembe	Area planted	4,039.80	5,892.21	8,597.69	8,259.15	9,927.13
	Area Harvested	1,647.41	4,087.57	4,004.64	5,454.84	4,237.26
Kalomo	Area planted	69,162.63	89,347.27	94,573.40	92,353.48	96,427.53
	Area Harvested	57,840.06	61,748.24	66,526.22	65,976.11	36,271.23
Kazungula	Area planted	26,531.17	28,793.18	31,392.13	22,999.42	32,499.87
	Area Harvested	20,063.28	23,842.18	19,577.04	16,475.52	8,663.72
Livingstone	Area planted	1,479.46	511.55	526.51	482.45	599.97
	Area Harvested	1,052.97	231.02	244.57	363.83	33.15
Mazabuka	Area planted	38,074.32	23,837.94	21,092.18	23,629.22	26,387.72
	Area Harvested	33,223.54	19,780.21	11,176.89	21,689.57	12,313.71
Monze	Area planted	41,041.57	36,559.82	42,467.75	39,870.95	41,502.94
	Area Harvested	34,671.25	25,892.01	25,143.97	35,101.88	12,526.46
Namwala	Area planted	24,725.49	28,943.81	36,772.07	33,806.11	36,697.72
	Area Harvested	17,608.63	18,586.03	14,277.10	22,328.31	15,161.13
Siavonga	Area planted	2,269.82	8,971.15	9,100.38	8,875.18	12,636.92
	Area Harvested	1,722.95	6,254.11	3,374.97	4,779.33	5,308.88
Sinazongwe	Area planted	12,319.17	12,288.61	12,036.96	13,996.73	17,004.97
	Area Harvested	7,579.16	9,061.71	5,969.50	10,556.49	3,619.76